Physics and Physical Oceanography Data Report 2000-1

Analysis of the Mean Circulation in Placentia Bay: Spring and Summer 1999

Douglas J. Schillinger, Paul Simmons and Brad deYoung,

© 2000
Department of Physics and Physical Oeanography
Memorial University of Newfoundland
St. John's, Newfoundland
A1B 3X7

Abstract

Seven moorings were deployed in Placentia Bay and recorded current velocity data from April to July 1999. The data were analysed to determine the circulation around the bay. Four of the moorings were deployed at the mouth of the bay and consisted of two current meters at depths of 20 m and either 45 or 55 m. The remaining three moorings each carried one Acoustic Doppler Current Profiler (ADCP). The observed circulation around the bay is cyclonic. The weekly mean currents measured at each mooring location are consistent in direction, but vary in magnitude. There is little correlation between the wind stress measured at Argentia and the observed currents at any depth. Results of tidal analysis and detided low-pass filtered currents are presented. The dominant source of variance in the circulation is at the M_2 tidal frequency.

Acknowledgements

We would like to thank our colleagues G. Rose and P. Snelgrove for their support with this work. We also thank Jack Foley for his help in the deployment and recovery of the instruments and Len Zedel for his help in the analysis and interpretation of the ADCP data. We thank the crews of the Mares and Shamook for their assistance with the field program. Funding support was provided by and NSERC research grant to B. deY.

Table of Contents

Abstract ii

Acknowledgements iii

Table of Contents iv

List of Figures v

List of Tables xi

Introduction 1

Station Information 2

Data Analysis 3

Summary of Findings 6

Mean Circulation 6

Tidal Analysis 7

References 11

Tabulated Results 12

Summary statistics of weekly mean currents for M1 to M7 in Earth co-ordinates 12

Summary Statistics at select depths for M1 to M6 in Earth co-ordinates 14

Summary Statistics in bay co-ordinates for M5, M6 and M7 15

Tidal Constituents measured at M5, in bay co-ordinates 17

Tidal Constituents measured at M6, in bay co-ordinates 20

Tidal Constituents measured at M7, in bay co-ordinates 23

Figures 25

Results from Mooring M5, in bay co-ordinates 38

Results from Mooring M6, in bay co-ordinates 56

Results from Mooring M7, in bay co-ordinates 72

List of Figures

Figure 1: Map of Placentia Bay, showing mooring placements used in the spring and summer of 1999. The moorings were in place from April to July 1999. Tidal height and wind information were obtained for Argentia. 25

Figure 2: Mean circulation at a depth of 20 m. Days 108 – 178, 1999. The results of covariance analysis are indicated in the figures by the solid axes. These axes show the standard deviation of the current along the direction of maximum variance and perpendicular to it. The scale for the standard deviation is four times the scale used for the current velocity (indicated by the open arrow in the top left-hand corner). The mean wind velocity is shown by the solid arrow in the upper left corner. 26

Figure 3: Weekly mean currents for the summer of 1999 in Placentia Bay at a depth of 20 m. 3(a) Days 108 - 115. 3(b) Days 115 - 122. 3(c) Days 122-129. 3(d) Days 129 - 136. The results using covariance analysis are indicated in the figures by the solid axes. The scale for the standard deviation is four times the scale used for the current velocity (indicated by the open arrow in the top left-hand corner). The mean wind velocity is included (the solid arrow below the scale). 27

Figure 3 (continued). Weekly mean currents for the summer of 1999 in Placentia Bay at a depth of 20 m. 3(e) Days 136 - 143. 3(f) Days 143 - 150. 3(g) Days 150 - 157. 3(h) Days 157 - 164. 28

Figure 3 (continued). Weekly mean currents for the summer of 1999 in Placentia Bay at a depth of 20 m. 3(i) Days 164 - 171. 3(j) Days 171 - 178. 29

Figure 4: Mean circulation in Placentia Bay at depths of 45–55m. Days 108-178, 1999. The results using covariance analysis are indicated in the figures by the solid axes. The scale for the standard deviation is four times the scale used for the current velocity (indicated by the open arrow in the top left-hand corner). The mean wind velocity is included (the solid arrow below the scale). 30

Figure 5: Weekly mean currents for the summer of 1999 in Placentia Bay at a depth of 45 m. 5(a) Days 108 - 115. 5(b) Days 115 - 122. 5(c) Days 122 - 129. 5(d) Days 129 - 136. The results using covariance analysis are indicated in the figures by the solid axes. The scale for the standard deviation is four times the scale used for the current velocity (indicated by the open arrow in the top left-hand corner). The mean wind velocity is included (the solid arrow below the scale). 31

Figure 5 (continued): Weekly mean currents for the summer of 1999 in Placentia Bay at a depth of 45 m. 5(e) Days 136 - 143. 5(f) Days 143 - 150. 5(g) Days 150 - 157. 5(h) Days 157 - 164. 32

Figure 5 (continued): Weekly mean currents for the summer of 1999 in Placentia Bay at a depth of 45 m. 5(i) Days 164 - 171. 5(j) Days 171 – 178 33

Figure 6: Mean circulation in Placentia Bay at 103 m depth, days 108-170, 1999. The results using covariance analysis are indicated in the figures by the solid axes. The scale for the standard deviation is four times the scale used for the current velocity (indicated by the open arrow in the top left hand corner). The mean wind velocity is included (the solid arrow below the scale). 34

Figure 7: Weekly mean currents for the summer of 1999 in Placentia Bay at a depth of 103 m. 5(a) Days 108 - 115. 5(b) Days 115 - 122. 5(c) Days 122 - 129. 5(d) Days 129 - 136. The results using covariance analysis are indicated in the figures by the solid axes. The scale for the standard deviation is four times the scale used for the current velocity (indicated by the open arrow in the top left hand corner). The mean wind velocity is included (the solid arrow below the scale). 35

Figure 7 (continued): Weekly mean currents for the summer of 1999 in Placentia Bay at a depth of 103 m. 5(e) Days 136 - 143. 5(f) Days 143 - 150. 5(g) Days 150 - 157. 5(h) Days 157 - 164. 36

Figure 7 (continued): Weekly mean currents for the summer of 1999 in Placentia Bay at a depth of 45 m. 5(i) Days 164 - 171. 37

Figure 8: Rotary spectrum for the velocities recorded at mooring M5 for each depth bin. There were 13 degrees of freedom in the rotary spectra calculation. 38

Figure 9: The surface elevation measured at Argentia, current velocities of the along bay component for 24, 60 and 100 m measured at M5, and the magnitude of the wind stress measured at Argentia..... 39

Figure 10: The surface elevation, current velocities of the cross bay component for 32, 56 and 84 m measured at M5, and the magnitude of the wind stress measured at Argentia..... 40

Figure 11: The K_1 tidal ellipses measured at M5. The N-S axis is the cross bay axis, while the E-W axis is the along bay axis. The red line connects the inclination of each ellipse for all depths. 41

Figure 12: The M_2 tidal ellipses measured at M5. The N-S axis is the cross bay axis, while the E-W axis is the along bay axis. The red line connects the inclination of each ellipse for all depths. 42

Figure 13: The subtidal along bay velocity and temperature measured by the ADCP at M5 along with the surface elevation and wind stress measured at Argentia. For the stick plot, wind is presented in the direction towards which the wind is blowing, with North at the top. 43

Figure 14: The subtidal cross bay velocity and temperature measured by the ADCP at M5 along with the surface elevation and wind stress measured at Argentia. For the stick plot, wind is presented in the direction towards which the wind is blowing, with North at the top. 44

Figure 15: The subtidal backscatter intensity and temperature measured by the ADCP at M5 along with the surface elevation and wind stress measured at Argentia. For the stick plot, wind is presented in the direction towards which the wind is blowing, with North at the top. 45

Figure 16: The subtidal along (blue solid line) and cross bay (red dashed line) velocity profiles measured at mooring M5. The standard deviation is included as error bars. 46

Figure 17: The surface elevation, along bay velocity, backscatter intensity, temperature and the wind stress for the hourly sampled data at M5 for Year Day 110 to 124. ... 47

Figure 18: The surface elevation, cross bay velocity, backscatter intensity, temperature and the wind stress for the hourly sampled data at M5 for Year Day 110 to 124. ... 48

Figure 19: The surface elevation, along bay velocity, backscatter intensity, temperature and the wind stress for the hourly sampled data at M5 for Year Day 118 to 124. ... 49

Figure 20: The surface elevation, cross bay velocity, backscatter intensity, temperature and the wind stress for the hourly sampled data at M5 for Year Day 118 to 124. ... 50

Figure 21: The surface elevation, along bay velocity, backscatter intensity, temperature and the wind stress for the hourly sampled data at M5 for Year Day 140 to 145. ... 51

Figure 22: The surface elevation, cross bay velocity, backscatter intensity, temperature and the wind stress for the hourly sampled data at M5 for Year Day 140 to 145. ... 52

Figure 23: The backscatter intensity at M5 at 20 minute intervals for four-day periods from days 110 to 170. The backscatter intensity is in arbitrary dB, while the y-axis is the depth in metres and the x-axis is the time line in Year Day. 53

Figure 24: The along bay component of current velocity (in cm s^{-1}) measured at M5 at 20 minute intervals for selected ranges of Year Day. The y-axis is the depth in metres and the x-axis is the time line in Year Day. Bad data are indicated by the black points in the plots. 54

Figure 25: The cross bay component of current velocity (in cm s^{-1}) measured at M5 at 20 minute intervals for selected ranges of Year Day. The y-axis is the depth in metres and the x-axis is the time line in Year Day. Bad data are indicated by the black points in the plots. 55

Figure 26: Rotary spectrum for the velocities recorded at mooring M6 for each depth bin. There were 13 degrees of freedom in the rotary spectral calculation. 56

Figure 27: The surface elevation measured at Argentia, current velocities of the along bay component for 24, 60 and 100 m at mooring M6, and the magnitude of the wind stress at Argentia. 57

Figure 28: The surface elevation measured at Argentia, current velocities of the cross bay component for 26, 60 and 100 m measured at mooring M6, and the magnitude of the wind stress measured at Argentia. 58

Figure 29: The K_1 tidal ellipses measured at mooring M6. The N-S axis is the cross bay axis, while the E-W axis is the along bay axis. The red line connects the inclination of each ellipse for all depths. 59

Figure 30: The M_2 tidal ellipses measured at mooring M6. The N-S axis is the cross bay axis, while the E-W axis is the along bay axis. The red line connects the inclination of each ellipse for all depths. 60

Figure 31: The subtidal along bay velocity and temperature measured by the ADCP at mooring M6 along with the surface elevation and wind stress measured at Argentia. For the stick plot, wind is presented in the direction towards which the wind is blowing, with North at the top. 61

Figure 32: The subtidal cross bay velocity and temperature measured by the ADCP at mooring M6 along with the surface elevation and wind stress measured at Argentia. For the stick plot, wind is presented in the direction towards which the wind is blowing, with North at the top. 62

Figure 33: The subtidal backscatter intensity and temperature measured by the ADCP at mooring M6 along with the surface elevation and wind stress measured at Argentia. For the stick plot, wind is presented in the direction towards which the wind is blowing, with North at the top. 63

Figure 34: The subtidal along (blue solid line) and cross bay (red dashed line) velocity profiles measured at mooring M6. The standard deviations are indicated by the error bars. 64

Figure 35: The surface elevation, along bay velocity, backscatter intensity, temperature and the wind stress for the hourly sampled data at mooring M6 for Year Day 118 to 124..... 65

Figure 36: The surface elevation, cross bay velocity, backscatter intensity, temperature and the wind stress for the hourly sampled data at mooring M6 for Year Day 118 to 124..... 66

Figure 37: The surface elevation, along bay velocity, backscatter intensity, temperature and the wind stress for the hourly sampled data at mooring M6 for Year Day 140 to 145..... 67

Figure 38: The surface elevation, along bay velocity, backscatter intensity, temperature and the wind stress for the hourly sampled data at mooring M6 for Year Day 140 to 145..... 68

Figure 39: The backscatter intensity at M6 at 20 minute intervals for four-day periods from days 110 to 170. The backscatter intensity is in arbitrary dB, while the y-axis is the depth in metres and the x-axis is the time line in Year Day. 69

Figure 40: The along bay component of current velocity (in cm s^{-1}) measured at M6 at 20 minute intervals for selected ranges of Year Day. The y-axis is the depth in metres and the x-axis is the time line in Year Day. Bad data are indicated by the black points in the plots. 70

Figure 41: The cross bay component of current velocity (in cm s^{-1}) measured at M6 at 20 minute intervals for selected ranges of Year Day. The y-axis is the depth in metres and the x-axis is the time line in Year Day. Bad data are indicated by the black points in the plots. 71

Figure 42: Rotary spectrum for the velocities recorded at Mooring M7 for each depth bin. There were 13 degrees of freedom in the rotary spectra calculation. 72

Figure 43: The surface elevation measured at Argentia, current velocities of the along bay component for 105, 125, and 140 m measured at M7, and the magnitude of the wind stress measured at Argentia. 73

Figure 44: The surface elevation measured at Argentia, current velocities of the cross bay component for 105, 125 and 140 m measured at M7, and the magnitude of the wind stress measured at Argentia..... 74

Figure 45: The subtidal along bay velocity intensity and the temperature measured by the ADCP at M7 along with the surface elevation and the wind stress measured at Argentia. For the stick plot, wind is presented in the direction towards which the wind is blowing, with North at the top. 75

Figure 46: The subtidal cross bay velocity intensity and the temperature measured by the ADCP at M7 along with the surface elevation and the wind stress measured at Argentia. For the stick plot, wind is presented in the direction towards which the wind is blowing, with North at the top. 76

Figure 47: The subtidal backscatter intensity and the temperature measured by the ADCP at M7 along with the surface elevation and the wind stress measured at Argentia. For the stick plot, wind is presented in the direction towards which the wind is blowing, with North at the top. 77

Figure 48: The subtidal along and cross bay velocity profiles measured at M7. The standard deviations are indicated by the error bars. 78

Figure 49: The surface elevation, along bay velocity, backscatter intensity, temperature and the wind stress for year day 140 to 145..... 79

Figure 50: The surface elevation, along bay velocity, backscatter intensity, temperature and the wind stress for year day 140 to 145..... 80

Figure 51: The rotary spectrum of the wind as measured at Argentia. There were 13 degrees of freedom in the rotary spectral calculation. 81

List of Tables

Table 1: Mooring locations and instrument configurations for April to June 1999 deployment. 3

Table 2: Weekly mean current heading and magnitude at mooring M1 12

Table 3: Weekly mean current heading and magnitude at mooring M2 12

Table 4: Weekly mean current heading and magnitude at mooring M3 12

Table 5: Weekly mean current heading and magnitude at mooring M4 13

Table 6: Weekly mean current heading and magnitude at mooring M5 13

Table 7: Weekly mean current heading and magnitude at mooring M6 13

Table 8: Weekly mean current heading and magnitude at mooring M7 14

Table 9: Statistical summary of currents at 20 m, Earth Axes 14

Table 10: Statistical summary of currents at 45-55 m , Earth Axes 14

Table 11: Statistical Summary for Depth Bins from Mooring M5, in Bay co-ordinates. 15

Table 12: Statistical Summary for depth bins at M6, in bay co-ordinates. 16

Table 13: The statistical summary for M7, in bay co-ordinates. 16

Table 14: The tidal constituents at M5, 24 m. 17

Table 15: The tidal constituents at M5, 32 m. 17

Table 16: The tidal constituents at M5, 40 m. 17

Table 17: The tidal constituents at M5, 48 m. 17

Table 18: The tidal constituents at M5, 56 m. 18

Table 19: The tidal constituents at M5, 64 m. 18

Table 20: The tidal constituents at M5, 72 m. 18

Table 21: The tidal constituents at M5, 80 m. 18

Table 22: The tidal constituents at M5, 88 m. 19

Table 23: The tidal constituents at M5, 96 m. 19

Table 24: The tidal constituents at M5, 104 m. 19
Table 25: The tidal constituents at M6, depth 24 m 20
Table 26: The tidal constituents at M6, depth 32 m 20
Table 27: The tidal constituents at M6, depth 40 m 20
Table 28: The tidal constituents at M6, depth 48 m 20
Table 29: The tidal constituents at M6, depth 56 m 21
Table 30: The tidal constituents at M6, depth 64 m 21
Table 31: The tidal constituents at M6, depth 72 m 21
Table 32: The tidal constituents at M6, depth 80 m 21
Table 33: The tidal constituents at M6, depth 88 m 21
Table 34: The tidal constituents at M6, depth 96 m 22
Table 35: The tidal constituents at M6, depth 104 m 22
Table 36: The tidal constituents at M7, 105m 23
Table 37: The tidal constituents at M7, 110m 23
Table 38: The tidal constituents at M7, 115m 23
Table 39: The tidal constituents at M7, 120m 23
Table 40: The tidal constituents at M7, 125m 24
Table 41: The tidal constituents at M7, 130m 24
Table 42: The tidal constituents at M7, 135m 24
Table 43: The tidal constituents at M7, 140m 24

Introduction

Placentia Bay is located between the Avalon and Burin Peninsulas on the island of Newfoundland, Canada. The shoreline has many bays and inlets, and is surrounded by fairly steep cliffs. There are many islands at the head of the bay, with the largest three being Merasheen, Red and Long Islands (indicated by the A, B and C on Figure 1). The centre of the mouth of the bay has a depth of 200 m, while much of the remainder of the bay is roughly 100 m deep. There are several areas with deep channels that run along the longitudinal axis of the Bay (Figure 1). There is heavy ship traffic to and from Argentia, on the eastern side of Placentia Bay, and Come-by-Chance located near the head of the Bay.

Seven current meter moorings were deployed in Placentia Bay during the spring and summer of 1999. The locations of the moorings are shown by the circled Xs in Figure 1, and are summarized in Table 1. Moorings M1, M2, M3, and M4 had InterOcean S4 at depths of 20 and Anderaa RCM7 current meters at 45 or 55 m depth respectively (see Table 1 for the set-up of each mooring). The current meter at 45m depth on mooring M3 malfunctioned and so no data were recovered. Moorings M5, M6, and M7 used Acoustic Doppler Current Profilers (ADCPs) to measure the current velocities. Of these, two were deployed in upward looking mode (M5 and M6) at depths of 110 m, while the third was deployed in downward looking mode (M7) at a depth of 100 m. This downward looking ADCP was configured to detect and measure the velocity of fish; however, it was also intended to observe water currents. The surface elevation was obtained from a meteorological station at Argentia via the MEDS web-site

(www.meds-sdmm.dfo-mpo.gc.ca/meds/Home_e.htm). The wind speed data were from the same location and were obtained from the Atmospheric Environment Services (AES). The wind speeds were converted to wind stress after rotation into the oceanographic convention (winds towards rather than from).

The mooring data are summarized by weekly mean magnitudes and direction in Tables 2 through 8 for moorings M1 through M7. The summary statistics for velocities at each depth oriented in Earth axes are listed in Tables 9 and 10 respectively. In addition, the data are summarized by maximum, minimum, mean, and standard deviation of velocity in along and cross bay axes (referred to as bay co-ordinates from hereon) in Tables 11, 23 and 35 for M5, M6 and M7 respectively. The mean and weekly averaged currents (Figures 2 to 7) reveal a fairly stable cyclonic circulation pattern around the Bay.

Station Information

The eastern side of the bay is a shipping channel, and the mooring locations had to be selected with care to avoid interference with passing ships. We expected to find a cyclonic circulation in the bay, so two moorings with two current meters were deployed on the western and eastern sides of the bay. In addition, two ADCPs were deployed near the large islands to determine the velocity profile around the islands. Finally, a third ADCP was deployed at the head of the bay to provide ancillary data with respect to the circulation around the bay. Table 1 summarizes the mooring location and instrument deployments.

Table 1: Mooring locations and instrument configurations for April to June 1999 deployment.

Station	Latitude (°N)	Longitude (°W)	Bottom depth (m)	Instrument and serial number	Instrument depth (m)
M1	47 11.61	54 42.80	106	S4 – 1555	20.0
				RCM – 10132	55.0
M2	47 09.07	54 34.98	182	S4 – 1556	20.0
				RCM – 10133	55.0
M3	47 02.79	54 18.02	165	S4 – 1557	20.0
				RCM – 10134	45.0
M4	47 01.17	54 12.59	55	S4 – 1558	20.0
				RCM – 10135	45.0
M5	47 24.63	54 24.17	428	ADCP - 718	110.0
M6	47 24.56	54 04.27	304	ADCP - 879	110.0
M7	47 44.57	54 08.31	147	ADCP - 266	140.0

Data Analysis

The data were analysed by computing the mean and weekly circulation at depths of 20 and 55 m for moorings M1 and M2 and at 20 and 45 m M4 to M6. The circulation for M3 is only presented at depth 20 m. The overall mean circulation is shown in Figures 2 and 4 for depths of 20 and 45/55 m respectively, while the overall mean circulation for M7 at depth 103 m is presented in Figure 6. The mean, weekly circulation for these depths are shown in Figures 3, 5 and 7 respectively. Summary statistics of the overall mean and weekly mean are given in Tables 2, 3 and 4. In each figure, the scale for the current velocity is shown by the arrow in the top left-hand corner. In addition to the current velocity, the variance in the current velocity is also quantified in Figures 2 to 7. The magnitude of the variance along perpendicular components is indicated by the axis

drawn at each mooring. The orientation of the set of perpendicular axes was determined using covariance analysis, which maximized the variance along one axis. The scale for the variance is shown by the line below the current scale in the top left hand corner of each figure. The mean wind speed and direction are also indicated on each figure by the solid arrow below the current velocity and variance scales.

In addition to the mean circulation, the data were also analyzed for flow at tidal and sub-tidal frequencies. We determined the along-channel and cross-channel axes through a covariance analysis, which maximized the variance along one component of a set of perpendicular axes. To rotate the co-ordinate system to the axes determined by the covariance analysis required a counter clockwise rotation of 45 ˚ to the Earth axes co-ordinates at M5. The analysis at the mooring required a uniform rotation angle with depth. At M6 however, the mean rotation angle was smaller, and not uniform with depth. To rotate the co-ordinate system to the determined set of axes required counter clockwise rotation of 42 ˚ at 20 m depth and decreased to approximately 35 ˚ for depths greater than 60 m. For consistency, a counter clockwise rotation of 45 ˚ was used for M5, M6, M7 for the remaining analysis (Tables 11 to 43, and Figures 8 to 50). This rotation set the positive x-axis approximately parallel to the axis of the Bay. For the few stick plots of the wind stress measured at Argentia, the wind has not been rotated to along and cross bay co-ordinates.

The surface was located at M5 and M6 by identifying the depth bin with the largest backscatter intensity. Additional bins were discarded based on the shear in the velocity profile. Four depth bins were discarded for M5 and five were discarded for M6. The vertical resolution of the depth bins for the upward looking ADCPs was 4 m. For the

downward looking ADCP at M7, the bottom was located in an identical fashion to the surface location technique used for M5 and M6. The depth of the instrument was then determined from the depth sounding at that mooring location. The resolution for this instrument was set to 1 m depth bins. The backscatter has been corrected for spherical spreading and chemical absorption along the acoustic path, and calibrated to dB (re: 1 μ Pa $Hz^{-1/2}$).

For tidal analysis, we applied the harmonic analysis routines of Foreman (1977) which required the data be sampled at hourly intervals. To this end, the data from M5 and M6 were filtered using a third order low-pass Butterworth filter with a stop band period of 2 hours and a pass band period of 3 hours in order to exclude high frequency fluctuations in the data. The data were then sub-sampled at 1-hour intervals as required by the tidal analysis software. The data from M7 was burst sampled every 10 minutes. Each burst sample consisted of 10 'pings' (the ADCP signal), each taken once per second. This data sampling scheme was chosen to monitor the velocity of fish. The data were averaged into 1-hour ensembles, as required by the tidal analysis software.

Although the length of the data sets allows for the determination of several additional tidal constituents, only five primary constituents are included: MSf, O_1, K_1, M_2, and S_2. The calculation was performed using a Rayleigh scaling of 3 and an observation parameter of 1. Both the axes of the representative tidal-ellipses and the corresponding Greenwich phase describe the main constituents of the tidal currents. The inclination of the ellipse indicates the angle the semi-major axis makes with the positive x-axis (45 ^{o} counter clockwise rotation from Earth axes). A positive value for the length

of the semi-major axis indicates that the current rotates counter clockwise around the tidal ellipse, while a negative value indicates a clockwise rotation.

In addition to the summary information provided from the harmonic analysis, the time series were filtered using a least squares method to remove tidal signals at the MSf, O_1, K_1, M_2 and S_2 frequencies. After this filter was applied, the energy at inertial frequencies was removed using complex demodulation (Emery and Thomson, 1999). The residual of this filter was then low-pass filtered with a third order Butterworth filter set to remove energy at periods shorter than 1.6 days.

Summary of Findings

Mean Circulation

The data for the spring and summer of 1999 indicate a general counter clockwise circulation around Placentia Bay, consistent with the results of Hart et al. (1999). Figures 2 and 4 show the mean circulation over the 70-day period for depths of 20 and 45 m respectively. As expected, the mean magnitude of the currents at 20 m depth are much larger than the deeper currents. For example, from Table 2, the magnitude of the weekly mean current during week 1 at 20 m depth is 11.98 cm s^{-1} while it is 7.80 cm s^{-1} at 55 m for mooring M1. Similar ratios exist for the other weeks, with the exception of weeks 4, 5, and 8 where the current at 20 m is approximately equal to the current at 55 m. Summary statistics for the weekly mean currents are listed for each site in Tables 2 to 8. Similar ratios are observed at each site. Included in these Tables is the standard deviation of the data within each week.

The currents move around the bay in a direction consistent with a topographically steered current, with the shoreline on the right. This is also the expected direction for the

propagation of Kelvin waves (de Young et. al. 1993). Water enters the bay on the eastern side of the mouth, propagates around the bay and leaves at the western side of the mouth of the bay. The only data that contradict this flow pattern are from the ADCP instrument at M6, where the flow is mainly towards the west-northwest at depth 45 m. This may indicate that the deeper current is being steered through the channel between Red Island (indicated by the B in Figure 1) and Long Island (C) instead of propagating around the head of the bay. The flow pattern around the group of islands at the head of the bay is not clear from these data, and may be quite complicated. For instance, when the winds blow to the west in weeks 2 and 6 (see Figures 3b and f) the flow at 20 m depth is through the islands (to the west).

The plots of the weekly mean currents (Figures 3, 5 and 7) show currents which are consistently in the same direction as the overall means (see Figures 2, 4 and 6) with the exception of M6, but vary significantly in their weekly magnitude. For example, the current meter at 20 m depth at mooring M3 recorded weekly means as high as 37.2 cm s^{-1} and as low as 12.6 cm s^{-1} (see Table 4). Comparison of Figures 3a to 3c shows that the magnitude of the currents at moorings M1, M4, M5, M6 all vary from the overall mean (see Tables 2 to 8 for summary statistics).

Tidal Analysis

The summary of the tidal constituents for moorings M5, M6 and M7 are given in Tables 14 to 24, 25 to 35 and 36 to 43 respectively. These results show a consistent trend: the M_2 tidal constituent is the strongest component of the flow for each site. However, there are some significant differences highlighted by comparing these tables. The currents at M7 are weak compared to M5 and M6. The mean flow (Z_0) is stronger at

M5 than at M6 at depths between 20 and 32 m. In addition, the strength of the MSf at M6 becomes stronger than Z_0 for depths below 48 m. This phenomenon is not repeated at M5, indicating that perhaps the flow around the islands is influence at this fortnightly frequency.

Rotary spectral analysis for each mooring was carried out for all measured depths (Figures 8, 26, and 42 for M5, M6 and M7). These results show the large energy at the M_2 and low frequencies. Figure 51 shows the rotary spectrum for the wind stress measured at Argentia. It is clear that there is a weak twice daily variation in the counter clockwise rotation (indicated by the peak at positive 2 cycles per day frequency). The largest energy is at periods of 4 days typical of storms, and also indicated counter clockwise rotation.

Inner and outer coherence squared analysis between the wind stress and the current velocities indicate there is little correlation to the wind stress at each of the moorings. Figures of the coherence squared are not included. Possible correlation exists at frequencies below long periods (0.25 cycles per day counter clockwise rotation) for depths greater than 60 m at M6 and depths less than 40 m at M5. There is no correlation at M7.

Time series plots of the surface elevation, along bay current velocities at selected depths (24, 60 and 100 m for both M5 and M6, and 105, 125 and 140 m for M7) and the wind stress are shown in Figures 9, 27 and 43 for M5, M6 and M7. Similar plots are shown for the cross bay velocity in Figures 10, 28 and 44. Not surprisingly, the M7 data, recorded at greater than 100 m depth, reveal currents much weaker (by roughly a factor of 3) than the surface currents measured at M5 and M6. The time series at the surface for

each site show the effects of the interpolation algorithm used to smooth out bad data. For example, at M5, between year days 160 and 170 there are high frequency fluctuations not present at depth. Likewise, at M6, between year days 140 and 150 there is a similar phenomenon. This is discussed further at the end of this Section.

The K_1 tidal ellipses are shown in Figures 11 and 29 for M5 and M6. The tidal ellipse plots for M7 are not included due to the weak signal at these frequencies. At each mooring, the inclination of the ellipses varies with depth. This variation is likely caused by aliasing of a low frequency signal contaminating the tidal analysis, due to the weak signal at K_1 frequencies. The M_2 tidal ellipses (Figures 12 and 30) show approximately constant strength with increasing depth, and a consistent inclination for each deployment.

Plots of surface elevation, along bay current velocity, temperature and wind stress are shown in Figures 13, 31 and 45 for M5, M6, M7 at sub-tidal frequencies. Similar plots for the cross bay current velocity are shown in Figures 14, 32 and 46 for M5, M6 and M7. The sub-tidal surface elevation is suspect because the 4 day period with no measurements corrupts the filters used to eliminate the tidal and inertial frequencies. To complete the sub-tidal velocity analysis, the mean sub-tidal velocities for each depth bin are shown for along (u) and cross (v) bay co-ordinates in Figures 16, 34 and 48 for M5, M6, M7.

Plots of surface elevation, the backscatter intensity corrected for spherical spreading and chemical absorption, temperature and wind stress (Figures 15, 33, and 47) show trends in the acoustic targets in the water column. At M6, there is a decrease in the overall number of acoustic reflectors. This is a cause of the increased occurrence of bad data which occur more frequently later in the time series at this mooring. The backscatter

from M5 shows a similar trend although the bad data at this mooring showed bad data spread at both the beginning and end of the time series.

Significant differences in the backscatter intensity from each mooring are apparent from the raw unfiltered data. Short period plots of along and cross bay velocities are plotted with backscatter intensity, surface elevation, temperature and wind stress for each deployment. Each deployment shows a diurnal pattern in backscatter intensity; M5 and M6 show an increase in backscatter intensity at the surface during the evening, while M7 shows an increase in backscatter intensity at depth during the day.

Figure 17 and 18 show the along and cross bay velocities for these short period backscatter intensity plots during April 20 to May 4 taken from M5. The evening diurnal migration of zooplankton is indicated by the green bars corresponding to increased backscatter intensity. There was a lack of acoustic scatterers near the surface on April 26th. Figures 19 and 20 show an even shorter period, ranging from April 28th to May 4th. In these figures, the lack of scatterers at mid-depths is apparent by the 75 dB reflections at depths of 50 to 70 m between the green peaks of April 30th and May 1st. Figures 21, and 22 (u, v) show decreased duration in the increased backscatter intensity for May 20th to May 24th.

The short time interval backscatter plots for mooring M6 show similar structure to M5. For April 28th to May 4th there are diurnal peaks in the backscatter intensity (Figures 35 and 36). The along and cross bay velocities show diurnal jets at the depths between 20 and 40 m for April 29th to May 3rd. The diurnal backscatter intensity decreases in duration for May 20th to May 24th (Figure 37 and 38). An example of temporal variability in the diurnal migration of scatters is the high concentrations of scatterers at depths of 20

to 40m and 60 to 100 m on May 22nd. Backscatter intensity plots for May 20th to May 24th at M7 show an inverse diurnal pattern compared to M5 and M6 (see Figures 49 and 50).

To further examine the effect of backscatter intensity, or the abundance of acoustic reflectors, the raw 20 minute time interval backscatter and velocity components are presented over 5 sets of 4 day intervals for M5 (Figures 23, 24 and 25) and M6 (Figures 39, 40 and 41). From these plots, it is apparent that when the backscatter intensity drops below 70 dB, the velocity is undefined. This problem could be corrected by reducing the threshold for the number of good pings per ensemble set for the ADCP at the time of deployment. The mean correlation between the individual beams of the ADCP would then be used as a flag to indicate when the reported velocity may be erroneous.

References

deYoung, B., Otterson, T. and R.. Greatbatch. 1993. The Local and Nonlocal Response of Conception Bay to Wind Forcing. *J. Phys. Ocean.*, **23**, pp. 2636-2649.

Emery, W., and R. Thomson. Data Analysis Methods in Physical Oceanography, 1997, pp. 402-404.

Foreman, M. Manual for Tidal Heights Analysis and Prediction, Pacific Marine Science Report 78-6, Institute of Ocean Science, Patricia Bay, Victoria B.C., (1977).

Hart, D., de Young, B., and Jack Foley. Observations of Currents, Temperature and Salinity in Placentia Bay 1998-9, Physics and Physical Oceanography Data Report 99-3, Memorial University of Newfoundland, St. John's NF, (1999).

Tabulated Results

Summary statistics of weekly mean currents for M1 to M7 in Earth co-ordinates

Table 2: Weekly mean current heading and magnitude at mooring M1

	Depth→	20 m				55 m			
Week	**Days**	**Heading (° T.N.)**	**Std. Dev.**	**Magnitude (cm/s)**	**Std. Dev.**	**Heading (° T.N.)**	**Std. Dev.**	**Magnitude (cm/s)**	**Std. Dev.**
1	108 - 115	235.1	117.5	11.98	10.14	223.4	91.4	7.80	5.78
2	115 - 122	232.5	108.2	17.56	10.14	227.8	86.0	8.13	5.39
3	122 - 129	209.1	77.5	5.83	4.81	215.6	92.5	3.51	4.42
4	129 - 136	243.2	118.5	4.03	8.72	224.8	94.1	4.67	7.15
5	136 - 143	241.1	121.5	4.43	6.28	223.6	106.0	4.29	6.04
6	143 - 150	224.7	106.9	5.43	7.03	239.6	110.3	2.04	5.17
7	150 - 157	231.8	116.8	8.20	7.38	226.4	84.4	5.99	5.39
8	157 - 164	215.9	107.5	5.01	7.20	217.2	81.9	5.50	7.74
9	164 -171	233.9	108.3	8.32	8.19	219.7	93.6	3.98	6.62
10	171 -178	224.8	100.8	5.73	5.88	211.2	96.5	2.11	4.97
Mean		229.2	108.4	7.65	7.58	222.9	93.7	4.80	5.87

Table 3: Weekly mean current heading and magnitude at mooring M2

	Depth →	20 m				55 m			
Week	**Days**	**Heading (° T.N.)**	**Std. Dev.**	**Magnitude (cm/s)**	**Std. Dev.**	**Heading (° T.N.)**	**Std. Dev.**	**Magnitude (cm/s)**	**Std. Dev.**
1	108 - 115	223.0	43.4	12.33	5.53	219.1	100.1	6.48	6.47
2	115 - 122	227.0	96.7	16.41	9.57	219.7	92.7	9.45	7.32
3	122 - 129	222.9	78.0	12.23	9.86	225.5	112.6	3.36	4.82
4	129 - 136	217.7	96.1	7.98	6.11	218.5	112.3	3.86	7.39
5	136 - 143	213.7	19.5	15.89	5.43	210.0	37.4	15.01	8.33
6	143 - 150	207.8	85.0	7.78	5.98	197.9	75.7	9.23	7.69
7	150 - 157	218.4	93.3	7.35	6.28	203.8	100.0	9.82	9.86
8	157 - 164	224.6	90.7	10.39	7.04	211.1	102.4	3.93	8.28
9	164 -171	228.6	89.5	11.94	6.44	216.0	100.1	6.98	8.53
10	171 -178	221.6	81.6	10.86	7.23	197.7	67.4	8.37	6.47
Mean		220.5	77.4	11.32	6.95	211.9	90.1	7.65	7.52

Table 4: Weekly mean current heading and magnitude at mooring M3

	Depth →	20 m			
Week	**Days**	**Heading (° T.N.)**	**Std. Dev.**	**Magnitude (cm/s)**	**Std. Dev.**
1	108 - 115	10.7	15.8	20.67	5.80
2	115 - 122	7.8	16.5	37.23	16.70
3	122 - 129	358.2	25.7	15.76	8.69
4	129 - 136	10.1	33.7	17.18	10.29
5	136 - 143	2.1	42.8	14.96	7.05
6	143 - 150	6.0	52.8	14.23	9.80
7	150 - 157	23.8	40.6	17.62	8.55
8	157 - 164	19.8	39.5	13.83	8.52
9	164 -171	10.5	58.4	15.10	9.80
10	171 -178	354.7	49.1	12.61	7.35
Mean		80.4	37.5	17.92	9.26

Table 5: Weekly mean current heading and magnitude at mooring M4

	Depth →	20 m				45 m			
Week	**Days**	**Heading (° T.N.)**	**Std. Dev.**	**Magnitude (cm/s)**	**Std. Dev.**	**Heading (° T.N.)**	**Std. Dev.**	**Magnitude (cm/s)**	**Std. Dev.**
1	108 - 115	21.7	59.1	16.98	11.00	19.9	31.3	10.84	6.61
2	115 - 122	23.4	68.7	9.57	9.93	29.2	85.7	3.30	7.36
3	122 - 129	3.4	96.7	4.72	9.94	197.8	91.7	0.47	6.65
4	129 - 136	26.6	46.5	16.10	10.50	20.5	74.2	5.99	7.41
5	136 - 143	19.3	67.1	9.08	8.76	31.3	95.1	1.92	5.19
6	143 - 150	19.9	81.9	14.60	17.34	25.5	89.4	3.42	9.59
7	150 - 157	25.9	31.4	17.81	10.50	24.4	84.9	5.22	7.66
8	157 - 164	16.3	92.6	8.36	12.56	25.0	95.1	2.79	9.31
9	164 -171	25.7	66.5	11.65	10.40	25.7	75.7	4.08	6.37
10	171 -178	28.2	96.3	2.70	7.75	38.3	91.9	1.33	4.64
Mean		21.0	70.7	11.16	10.87	43.8	81.5	3.94	7.08

Table 6: Weekly mean current heading and magnitude at mooring M5

	Depth →	20 m				45 m			
Week	**Days**	**Heading (° T.N.)**	**Std. Dev.**	**Magnitude (cm/s)**	**Std. Dev.**	**Heading (° T.N.)**	**Std. Dev.**	**Magnitude (cm/s)**	**Std. Dev.**
1	108 - 115	224.2	54.6	19.17	16.82	222.9	83.9	7.52	5.99
2	115 - 122	232.5	113.1	16.34	18.54	153.6	93.7	0.87	9.12
3	122 - 129	275.1	109.3	0.92	8.20	75.8	76.5	2.48	5.18
4	129 - 136	208.0	91.3	3.52	12.08	204.3	90.6	1.91	6.41
5	136 - 143	230.4	107.9	11.21	13.84	221.4	82.0	6.54	5.06
6	143 - 150	359.4	109.6	2.26	13.74	203.5	98.6	1.19	5.44
7	150 - 157	234.3	104.3	10.83	13.15	134.2	87.6	1.37	6.53
8	157 - 164	230.9	102.4	9.41	16.97	226.0	106.6	4.66	10.35
9	164 -171	237.0	113.5	8.11	14.68	203.9	97.1	2.93	6.62
10	171 -178	267.3	104.9	1.00	10.48	194.6	93.2	2.49	9.64
Mean		249.9	101.1	8.28	6.95	184.0	91.0	3.20	7.03

Table 7: Weekly mean current heading and magnitude at mooring M6

	Depth →	20 m				45 m			
Week	**Days**	**Heading (° T.N.)**	**Std. Dev.**	**Magnitude (cm/s)**	**Std. Dev.**	**Heading (° T.N.)**	**Std. Dev.**	**Magnitude (cm/s)**	**Std. Dev.**
1	108 - 115	349.2	102.8	5.33	20.53	312.8	118.8	7.02	8.45
2	115 - 122	303.9	112.1	3.49	23.90	6.0	89.3	2.44	10.53
3	122 - 129	21.8	66.8	19.35	22.63	269.4	115.4	1.04	4.70
4	129 - 136	17.5	55.8	22.54	22.20	256.5	122.1	3.53	5.84
5	136 - 143	15.8	82.6	15.70	34.25	51.1	100.9	0.61	5.43
6	143 - 150	342.6	96.9	12.65	32.40	302.8	109.8	1.48	4.77
7	150 - 157	6.8	87.8	15.62	36.53	273.6	138.5	4.92	6.09
8	157 - 164	17.3	81.0	24.10	29.75	302.1	116.3	3.07	6.98
9	164 -171	352.6	98.8	13.30	36.60	241.4	114.2	5.30	8.11
10	171 -178	356.7	94.9	11.54	36.95	314.9	122.2	4.45	7.32
Mean		178.4	88.0	14.36	29.57	233.1	114.8	3.39	6.82

Table 8: Weekly mean current heading and magnitude at mooring M7

	Depth →		103 m		
Week	**Days**	**Heading (° T.N.)**	**Std. Dev.**	**Magnitude (cm/s)**	**Std. Dev.**
1	107 - 114	239.3	116.7	2.28	3.74
2	114 - 121	219.3	115.7	3.27	4.91
3	121 - 128	225.2	116.2	2.26	3.48
4	128 - 135	157.3	88.8	2.27	3.18
5	135 - 142	219.1	109.6	1.00	3.28
6	142 - 149	144.5	94.5	1.22	2.79
7	149 - 156	193.3	106.5	0.70	3.30
8	156 - 163	172.5	94.4	2.48	4.24
9	163 -170	310.4	109.4	0.74	3.28
10					
Mean		209.0	105.8	1.80	3.58

Summary Statistics at select depths for M1 to M6 in Earth co-ordinates

Table 9: Statistical summary of currents at 20 m, Earth Axes

Mooring	**Depth (m)**	**Component**	**Mean ($cm\ s^{-1}$)**	**Maximum ($cm\ s^{-1}$)**	**Minimum ($cm\ s^{-1}$)**	**Standard deviation**
M1	20.0	u	-7.55	47.27	0.00	8.62
		v	0.68	24.90	0.00	5.05
M2	20.0	u	-11.24	46.53	0.00	7.65
		v	-0.76	27.20	0.00	5.78
M3	20.0	u	14.39	63.35	0.00	10.63
		v	10.51	50.49	0.00	8.76
M4	20.0	u	10.35	56.61	0.00	11.99
		v	4.36	23.21	0.00	4.95
M5	20.0	u	-7.55	136.05	0.00	15.56
		v	0.92	141.21	0.00	8.78
M6	20.0	u	10.96	78.35	0.00	28.76
		v	8.48	51.41	0.00	15.70

Table 10: Statistical summary of currents at 45-55 m , Earth Axes

Mooring	**Depth (m)**	**Component**	**Mean ($cm\ s^{-1}$)**	**Maximum ($cm\ s^{-1}$)**	**Minimum ($cm\ s^{-1}$)**	**Standard deviation**
M1	55.0	u	-4.81	27.25	0.01	6.26
		v	-0.14	14.74	0.00	3.08
M2	55.0	u	-7.30	40.02	0.00	7.81
		v	-1.92	29.85	0.01	5.43
M4	45.0	u	3.61	42.39	0.00	7.43
		v	1.38	26.12	0.01	4.22
M5	45.0	u	-2.46	42.42	0.00	7.72
		v	-0.73	52.89	0.00	3.84
M6	45.0	u	-1.06	37.55	0.00	6.99
		v	2.50	41.44	0.00	5.08

Summary Statistics in bay co-ordinates for M5, M6 and M7

Table 11: Statistical Summary for Depth Bins from Mooring M5, in Bay co-ordinates

Depth	Component	Mean	Max	Min	Standard Deviation
20	u	-8.08	82.71	0.02	15.28
	v	0.83	84.58	0.00	8.38
28	u	-4.66	63.04	0.00	11.86
	v	0.20	38.27	0.01	6.32
36	u	-2.92	40.42	0.01	9.05
	v	-0.38	35.55	0.00	4.85
44	u	-2.49	32.19	0.03	7.54
	v	-0.75	15.24	0.01	3.43
52	u	-1.96	25.76	0.01	7.20
	v	-1.24	13.31	0.00	3.42
60	u	-1.73	31.37	0.00	7.35
	v	-1.30	13.53	0.00	3.45
68	u	-1.40	23.68	0.02	7.14
	v	-1.17	20.02	0.00	3.37
76	u	-1.12	20.48	0.01	7.17
	v	-1.14	20.14	0.00	3.32
84	u	-0.94	21.59	0.01	7.05
	v	-1.12	16.93	0.01	3.16
92	u	-0.64	20.70	0.00	6.55
	v	-1.06	12.62	0.00	2.82
100	u	-0.47	19.07	0.00	5.96
	v	-1.06	12.93	0.01	2.50

Table 12: Statistical Summary for depth bins at M6, in bay co-ordinates.

Depth	Component	Mean	Max	Min	Standard Deviation
24	u	-0.45	63.00	0.01	9.17
	v	2.26	72.91	0.00	7.94
32	u	-0.62	29.38	0.00	7.55
	v	2.76	35.45	0.01	6.04
40	u	-1.03	27.60	0.00	7.06
	v	2.73	31.49	0.01	5.35
48	u	-1.27	28.66	0.00	6.53
	v	2.11	21.68	0.00	4.75
56	u	-1.25	21.17	0.01	5.62
	v	0.86	12.40	0.00	3.11
64	u	-1.50	18.81	0.01	5.70
	v	1.14	19.60	0.00	4.29
72	u	-1.35	20.81	0.00	5.52
	v	0.94	16.63	0.00	4.25
80	u	-1.21	21.42	0.00	5.37
	v	0.86	16.04	0.00	3.88
88	u	-1.08	20.74	0.00	5.27
	v	0.86	12.85	0.00	3.48
96	u	-1.05	19.65	0.00	5.11
	v	0.93	12.60	0.01	3.13
104	u	-1.13	19.60	0.00	5.24
	v	0.88	12.75	0.00	3.09

Table 13: The statistical summary for M7, in bay co-ordinates.

Depth	Component	Mean	Max	Min	Standard Deviation
104	u	-0.76	19.19	0.00	3.33
	v	-0.56	15.59	0.00	3.59
112	u	-0.72	14.36	0.00	3.42
	v	-0.68	13.60	0.00	3.65
120	u	-0.03	11.47	0.00	3.33
	v	-0.38	14.97	0.01	3.96
128	u	0.44	11.53	0.00	3.45
	v	-0.29	13.35	0.00	3.90
136	u	0.65	14.11	0.00	3.49
	v	-0.06	11.79	0.00	3.79
143	u	-0.08	23.37	0.00	5.66
	v	-0.04	21.86	0.00	5.52

Tidal Constituents measured at M5, in bay co-ordinates

Table 14: The tidal constituents at M5, 24 m.

Name	Frequency	Major Axis (cm s^{-1})	Minor Axis (cm s^{-1})	Inclination	G. Phase
Z_0	0.000000	6.43	0.00	174.1	360
MSf	0.002822	2.58	0.34	176.4	164
O_1	0.038731	1.50	-0.42	127.7	210.5
K_1	0.041781	2.30	-1.14	13.8	216
M_2	0.080511	4.42	-0.81	9.9	206.8
S_2	0.083333	1.37	-0.41	19	325.8

Table 15: The tidal constituents at M5, 32 m.

Name	Frequency	Major Axis (cm s^{-1})	Minor Axis (cm s^{-1})	Inclination	G. Phase
Z_0	0.000000	3.46	0.00	179.6	360
MSf	0.002822	1.18	0.00	5.7	326.7
O_1	0.038731	0.76	-0.14	107.1	203
K_1	0.041781	1.31	-1.18	159	67
M_2	0.080511	3.77	-0.88	17.1	202.7
S_2	0.083333	1.25	-0.59	29.2	321.1

Table 16: The tidal constituents at M5, 40 m.

Name	Frequency	Major Axis (cm s^{-1})	Minor Axis (cm s^{-1})	Inclination	G. Phase
Z_0	0.000000	2.73	0.00	11.4	180
MSf	0.002822	0.78	-0.22	2.7	41.3
O_1	0.038731	0.37	-0.16	0.6	337.1
K_1	0.041781	0.59	-0.47	122.2	65.9
M_2	0.080511	3.96	-0.34	18.5	200.5
S_2	0.083333	1.05	-0.43	34.6	326.9

Table 17: The tidal constituents at M5, 48 m.

Name	Frequency	Major Axis (cm s^{-1})	Minor Axis (cm s^{-1})	Inclination	G. Phase
Z_0	0.000000	2.41	0.00	26	180
MSf	0.002822	0.75	-0.30	158.3	273.7
O_1	0.038731	0.48	0.13	163.4	189.3
K_1	0.041781	0.26	0.01	118.2	43
M_2	0.080511	3.91	-0.21	21.5	202.9
S_2	0.083333	0.96	-0.16	27.7	335.3

Table 18: The tidal constituents at M5, 56 m.

Name	Frequency	Major Axis (cm s^{-1})	Minor Axis (cm s^{-1})	Inclination	G. Phase
Z_0	0.000000	2.13	0.00	37.3	180
MSf	0.002822	1.19	-0.33	168.7	252.2
O_1	0.038731	0.63	0.09	15.6	30.9
K_1	0.041781	0.39	0.12	76.9	25.4
M_2	0.080511	4.16	-0.02	20	197.4
S_2	0.083333	0.96	-0.11	26.4	325.9

Table 19: The tidal constituents at M5, 64 m.

Name	Frequency	Major Axis (cm s^{-1})	Minor Axis (cm s^{-1})	Inclination	G. Phase
Z_0	0.000000	1.79	0.00	40.4	180
MSf	0.002822	1.12	-0.26	172.9	249.7
O_1	0.038731	0.60	-0.28	166.5	210.5
K_1	0.041781	0.15	0.01	41.8	53.5
M_2	0.080511	4.31	0.02	18.3	191.5
S_2	0.083333	1.11	0.01	23.3	324.3

Table 20: The tidal constituents at M5, 72 m.

Name	Frequency	Major Axis (cm s^{-1})	Minor Axis (cm s^{-1})	Inclination	G. Phase
Z_0	0.000000	1.57	0.00	45.5	180
MSf	0.002822	1.24	-0.11	5.3	53.5
O_1	0.038731	0.38	-0.08	8.2	357
K_1	0.041781	0.13	-0.05	167.8	251.3
M_2	0.080511	4.24	-0.04	14.6	188.6
S_2	0.083333	1.29	0.08	14.5	322.1

Table 21: The tidal constituents at M5, 80 m.

Name	Frequency	Major Axis (cm s^{-1})	Minor Axis (cm s^{-1})	Inclination	G. Phase
Z_0	0.000000	1.45	0.00	49.8	180
MSf	0.002822	0.99	-0.03	14.7	33.3
O_1	0.038731	0.33	0.02	42.5	355.9
K_1	0.041781	0.12	0.09	93.5	75.5
M_2	0.080511	4.34	-0.26	11	186.5
S_2	0.083333	1.28	0.00	10.8	316.6

Table 22: The tidal constituents at M5, 88 m.

Name	Frequency	Major Axis (cm s^{-1})	Minor Axis (cm s^{-1})	Inclination	G. Phase
Z_0	0.000000	1.23	0.00	58.2	180
MSf	0.002822	0.78	0.23	37.7	18.2
O_1	0.038731	0.53	-0.07	53.9	3.2
K_1	0.041781	0.30	0.03	38.7	26.2
M_2	0.080511	4.40	-0.38	11.4	186.4
S_2	0.083333	1.26	-0.06	9.3	316.3

Table 23: The tidal constituents at M5, 96 m.

Name	Frequency	Major Axis (cm s^{-1})	Minor Axis (cm s^{-1})	Inclination	G. Phase
Z_0	0.000000	1.16	0.00	64.8	180
MSf	0.002822	0.68	0.33	45	354.8
O_1	0.038731	0.37	-0.16	38.6	355.9
K_1	0.041781	0.44	0.03	20.4	26.9
M_2	0.080511	4.35	-0.34	13.1	187
S_2	0.083333	1.10	-0.10	8.1	314.7
S_2	0.083333	1.09	-0.07	7.9	312.7

Table 24: The tidal constituents at M5, 104 m.

Name	Frequency	Major Axis (cm s^{-1})	Minor Axis (cm s^{-1})	Inclination	G. Phase
Z_0	0.000000	1.11	0.00	71.7	180
MSf	0.002822	0.70	0.40	176.5	112.4
O_1	0.038731	0.14	-0.14	28.1	28.7
K_1	0.041781	0.29	0.02	25.9	31
M_2	0.080511	4.69	-0.55	12.2	186
S_2	0.083333	1.10	-0.02	9.8	314

Tidal Constituents measured at M6, in bay co-ordinates

Table 25: The tidal constituents at M6, depth 24 m

Name	Frequency	Major Axis (cm s^{-1})	Minor Axis (cm s^{-1})	Inclination	G. Phase
Z_0	0.00000000	2.26	0.00	99.8	360
MSf	0.00282193	1.61	1.19	22.6	131
O_1	0.03873065	0.49	-0.17	147.6	322.6
K_1	0.04178075	1.12	-0.35	6.1	132.3
M_2	0.08051140	2.49	-0.51	4.3	347.2
S_2	0.08333334	1.21	-0.25	30.3	94.6

Table 26: The tidal constituents at M6, depth 32 m

Name	Frequency	Major Axis (cm s^{-1})	Minor Axis (cm s^{-1})	Inclination	G. Phase
Z_0	0.00000000	2.76	0.00	101.1	360
MSf	0.00282193	1.92	0.38	18.7	127.4
O_1	0.03873065	0.40	0.31	91.7	9.4
K_1	0.04178075	0.79	0.11	98.8	191.8
M_2	0.08051140	2.94	-0.59	178.2	183.1
S_2	0.08333334	0.90	-0.17	175.5	268.4

Table 27: The tidal constituents at M6, depth 40 m

Name	Frequency	Major Axis (cm s^{-1})	Minor Axis (cm s^{-1})	Inclination	G. Phase
Z_0	0.00000000	2.82	0.00	109.7	360
MSf	0.00282193	1.22	0.34	175.4	309.1
O_1	0.03873065	0.34	0.03	41.6	202.2
K_1	0.04178075	0.84	-0.40	131.3	168.8
M_2	0.08051140	3.33	-0.88	10.8	1.8
S_2	0.08333334	1.13	-0.40	160.9	270.9

Table 28: The tidal constituents at M6, depth 48 m

Name	Frequency	Major Axis (cm s^{-1})	Minor Axis (cm s^{-1})	Inclination	G. Phase
Z_0	0.00000000	2.37	0.00	120.6	360
MSf	0.00282193	1.31	0.70	43	215.8
O_1	0.03873065	0.31	0.26	29.7	163.6
K_1	0.04178075	0.39	-0.27	57.5	218.7
M_2	0.08051140	3.75	-1.02	17.6	1.7
S_2	0.08333334	0.58	-0.18	147.3	270.6

Table 29: The tidal constituents at M6, depth 56 m

Name	Frequency	Major Axis (cm s^{-1})	Minor Axis (cm s^{-1})	Inclination	G. Phase
Z_0	0.00000000	1.98	0.00	135.2	360.0
MSf	0.00282193	2.55	0.57	32.2	228.8
O_1	0.03873065	0.23	0.04	168.4	320.2
K_1	0.04178075	0.67	-0.41	48.6	191.8
M_2	0.08051140	3.42	-0.46	20.4	6.5
S_2	0.08333334	0.50	0.03	25.0	115.1

Table 30: The tidal constituents at M6, depth 64 m

Name	Frequency	Major Axis (cm s^{-1})	Minor Axis (cm s^{-1})	Inclination	G. Phase
Z_0	0.00000000	1.83	0.00	143.1	360
MSf	0.00282193	3.00	0.29	33.8	229.2
O_1	0.03873065	0.12	0.05	25.4	170.4
K_1	0.04178075	0.31	-0.18	58.5	172.5
M_2	0.08051140	3.45	-0.55	19.9	8.6
S_2	0.08333334	0.73	0.03	24.3	120

Table 31: The tidal constituents at M6, depth 72 m

Name	Frequency	Major Axis (cm s^{-1})	Minor Axis (cm s^{-1})	Inclination	G. Phase
Z_0	0.00000000	1.59	0.00	145.1	360
MSf	0.00282193	2.76	0.10	37.8	224.2
O_1	0.03873065	0.25	-0.11	76.6	180.2
K_1	0.04178075	0.38	-0.15	157.5	324.2
M_2	0.08051140	3.32	-0.40	22.6	11.7
S_2	0.08333334	0.92	-0.21	25.7	124.7

Table 32: The tidal constituents at M6, depth 80 m

Name	Frequency	Major Axis (cm s^{-1})	Minor Axis (cm s^{-1})	Inclination	G. Phase
Z_0	0.00000000	1.45	0.00	144.2	360
MSf	0.00282193	2.43	-0.11	44.7	222.7
O_1	0.03873065	0.14	-0.02	83.7	133.4
K_1	0.04178075	0.34	-0.06	7.7	125.6
M_2	0.08051140	3.10	-0.03	23.2	14.1
S_2	0.08333334	0.90	-0.21	19.9	120.7

Table 33: The tidal constituents at M6, depth 88 m

Name	Frequency	Major Axis (cm s^{-1})	Minor Axis (cm s^{-1})	Inclination	G. Phase
Z_0	0.00000000	1.34	0.00	141.2	360
MSf	0.00282193	2.11	0.06	48.4	220.3
O_1	0.03873065	0.22	0.06	57.7	113.5
K_1	0.04178075	0.37	-0.05	165.1	303.5
M_2	0.08051140	3.01	0.09	27.5	21.3
S_2	0.08333334	0.79	-0.04	27.4	128.2

Table 34: The tidal constituents at M6, depth 96 m

Name	Frequency	Major Axis (cm s^{-1})	Minor Axis (cm s^{-1})	Inclination	G. Phase
Z_0	0.00000000	1.36	0.00	138.1	360
MSf	0.00282193	1.86	0.11	50	224.7
O_1	0.03873065	0.20	0.10	131.3	203.6
K_1	0.04178075	0.47	-0.11	169.8	318.5
M_2	0.08051140	2.86	0.26	35.6	29.3
S_2	0.08333334	0.59	0.11	40.4	137.8

Table 35: The tidal constituents at M6, depth 104 m

Name	Frequency	Major Axis (cm s^{-1})	Minor Axis (cm s^{-1})	Inclination	G. Phase
Z_0	0.00000000	1.48	0.00	145.30	360.00
MSf	0.00282193	1.62	0.04	54.70	225.30
O_1	0.03873065	0.12	-0.05	53.30	106.10
K_1	0.04178075	0.40	0.02	167.90	327.80
M_2	0.08051140	2.99	0.24	35.90	31.80
S_2	0.08333334	0.53	0.20	57.50	172.10

Tidal Constituents measured at M7, in bay co-ordinates

Table 36: The tidal constituents at M7, 105m

Name	Frequency	Major Axis (cm s-1)	Minor Axis (cm s-1)	Inclination	G. Phase
Z_0	0.000000	1.14	0.00	24.8	180.0
MSf	0.002822	0.80	0.06	116.1	254.7
O_1	0.038731	0.16	-0.06	89.8	35.3
K_1	0.041781	0.25	0.02	129.8	92.3
M_2	0.080511	1.15	0.05	129.7	9.9
S_2	0.083333	0.56	-0.13	146.8	184.9

Table 37: The tidal constituents at M7, 110m

Name	Frequency	Major Axis (cm s-1)	Minor Axis (cm s-1)	Inclination	G. Phase
Z_0	0.000000	0.87	0.00	37.9	180.0
MSf	0.002822	0.65	0.22	113.2	258.4
O_1	0.038731	0.19	0.06	159.4	328.2
K_1	0.041781	0.44	0.20	145.1	107.7
M_2	0.080511	0.99	0.11	123.2	14.5
S_2	0.083333	0.60	-0.05	164.6	167.5

Table 38: The tidal constituents at M7, 115m

Name	Frequency	Major Axis (cm s-1)	Minor Axis (cm s-1)	Inclination	G. Phase
Z_0	0.000000	0.77	0.00	55.7	180.0
MSf	0.002822	0.55	0.12	130.2	278.1
O_1	0.038731	0.28	-0.11	127.6	105.0
K_1	0.041781	0.17	-0.04	154.8	80.1
M_2	0.080511	0.95	0.27	129.3	5.9
S_2	0.083333	0.71	-0.07	147.1	189.4

Table 39: The tidal constituents at M7, 120m

Name	Frequency	Major Axis (cm s-1)	Minor Axis (cm s-1)	Inclination	G. Phase
Z_0	0.000000	0.34	0.00	85.7	180.0
MSf	0.002822	0.45	-0.03	116.1	267.5
O_1	0.038731	0.20	0.05	70.2	138.1
K_1	0.041781	0.37	-0.07	116.0	54.9
M_2	0.080511	0.81	-0.06	128.5	16.0
S_2	0.083333	0.45	-0.34	74.5	220.3

Table 40: The tidal constituents at M7, 125m

Name	Frequency	Major Axis (cm s-1)	Minor Axis (cm s-1)	Inclination	G. Phase
Z_0	0.000000	0.36	0.00	132.8	180.0
MSf	0.002822	0.53	-0.19	125.2	259.8
O_1	0.038731	0.39	0.02	34.3	190.2
K_1	0.041781	0.52	-0.06	124.3	87.1
M_2	0.080511	1.02	0.12	132.9	20.7
S_2	0.083333	0.61	-0.14	124.9	126.3

Table 41: The tidal constituents at M7, 130m

Name	Frequency	Major Axis (cm s-1)	Minor Axis (cm s-1)	Inclination	G. Phase
Z_0	0.000000	0.62	0.00	155.1	180.0
MSf	0.002822	0.54	-0.13	128.4	269.0
O_1	0.038731	0.16	0.07	171.2	220.1
K_1	0.041781	0.53	0.08	152.3	53.3
M_2	0.080511	1.04	0.06	146.9	34.7
S_2	0.083333	0.40	0.11	128.0	105.1

Table 42: The tidal constituents at M7, 135m

Name	Frequency	Major Axis (cm s-1)	Minor Axis (cm s-1)	Inclination	G. Phase
Z_0	0.000000	0.55	0.00	156.7	180.0
MSf	0.002822	0.27	-0.08	153.6	226.5
O_1	0.038731	0.18	-0.01	24.6	294.6
K_1	0.041781	0.39	-0.10	170.0	68.3
M_2	0.080511	1.16	0.08	140.2	17.7
S_2	0.083333	0.40	0.18	115.8	126.4

Table 43: The tidal constituents at M7, 140m

Name	Frequency	Major Axis (cm s-1)	Minor Axis (cm s-1)	Inclination	G. Phase
Z_0	0.000000	0.41	0.00	178.4	180.0
MSf	0.002822	0.27	-0.10	145.8	244.5
O_1	0.038731	0.40	0.07	39.3	207.8
K_1	0.041781	0.46	-0.08	171.0	46.9
M_2	0.080511	1.43	0.12	143.8	17.3
S_2	0.083333	0.40	0.01	125.4	128.2

Figures

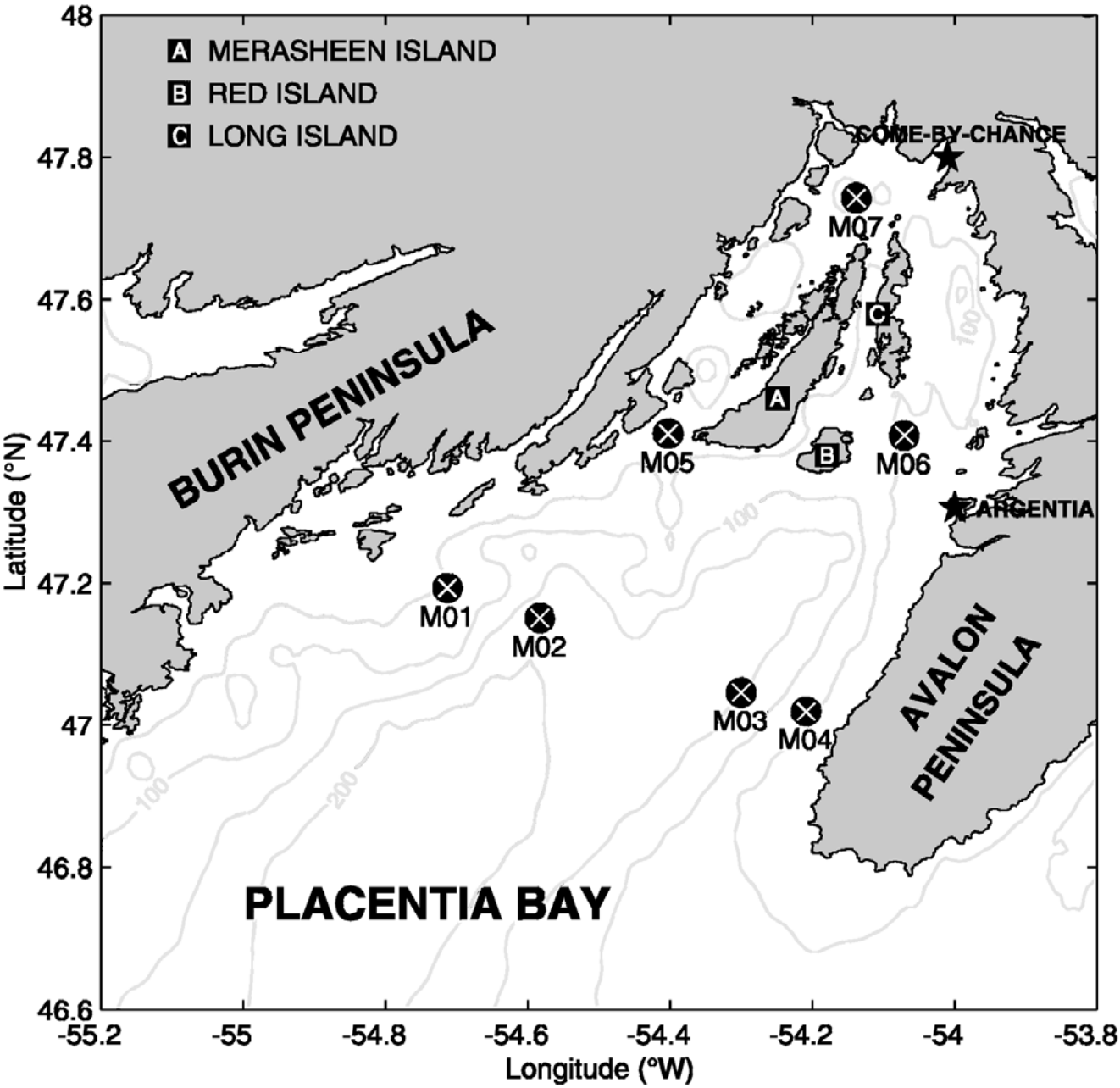

Figure 1: Map of Placentia Bay, showing mooring placements used in the spring and summer of 1999. The moorings were in place from April to July 1999. Tidal height and wind information were obtained for Argentia.

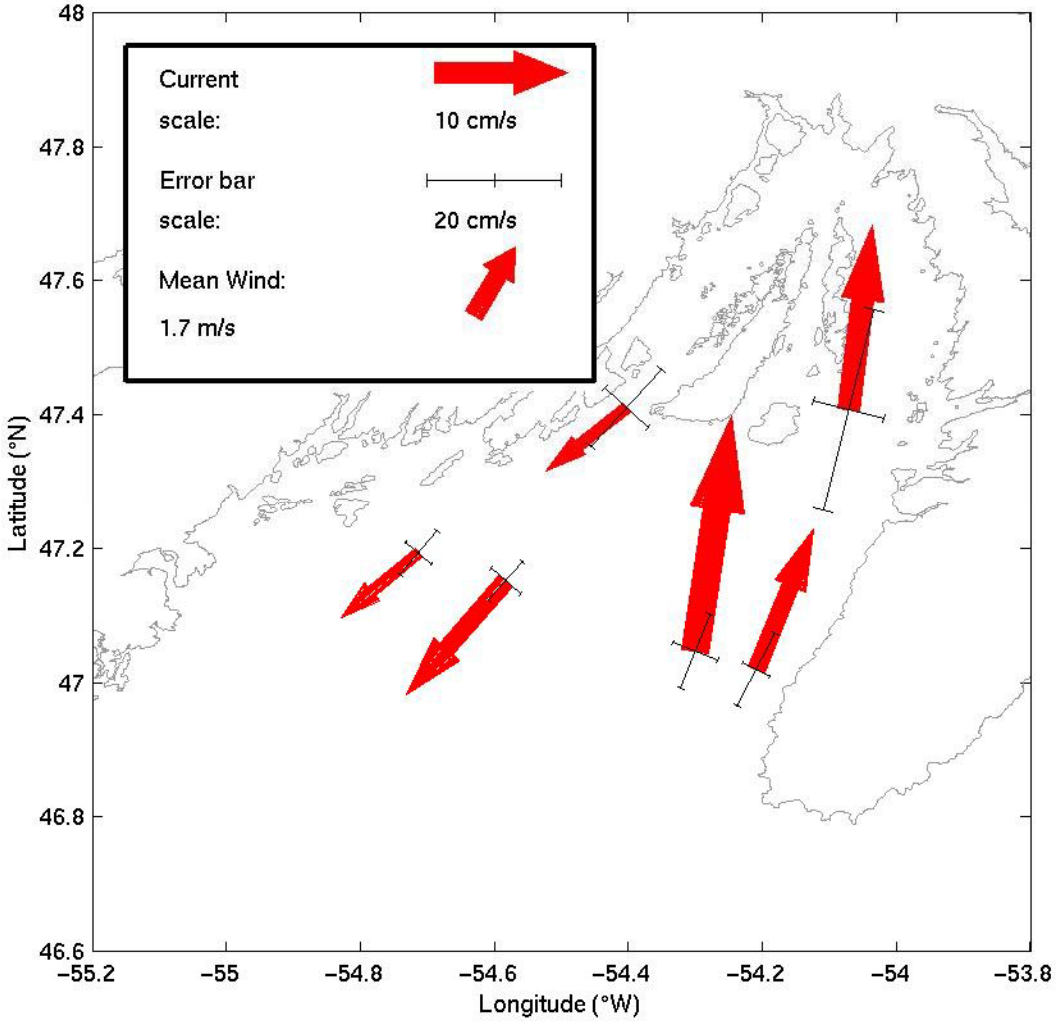

Figure 2: Mean circulation at a depth of 20 m. Days 108 – 178, 1999. The results of covariance analysis are indicated in the figures by the solid axes. These axes show the standard deviation of the current along the direction of maximum variance and perpendicular to it. The scales for the current velocity (open arrow) and the variance (solid line) are included in the left-hand corner. The mean wind velocity is included (solid arrow) with the scales.

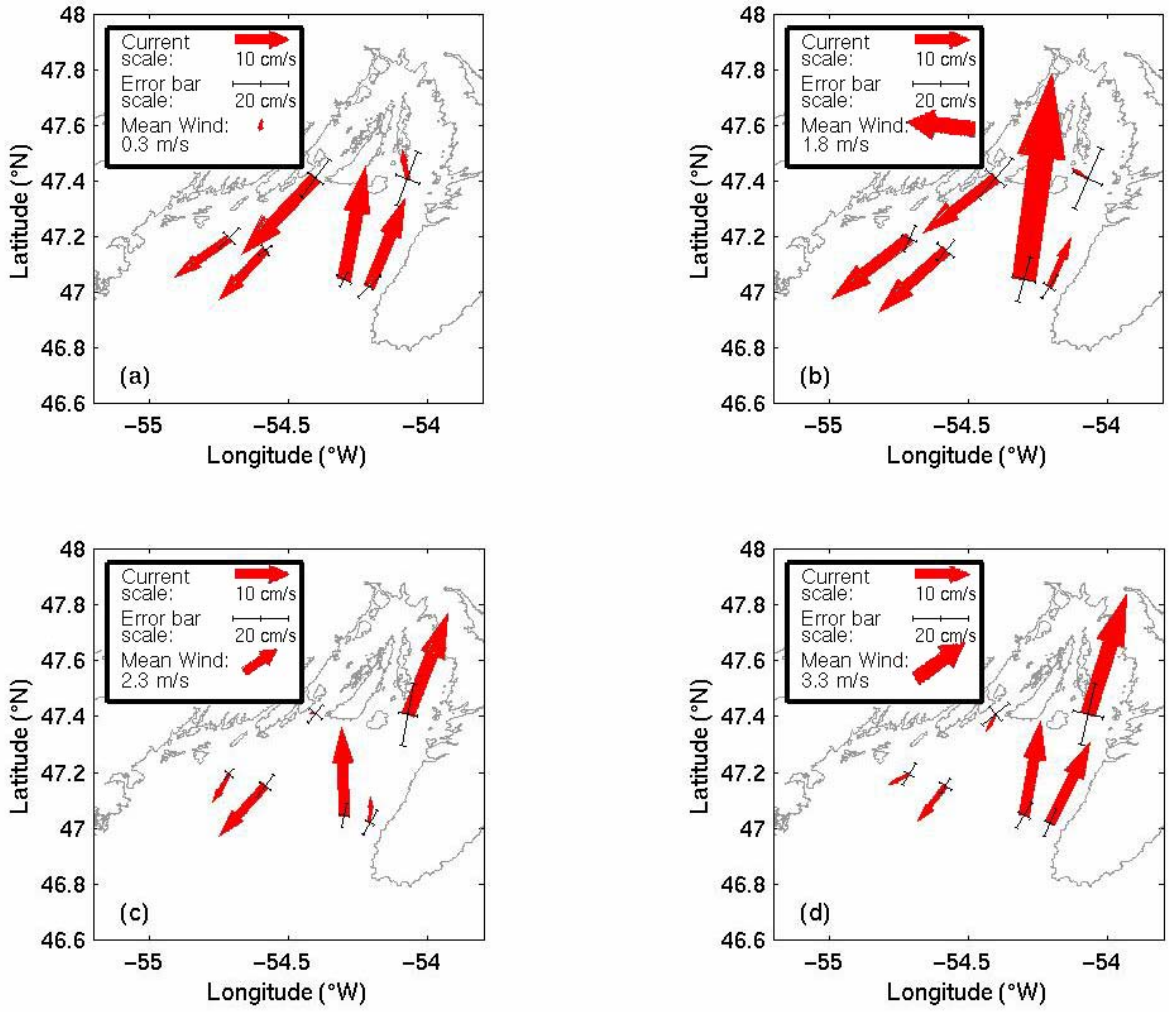

Figure 3: Weekly mean currents for the spring and summer of 1999 in Placentia Bay at a depth of 20 m. 3(a) Days 108 - 115. 3(b) Days 115 - 122. 3(c) Days 122 - 129. 3(d) Days 129 - 136. The results using covariance analysis are indicated in the figures by the solid axes. The scales for the current velocity (open arrow) and the variance (solid line) are included in the left-hand corner. The mean wind velocity is included (solid arrow) with the scales.

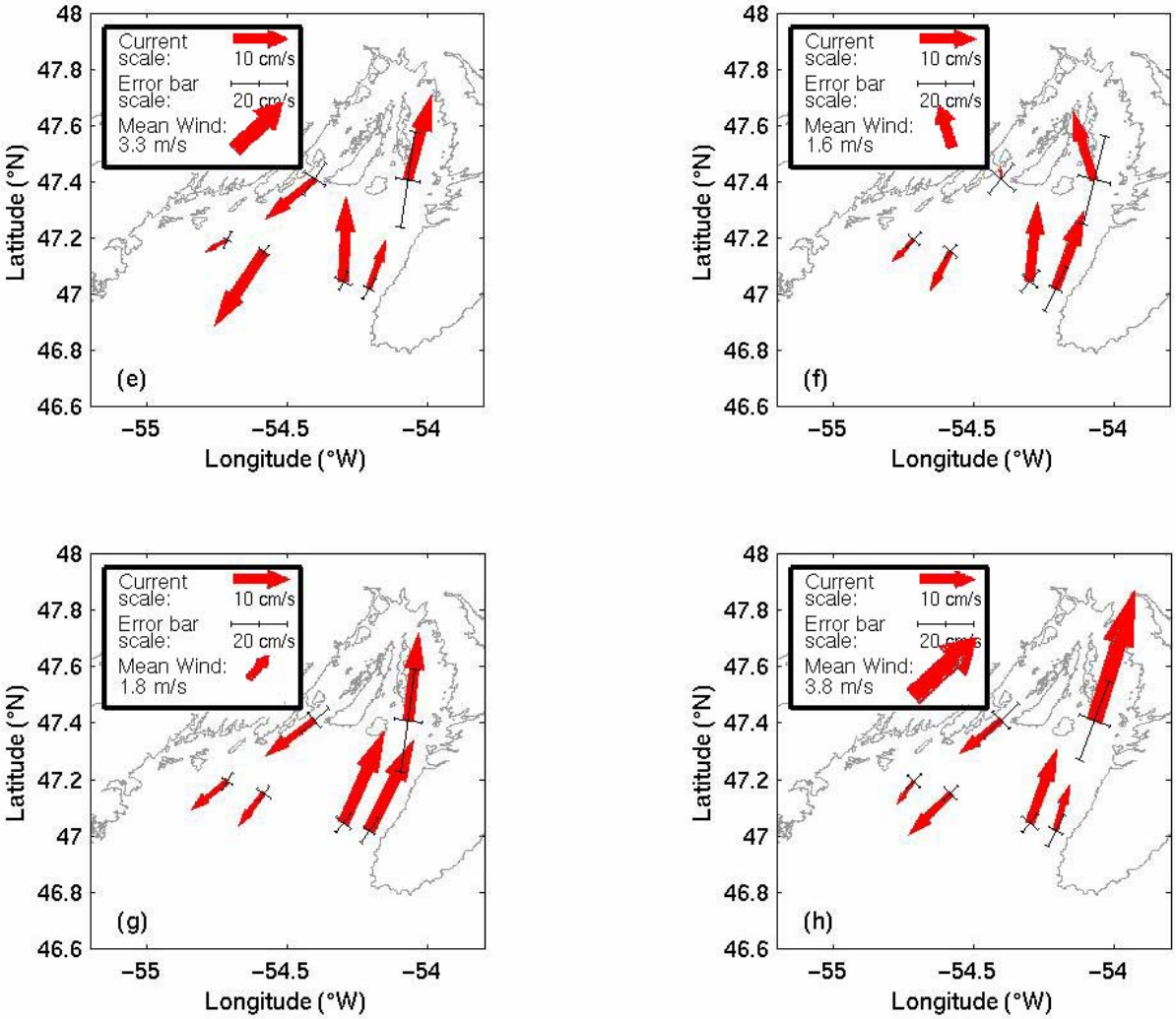

Figure 3 (continued). Weekly mean currents for the spring and summer of 1999 in Placentia Bay at a depth of 20 m. 3(e) Days 136 - 143. 3(f) Days 143 - 150. 3(g) Days 150 - 157. 3(h) Days 157 - 164.

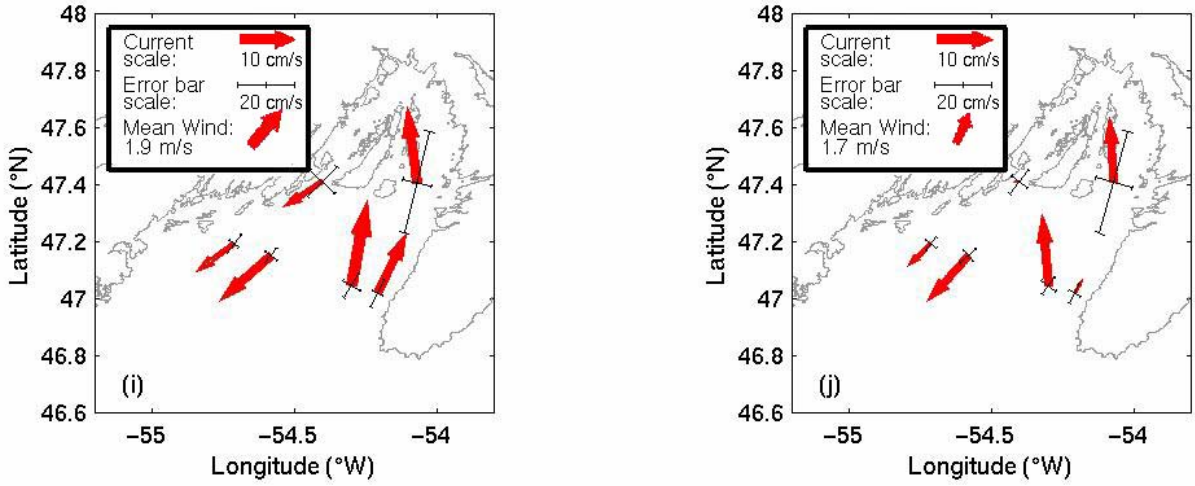

Figure 3 (continued). Weekly mean currents for the spring and summer of 1999 in Placentia Bay at a depth of 20 m. 3(i) Days 164 - 171. 3(j) Days 171 - 178.

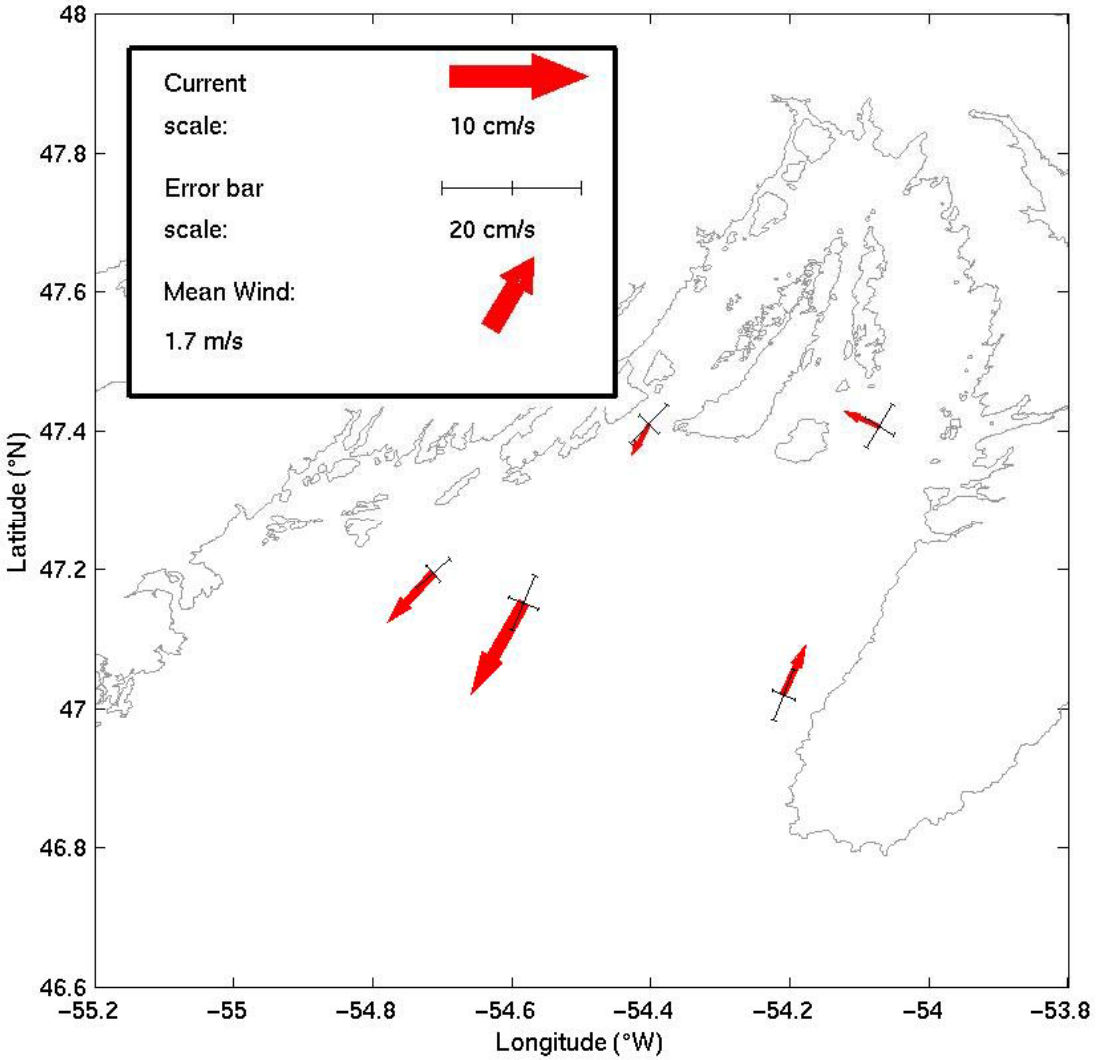

Figure 4: Mean circulation in Placentia Bay at depths of 45–55m. Days 108-178, 1999. The results using covariance analysis are indicated in the figures by the solid axes. The scales for the current velocity (open arrow) and the variance (solid line) are included in the left-hand corner. The mean wind velocity is included (solid arrow) with the scales.

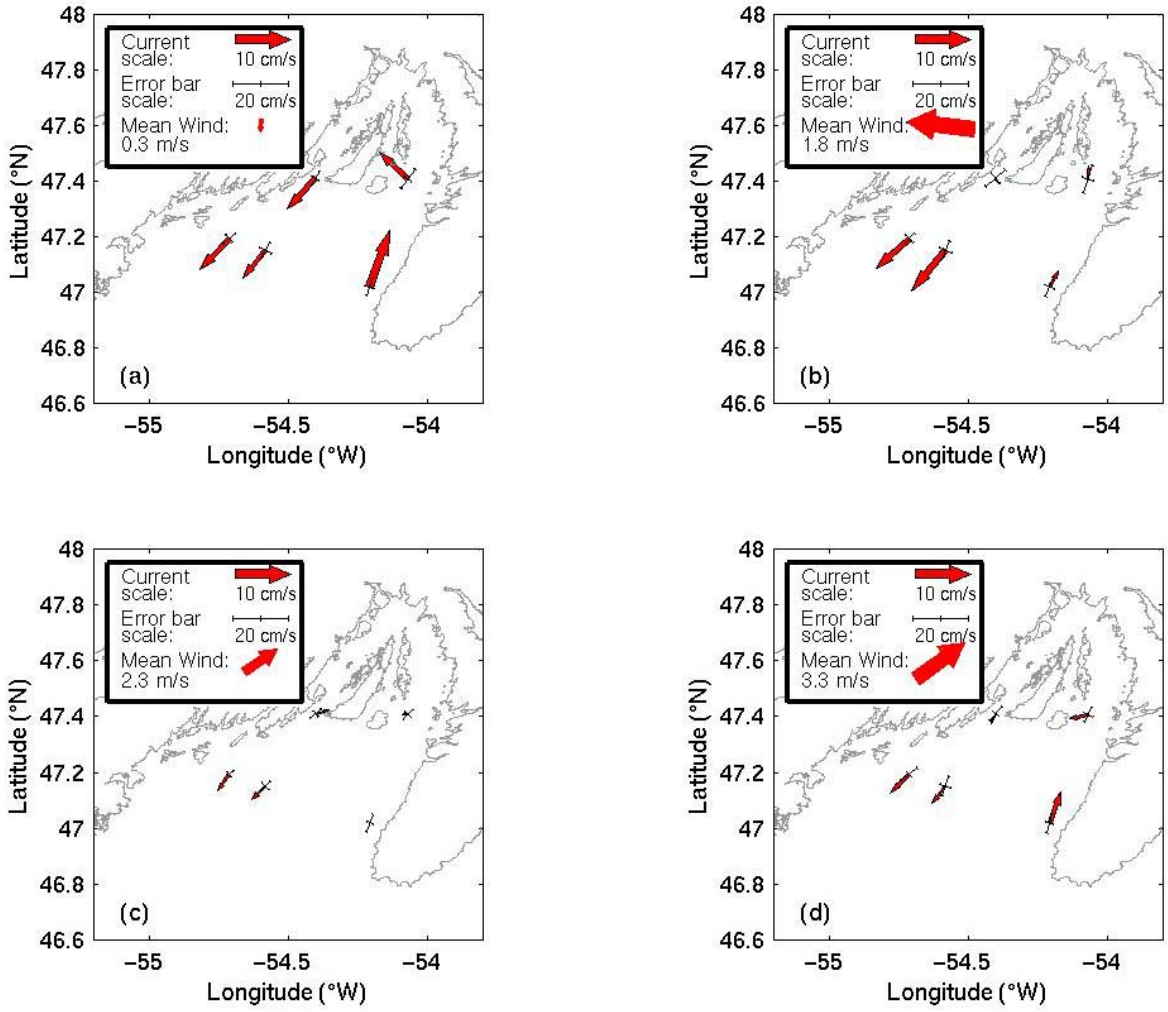

Figure 5: Weekly mean currents for the spring and summer of 1999 in Placentia Bay at a depth of 45 m. 5(a) Days 108 - 115. 5(b) Days 115 - 122. 5(c) Days 122 - 129. 5(d) Days 129 - 136. The results using covariance analysis are indicated in the figures by the solid axes. The scales for the current velocity (open arrow) and the variance (solid line) are included in the left-hand corner. The mean wind velocity is included (solid arrow) with the scales.

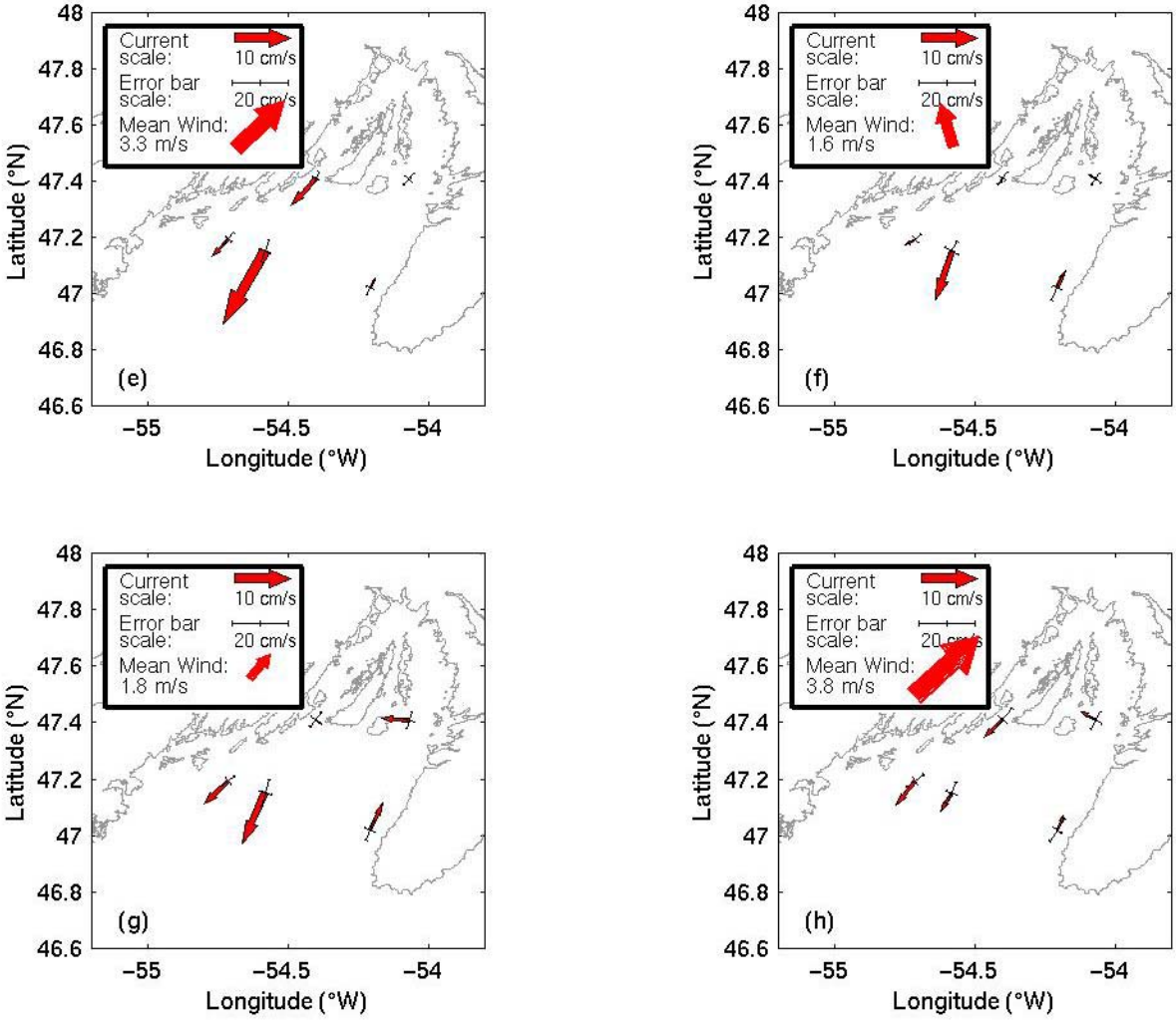

Figure 5 (continued): Weekly mean currents for the spring and summer of 1999 in Placentia Bay at a depth of 45 m. 5(e) Days 136 - 143. 5(f) Days 143 - 150. 5(g) Days 150 - 157. 5(h) Days 157 - 164.

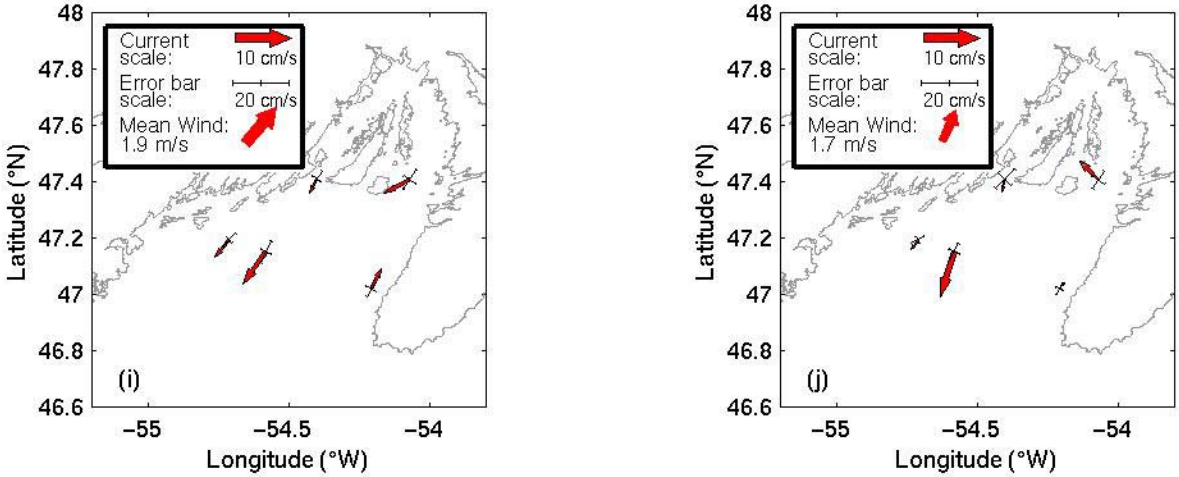

Figure 5 (continued): Weekly mean currents for the spring and summer of 1999 in Placentia Bay at a depth of 45 m. 5(i) Days 164 - 171. 5(j) Days 171 – 178

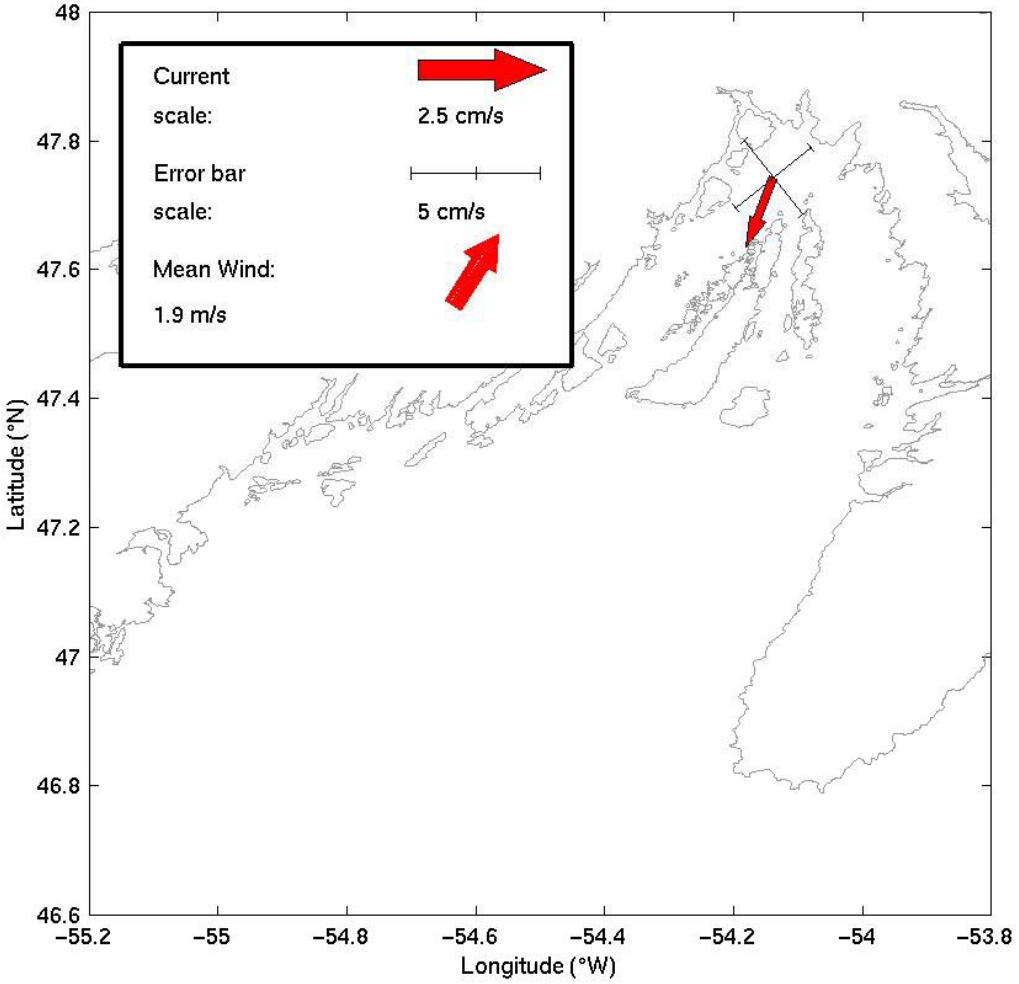

Figure 6: Mean circulation in Placentia Bay at 103 m depth, days 108-170, 1999. The results using covariance analysis are indicated in the figures by the solid axes. The scales for the current velocity (open arrow) and the variance (solid line) are included in the left-hand corner. The mean wind velocity is included (solid arrow) with the scales.

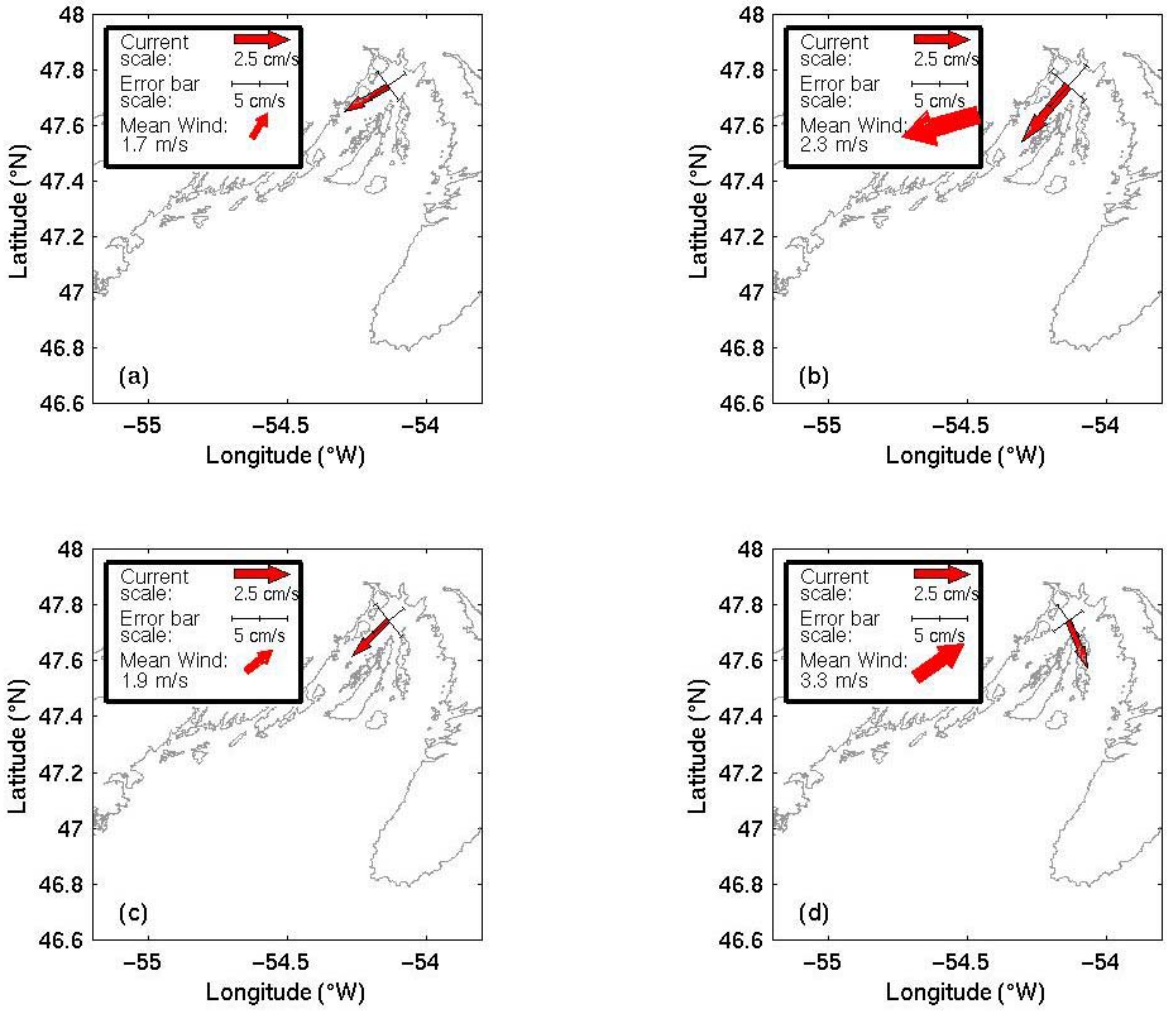

Figure 7: Weekly mean currents for the spring and summer of 1999 in Placentia Bay at a depth of 103 m. 5(a) Days 108 - 115. 5(b) Days 115 - 122. 5(c) Days 122 - 129. 5(d) Days 129 - 136. The results using covariance analysis are indicated in the figures by the solid axes. The scales for the current velocity (open arrow) and the variance (solid line) are included in the left-hand corner. The mean wind velocity is included (solid arrow) with the scales.

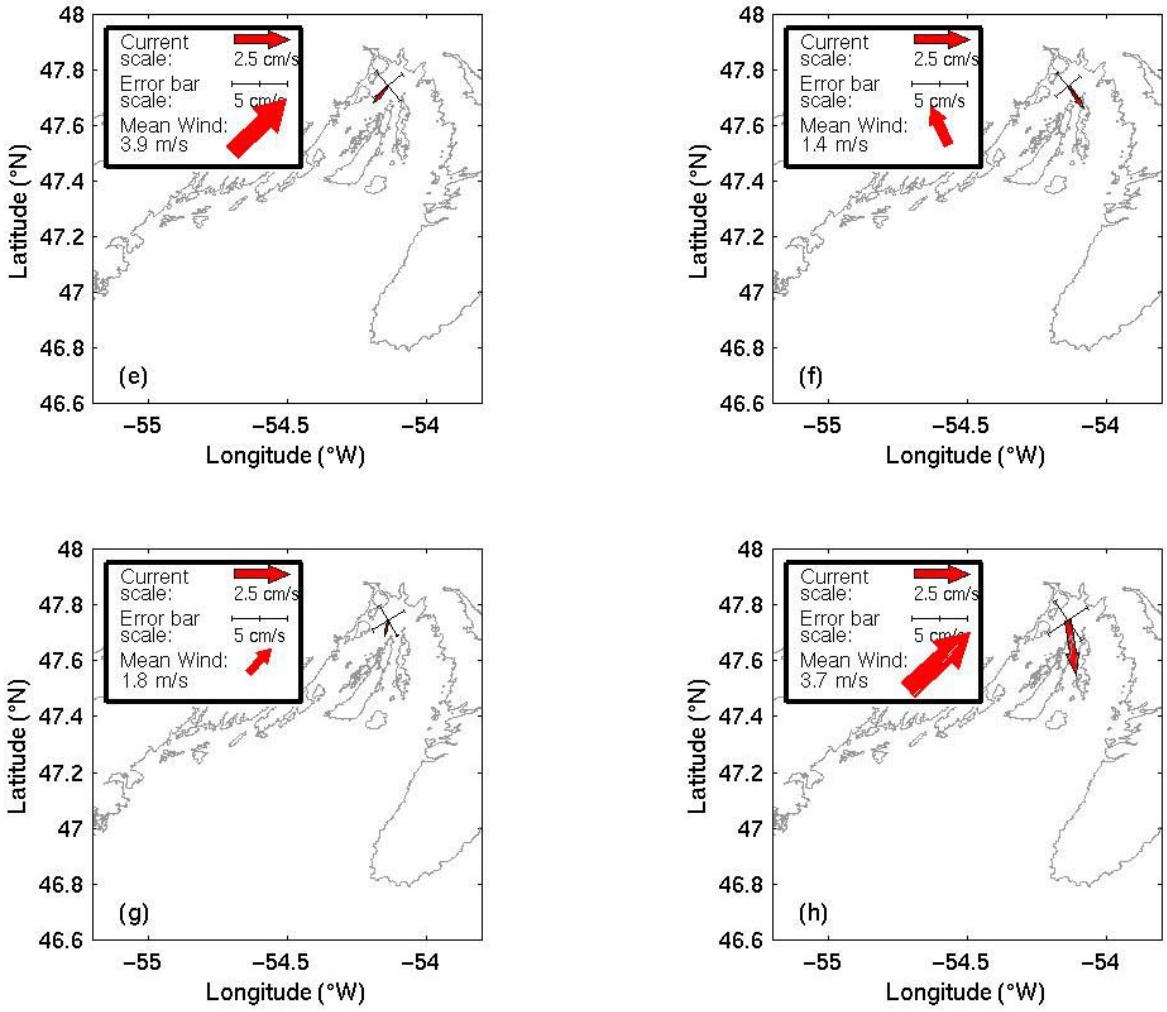

Figure 7 (continued): Weekly mean currents for the spring and summer of 1999 in Placentia Bay at a depth of 103 m. 5(e) Days 136 - 143. 5(f) Days 143 - 150. 5(g) Days 150 - 157. 5(h) Days 157 - 164.

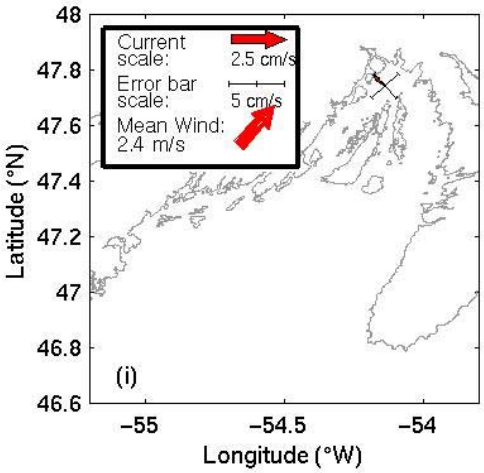

Figure 7 (continued): Weekly mean currents for the spring and summer of 1999 in Placentia Bay at a depth of 45 m. 5(i) Days 164 - 171.

Results from Mooring M5, in bay co-ordinates

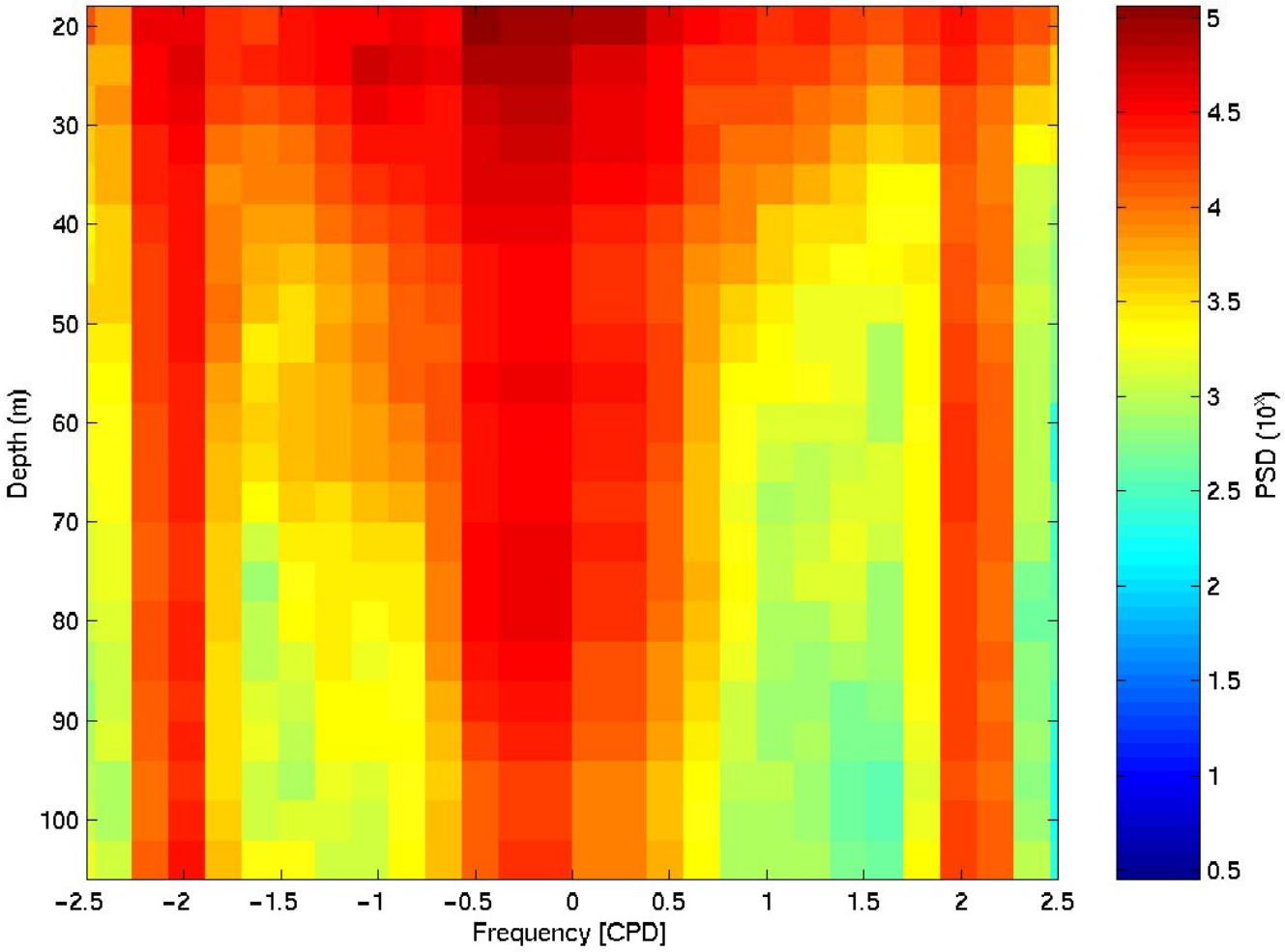

Figure 8: Rotary spectrum for the velocities recorded at mooring M5 for each depth bin. There were 13 degrees of freedom in the rotary spectra calculation.

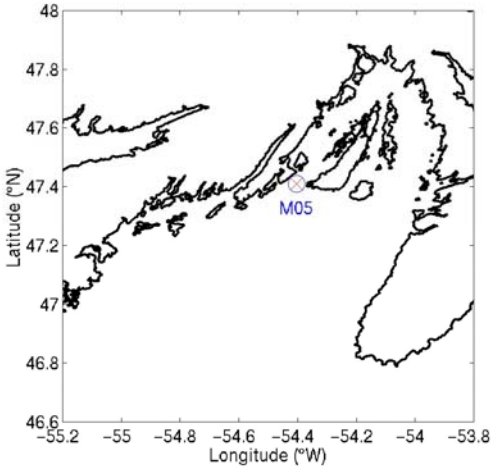

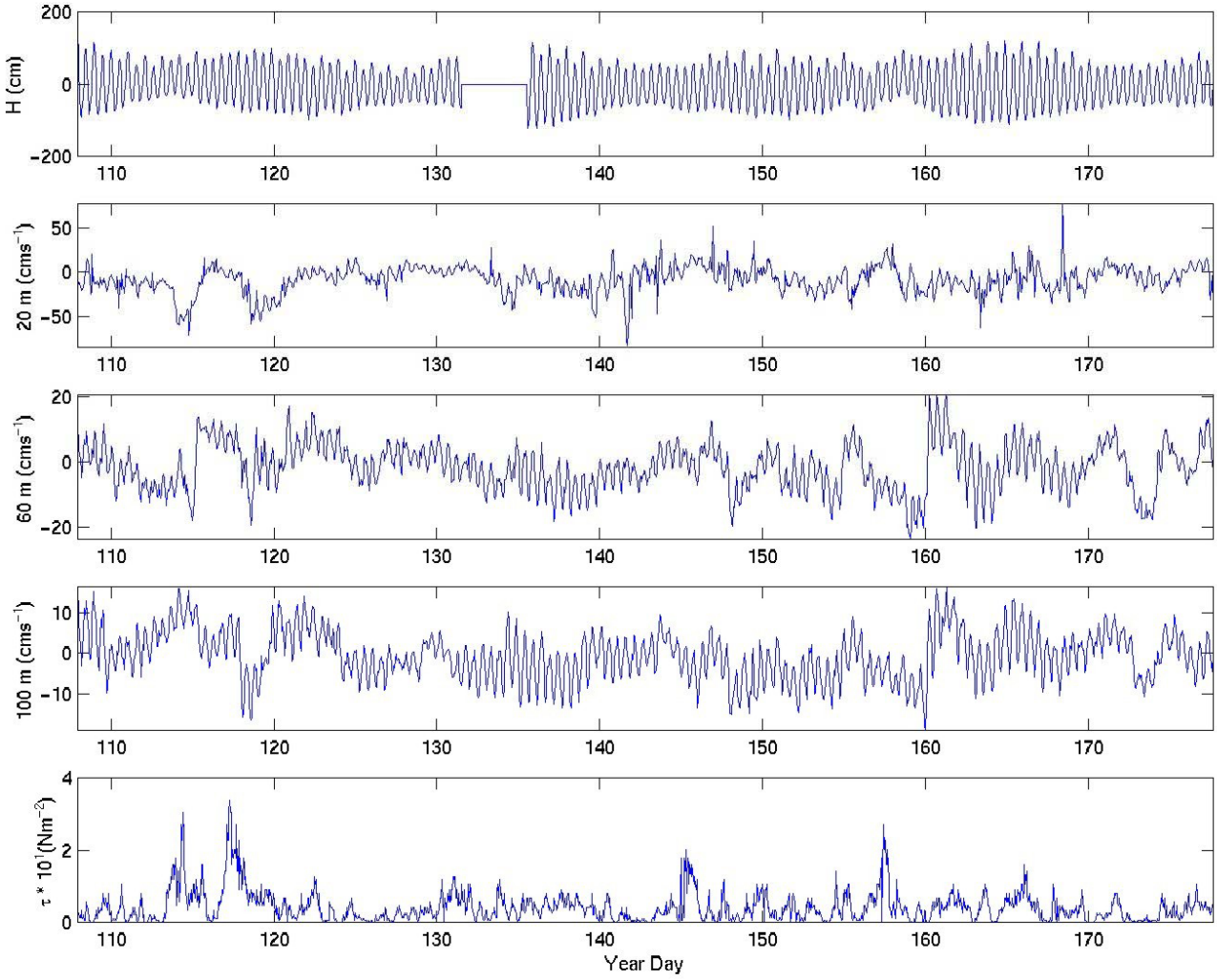

Figure 9: The surface elevation measured at Argentia, current velocities of the along bay component for 24, 60 and 100 m measured at M5, and the magnitude of the wind stress measured at Argentia.

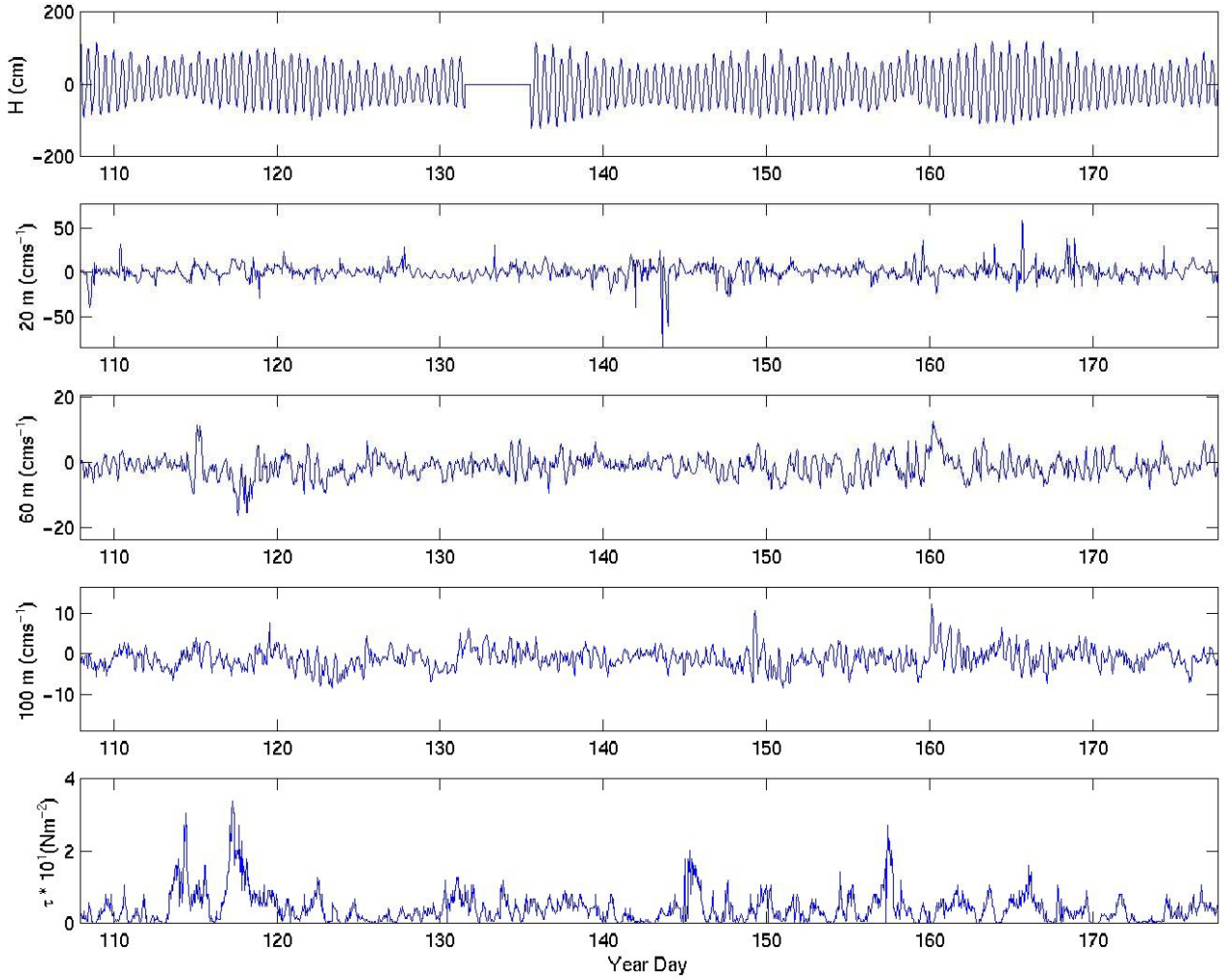

Figure 10: The surface elevation, current velocities of the cross bay component for 32, 56 and 84 m measured at M5, and the magnitude of the wind stress measured at Argentia.

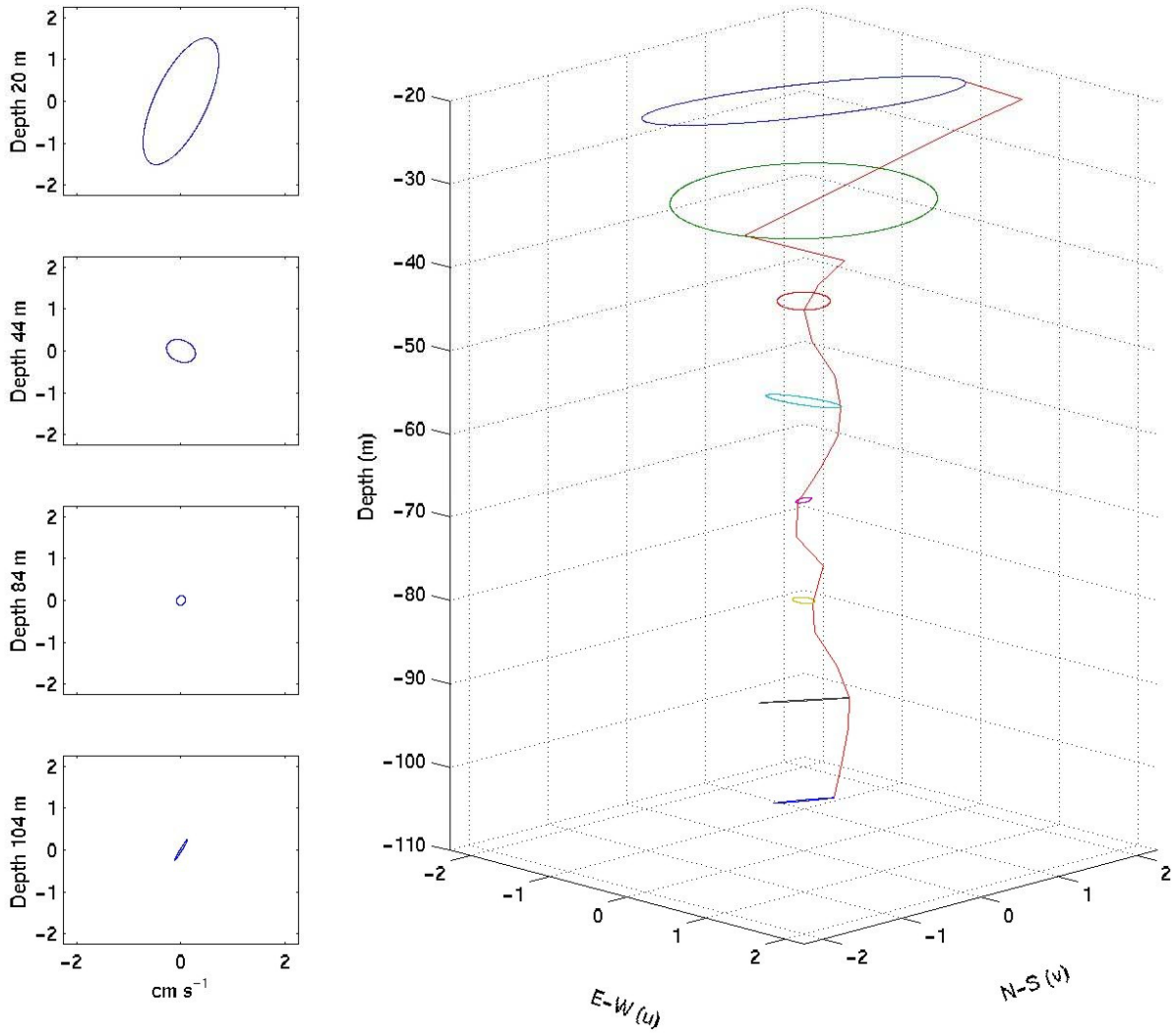

Figure 11: The K_1 tidal ellipses measured at M5. The N-S axis is the cross bay axis, while the E-W axis is the along bay axis. The red line connects the inclination of each ellipse for all depths.

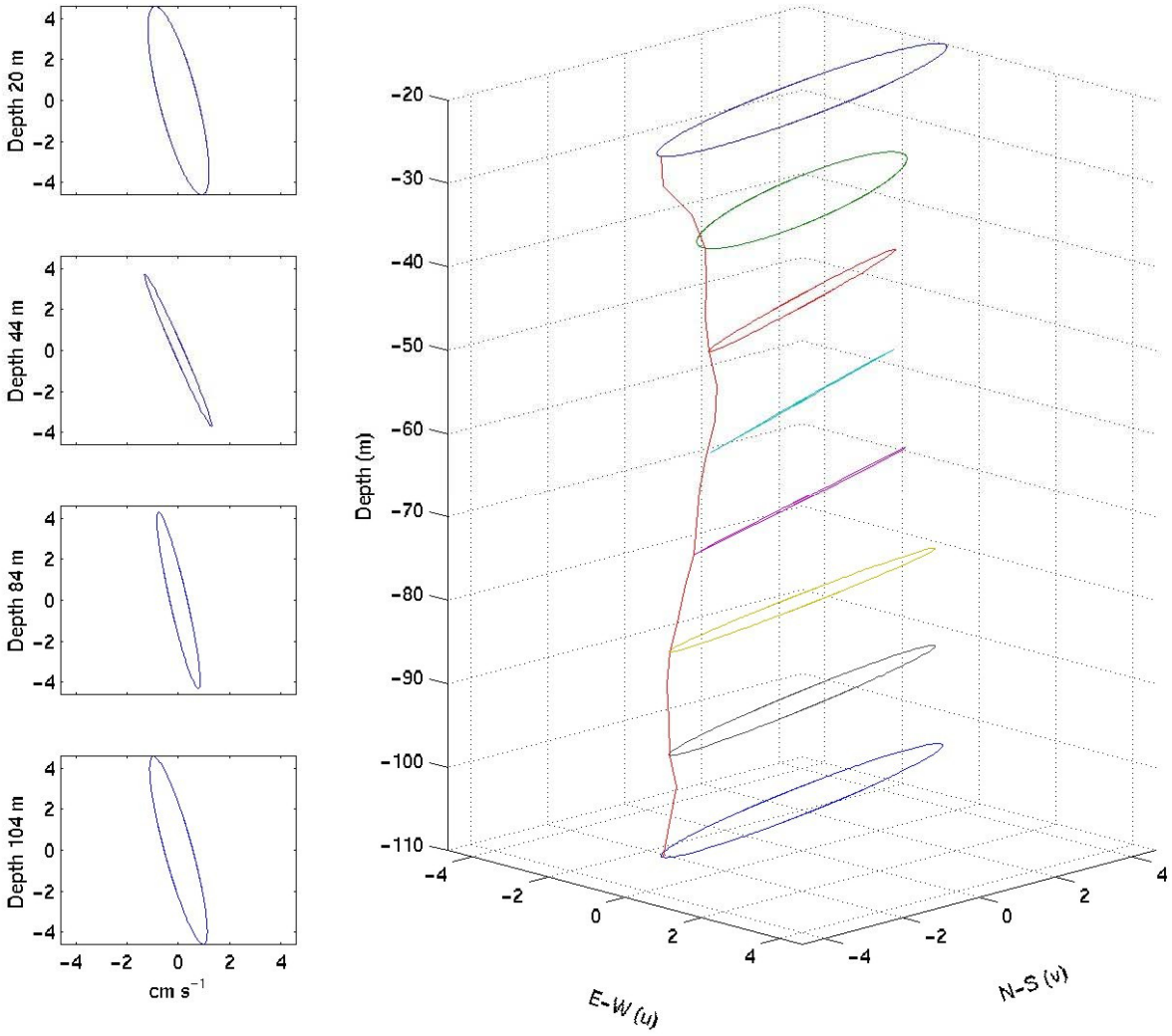

Figure 12: The M_2 tidal ellipses measured at M5. The N-S axis is the cross bay axis, while the E-W axis is the along bay axis. The red line connects the inclination of each ellipse for all depths.

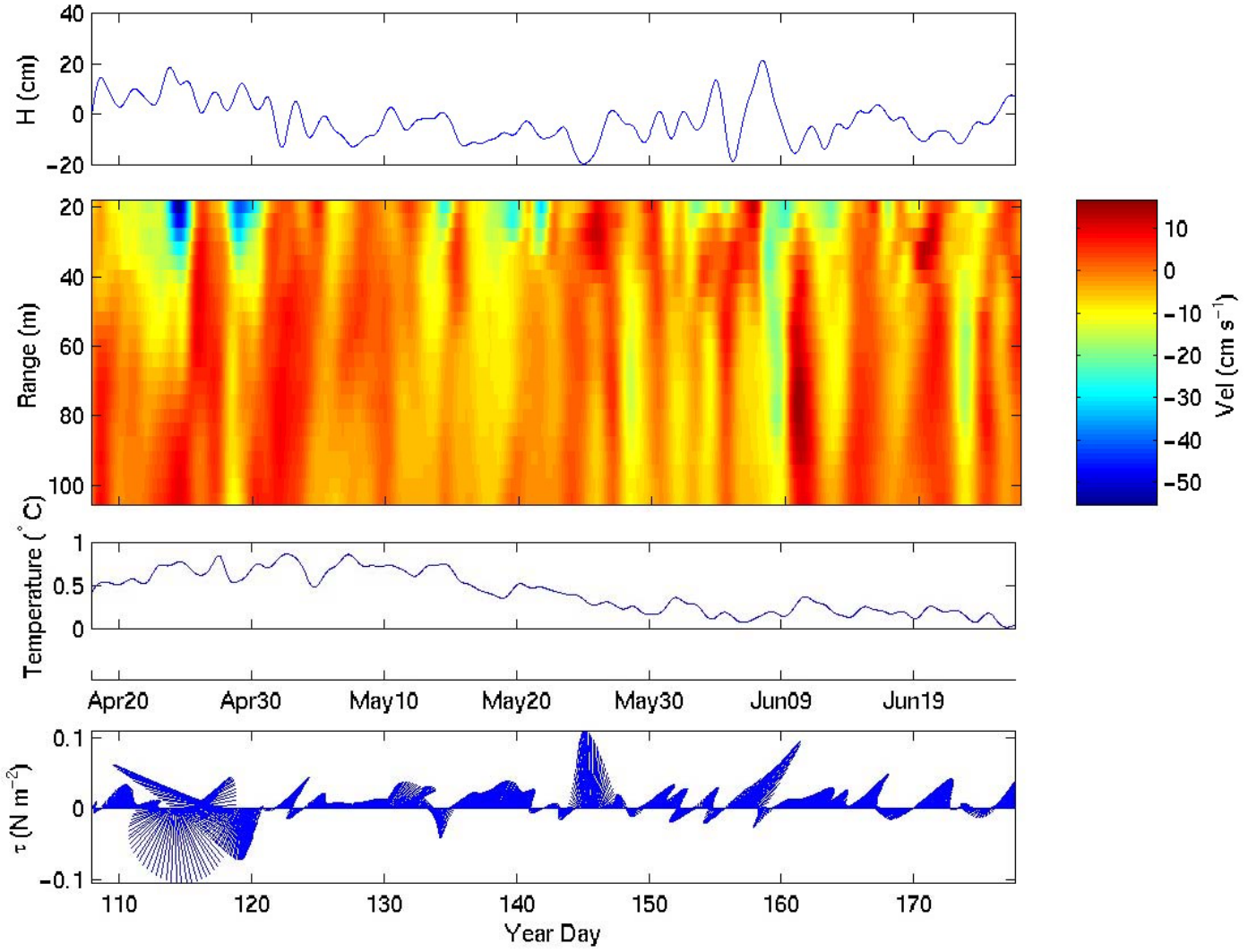

Figure 13: The subtidal along bay velocity and temperature measured by the ADCP at M5 along with the surface elevation and wind stress measured at Argentia. For the stick plot, wind is presented in the direction towards which the wind is blowing, with North at the top.

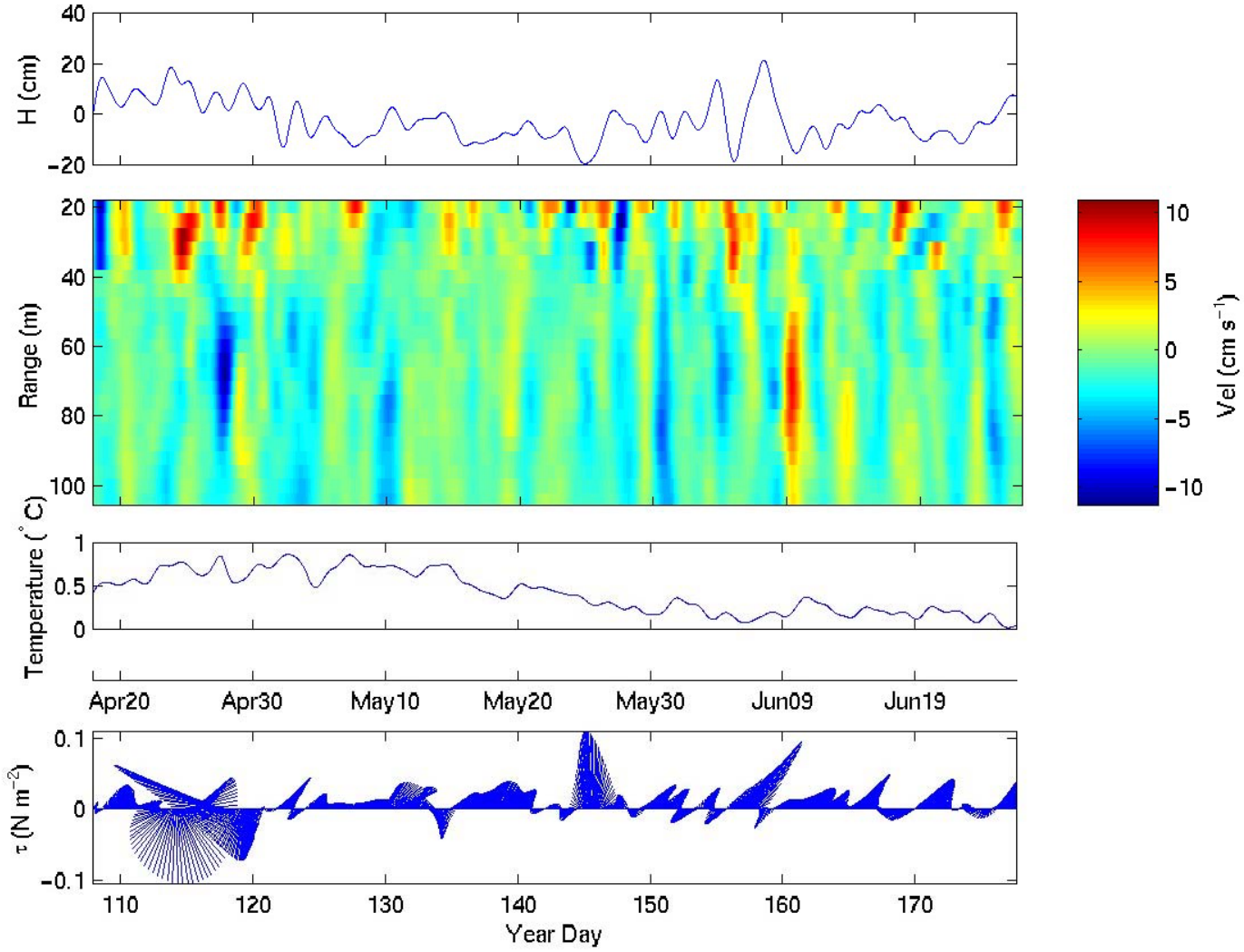

Figure 14: The subtidal cross bay velocity and temperature measured by the ADCP at M5 along with the surface elevation and wind stress measured at Argentia. For the stick plot, wind is presented in the direction towards which the wind is blowing, with North at the top.

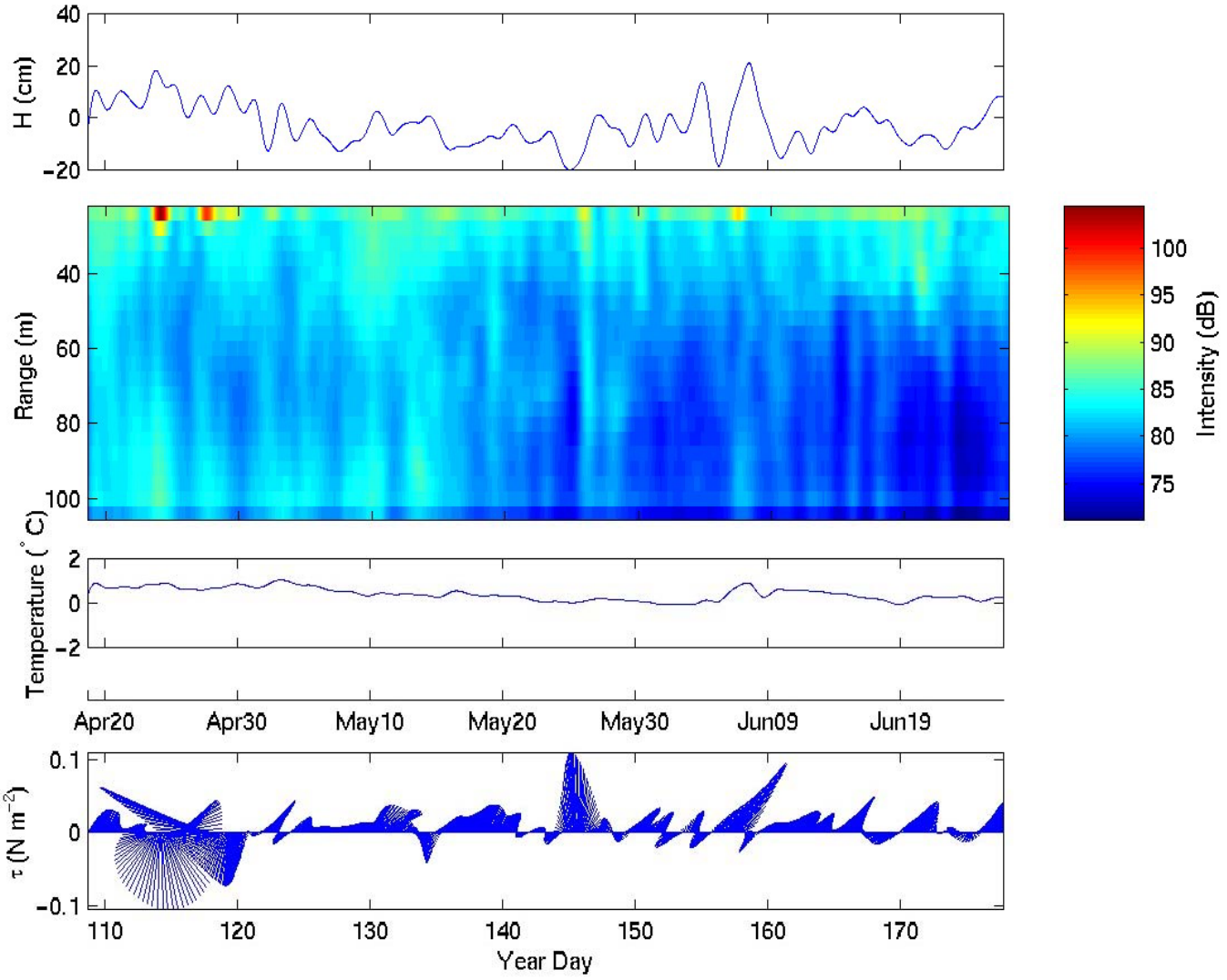

Figure 15: The subtidal backscatter intensity and temperature measured by the ADCP at M5 along with the surface elevation and wind stress measured at Argentia. For the stick plot, wind is presented in the direction towards which the wind is blowing, with North at the top.

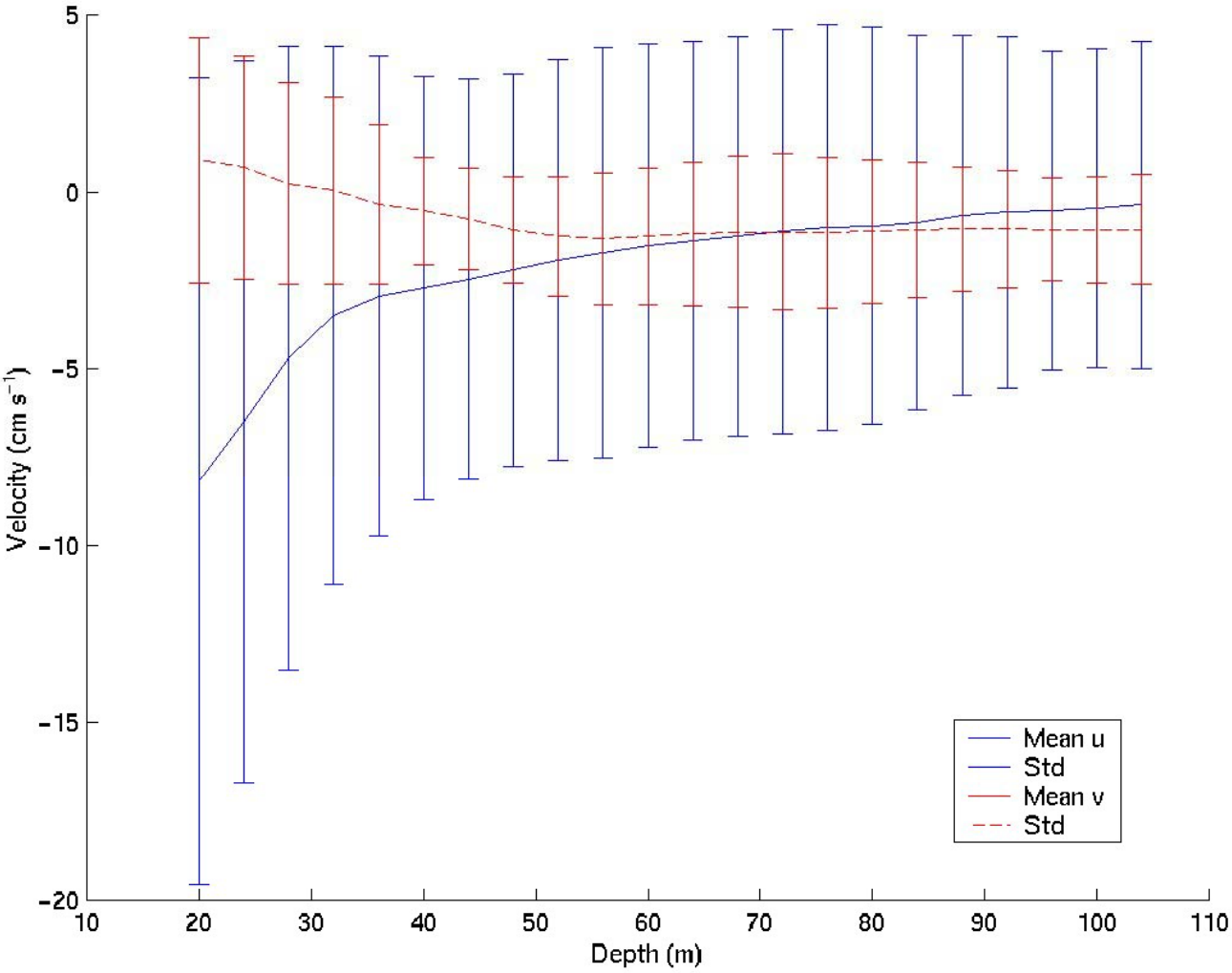

Figure 16: The subtidal along (blue solid line) and cross bay (red dashed line) velocity profiles measured at mooring M5. The standard deviation is included as error bars.

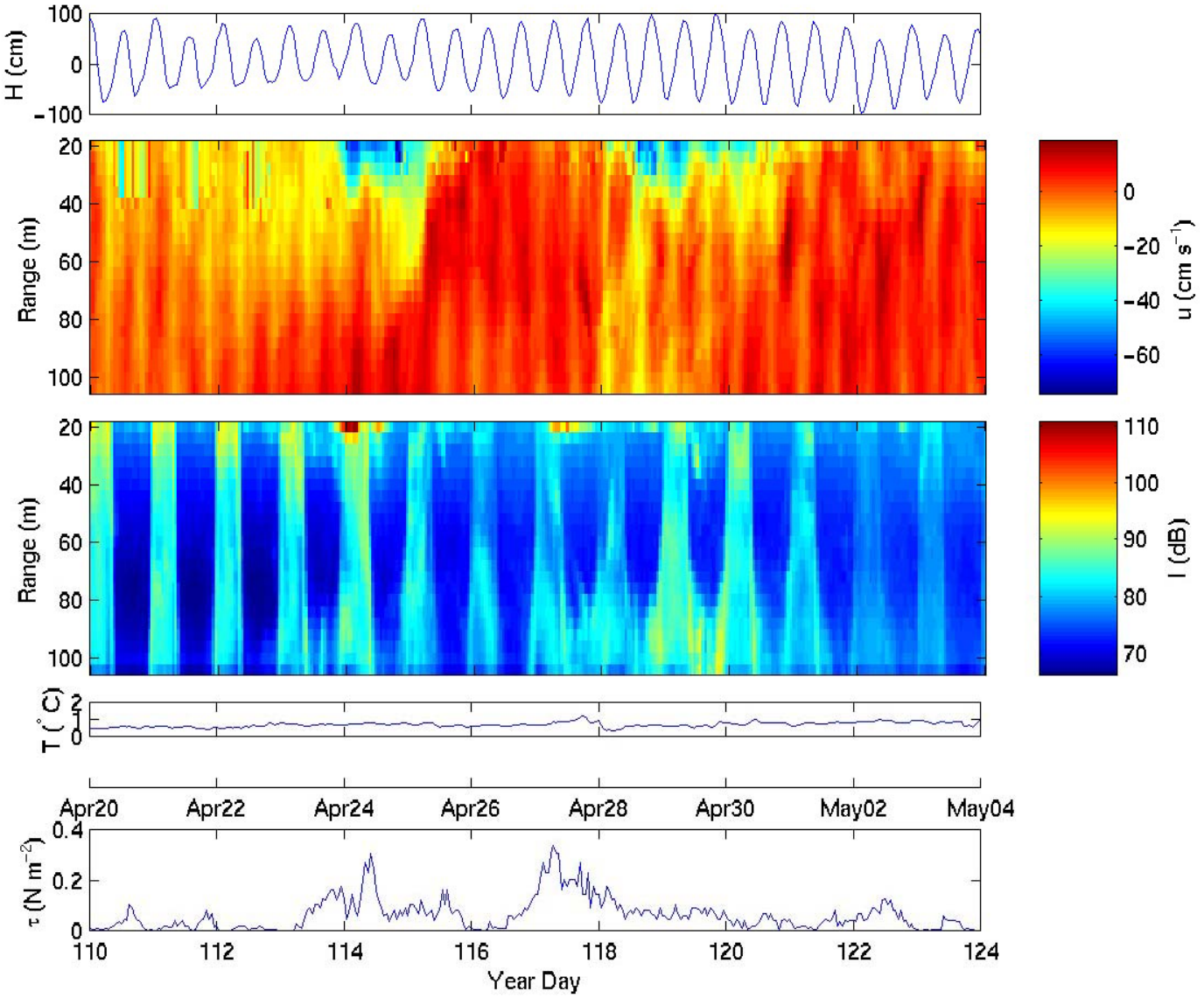

Figure 17: The surface elevation, along bay velocity, backscatter intensity, temperature and the wind stress for the hourly sampled data at M5 for Year Day 110 to 124.

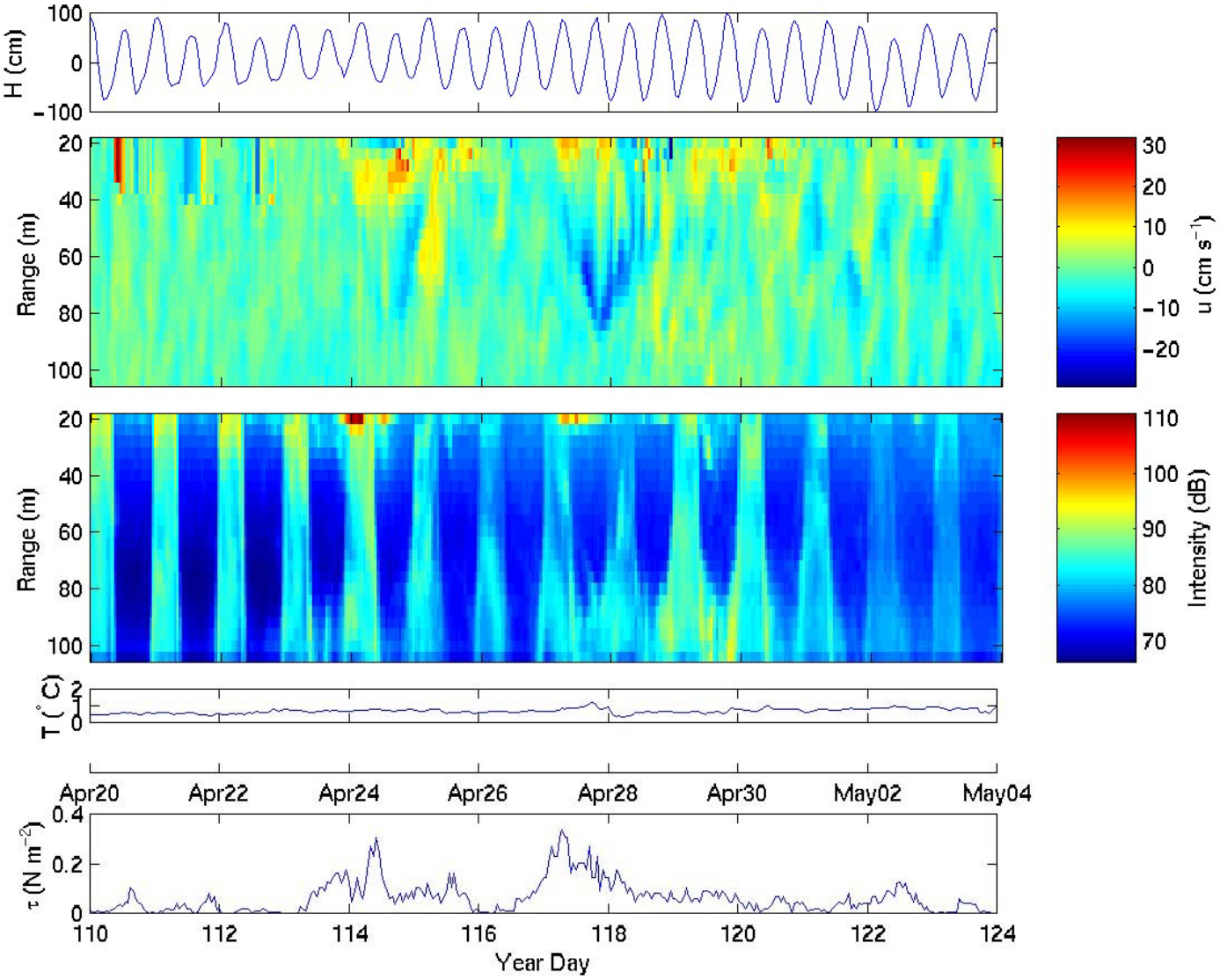

Figure 18: The surface elevation, cross bay velocity, backscatter intensity, temperature and the wind stress for the hourly sampled data at M5 for Year Day 110 to 124.

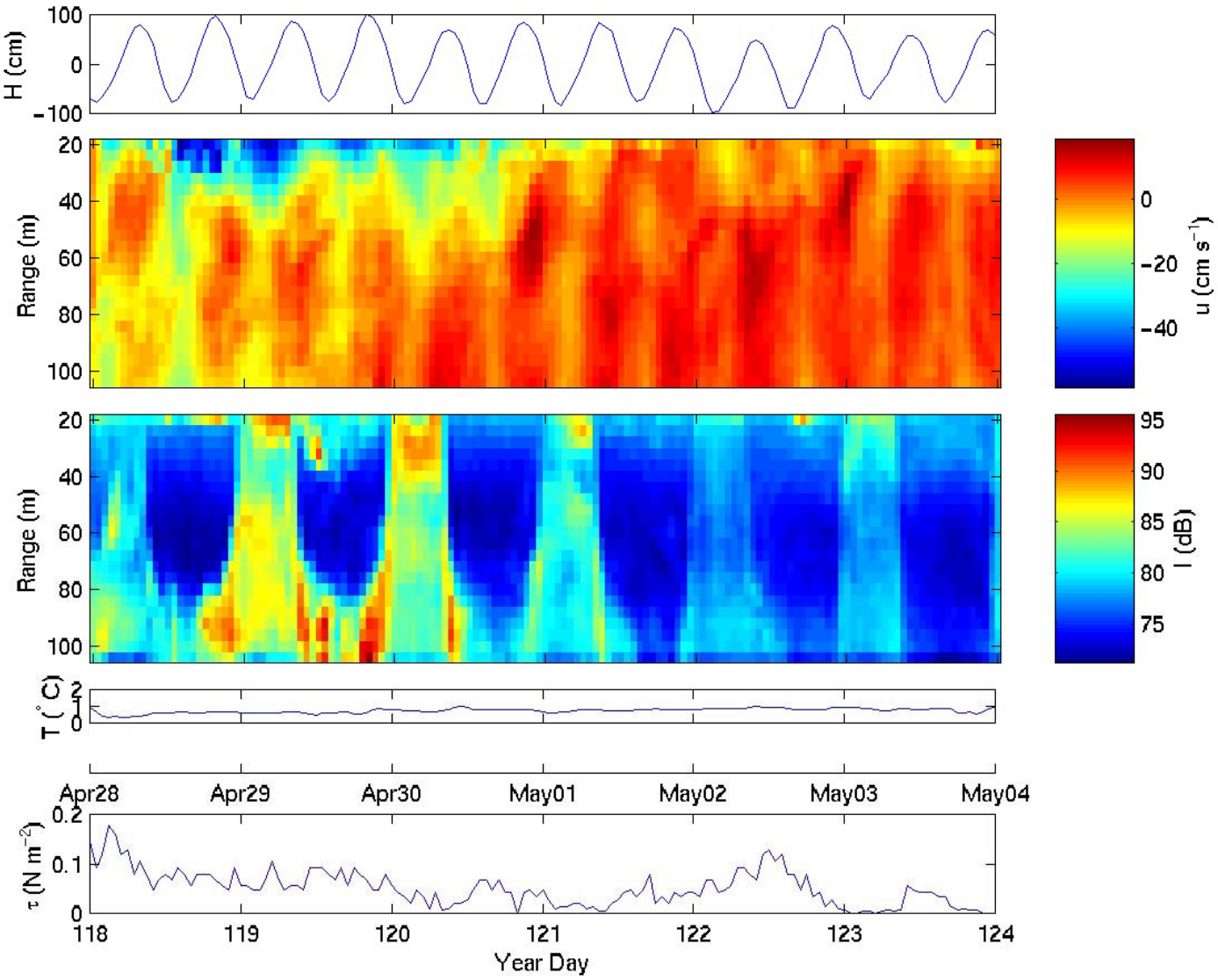

Figure 19: The surface elevation, along bay velocity, backscatter intensity, temperature and the wind stress for the hourly sampled data at M5 for Year Day 118 to 124.

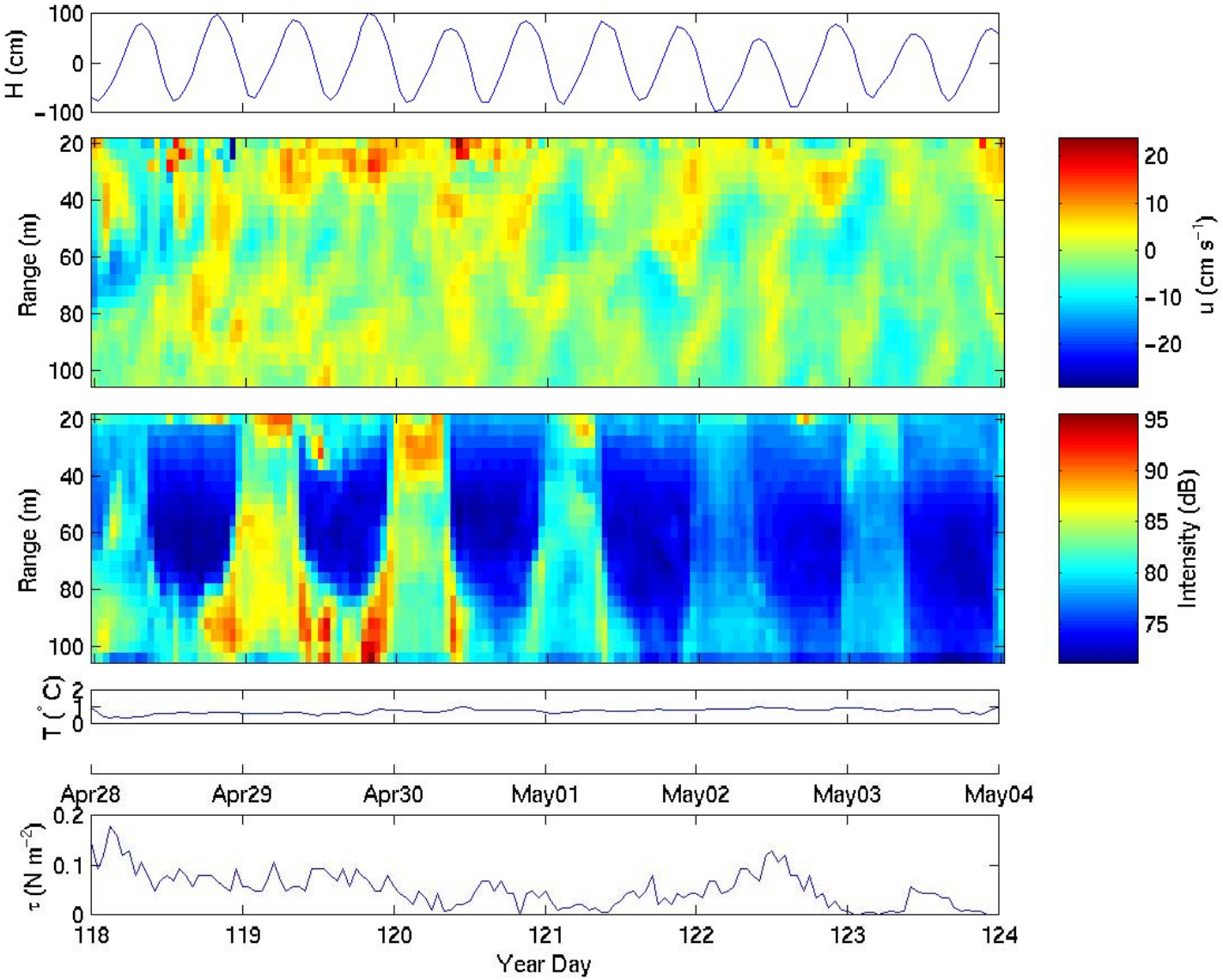

Figure 20: The surface elevation, cross bay velocity, backscatter intensity, temperature and the wind stress for the hourly sampled data at M5 for Year Day 118 to 124.

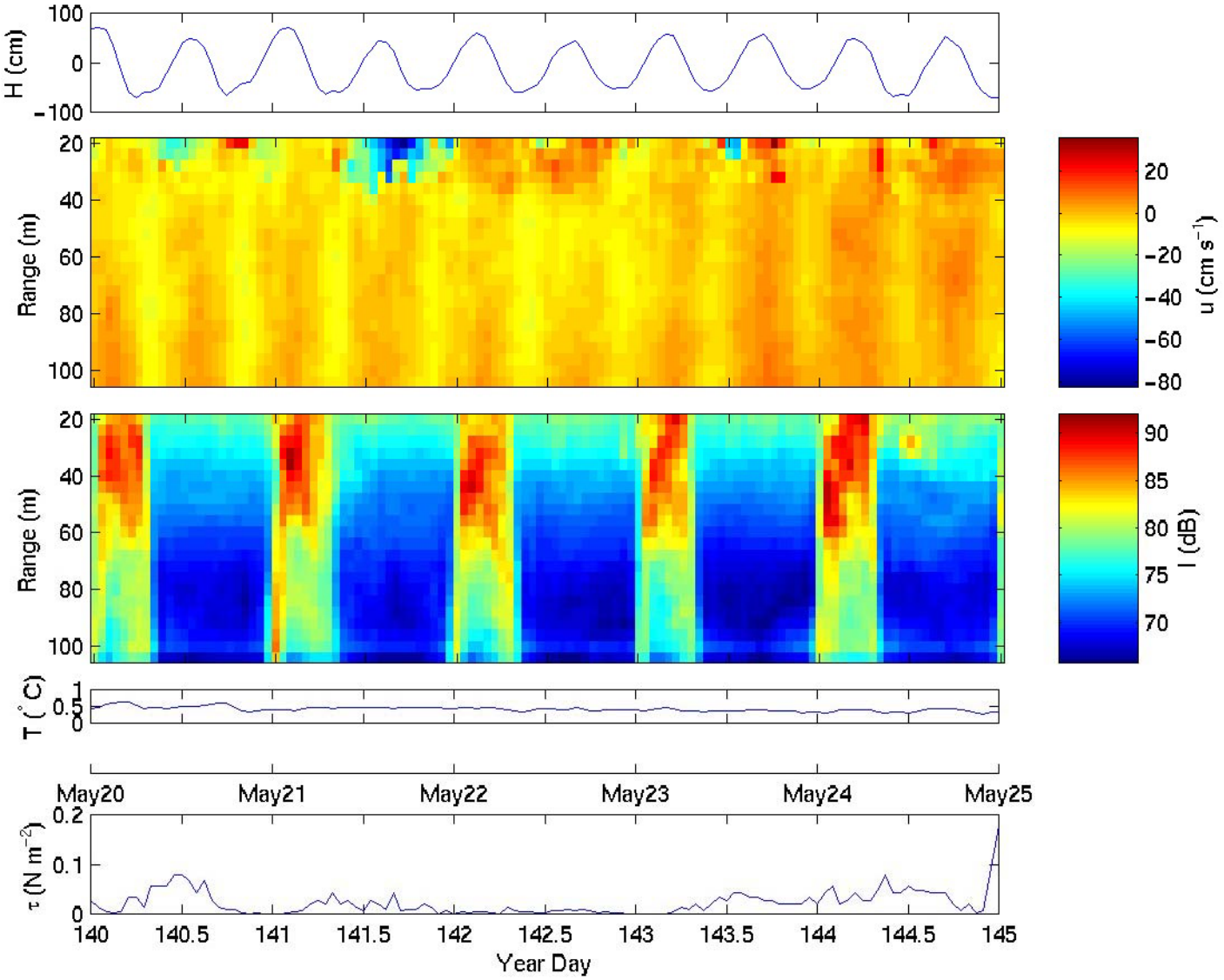

Figure 21: The surface elevation, along bay velocity, backscatter intensity, temperature and the wind stress for the hourly sampled data at M5 for Year Day 140 to 145.

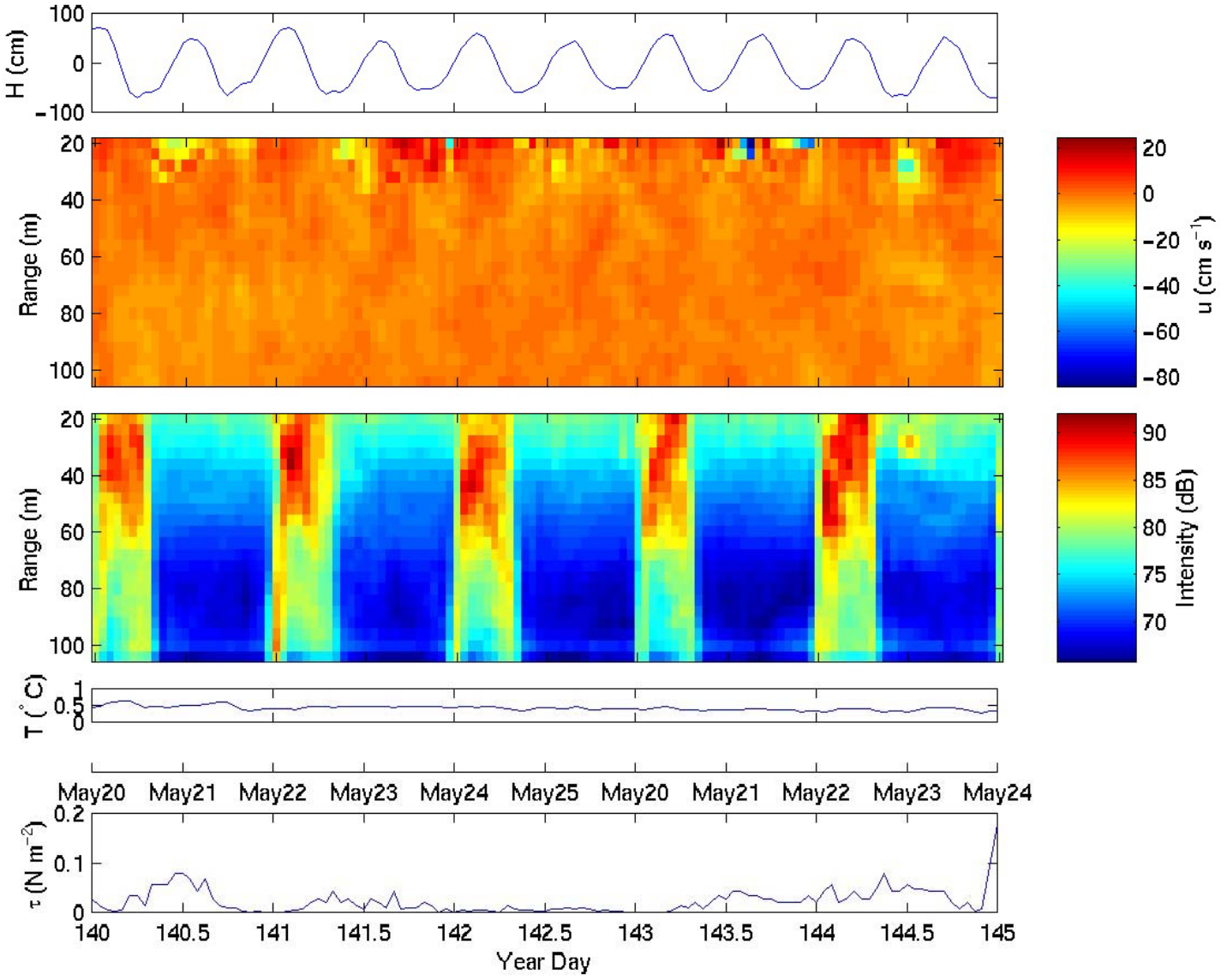

Figure 22: The surface elevation, cross bay velocity, backscatter intensity, temperature and the wind stress for the hourly sampled data at M5 for Year Day 140 to 145.

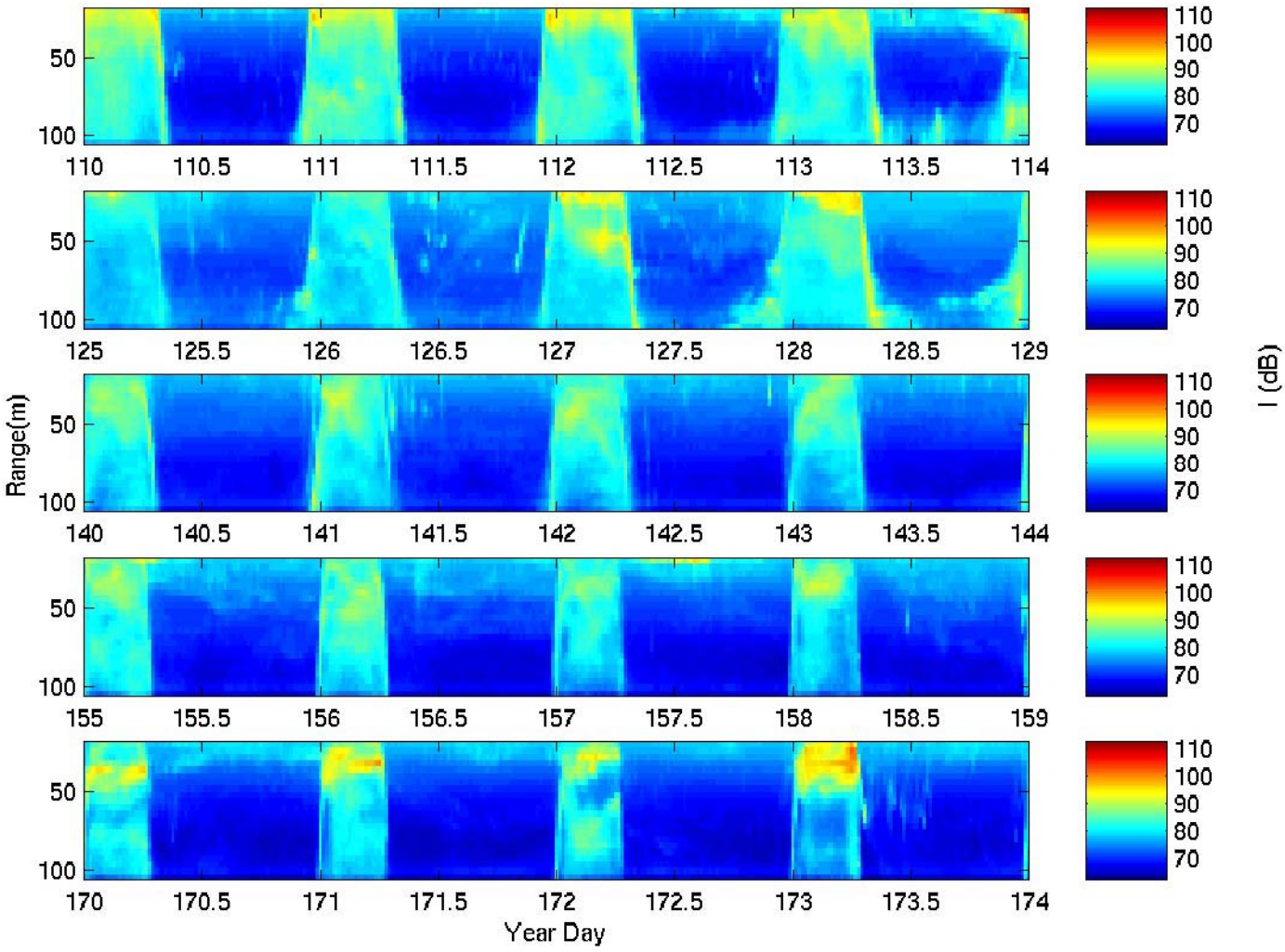

Figure 23: The backscatter intensity at M5 at 20 minute intervals for four-day periods from days 110 to 170. The backscatter intensity is in arbitrary dB, while the y-axis is the depth in metres and the x-axis is the time line in Year Day.

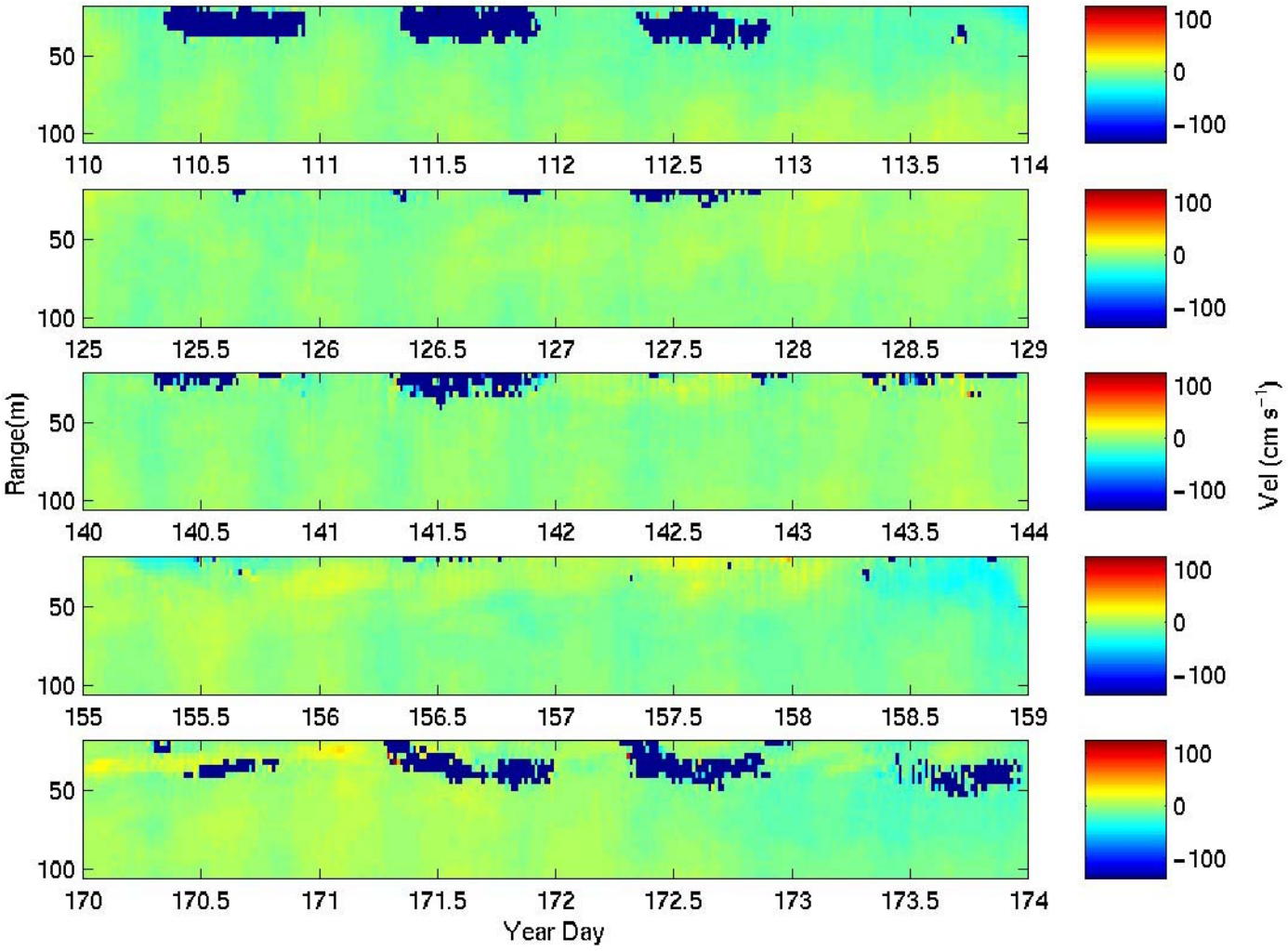

Figure 24: The along bay component of current velocity (in cm s^{-1}) measured at M5 at 20 minute intervals for selected ranges of Year Day. The y-axis is the depth in metres and the x-axis is the time line in Year Day. Bad data are indicated by the black points in the plots.

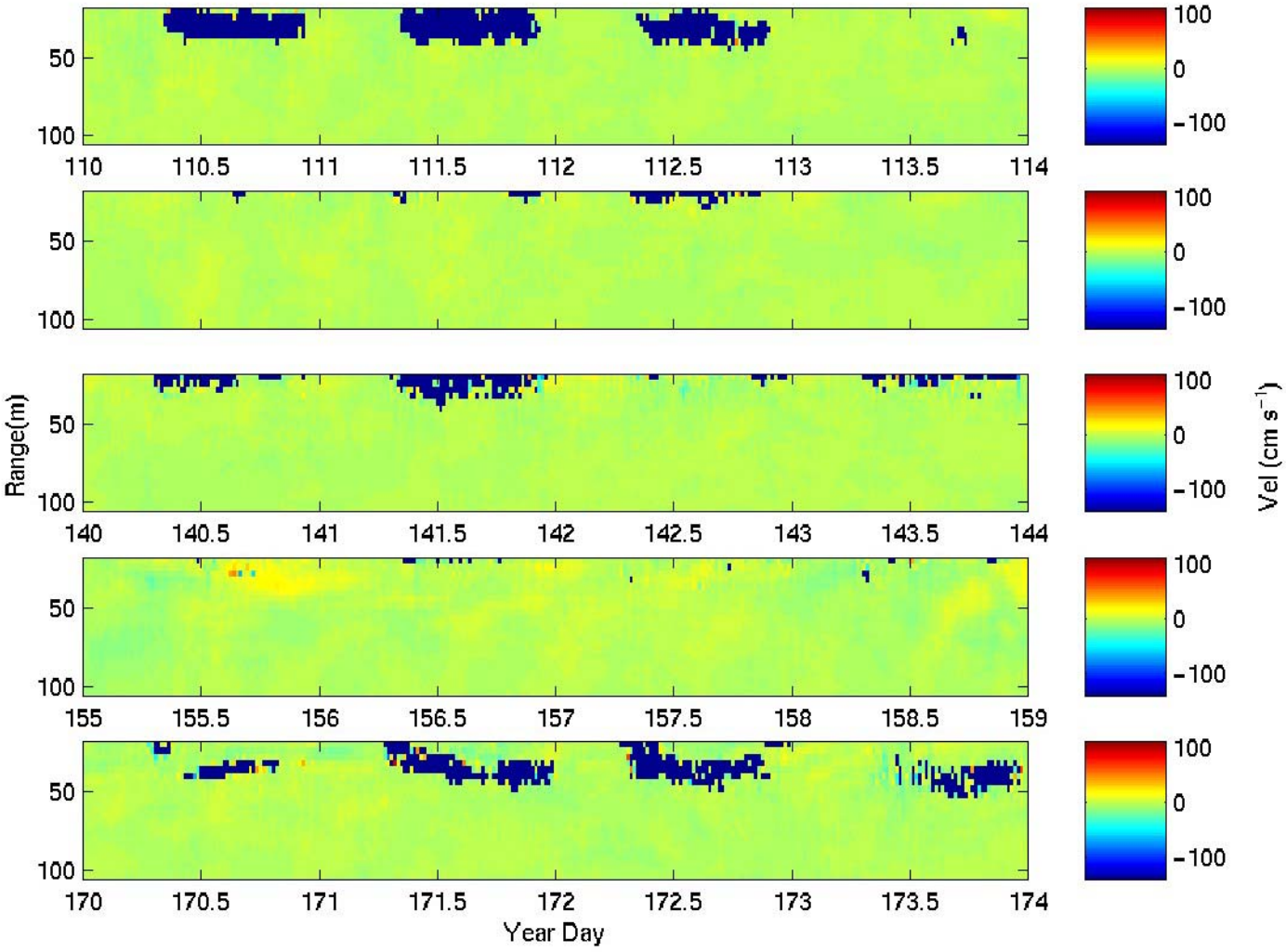

Figure 25: The cross bay component of current velocity (in cm s^{-1}) measured at M5 at 20 minute intervals for selected ranges of Year Day. The y-axis is the depth in metres and the x-axis is the time line in Year Day. Bad data are indicated by the black points in the plots.

Results from Mooring M6, in bay co-ordinates

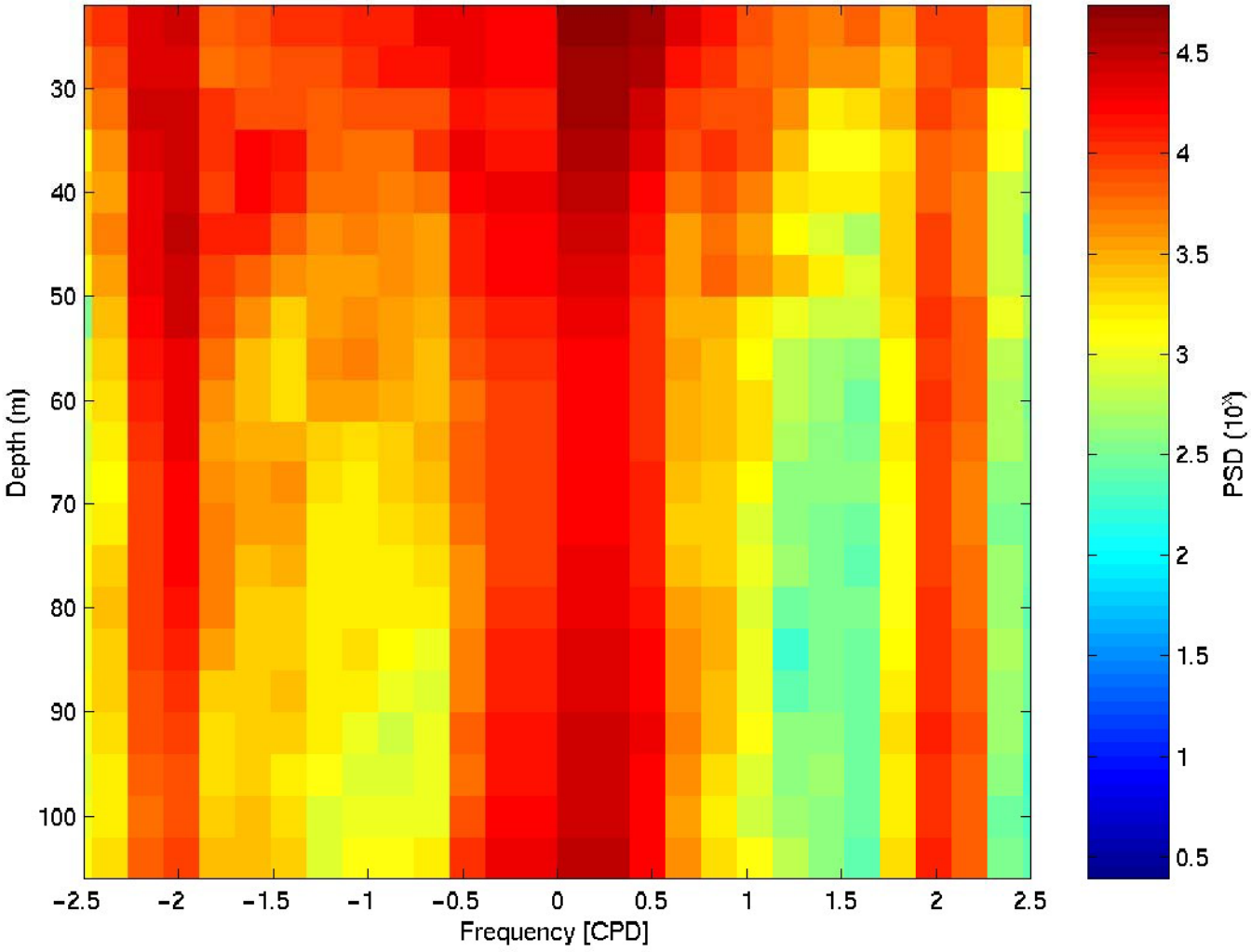

Figure 26: Rotary spectrum for the velocities recorded at mooring M6 for each depth bin. There were 13 degrees of freedom in the rotary spectral calculation.

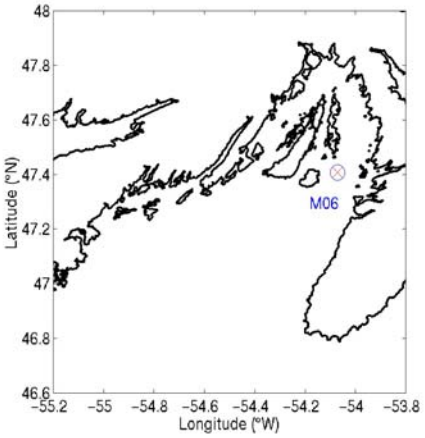

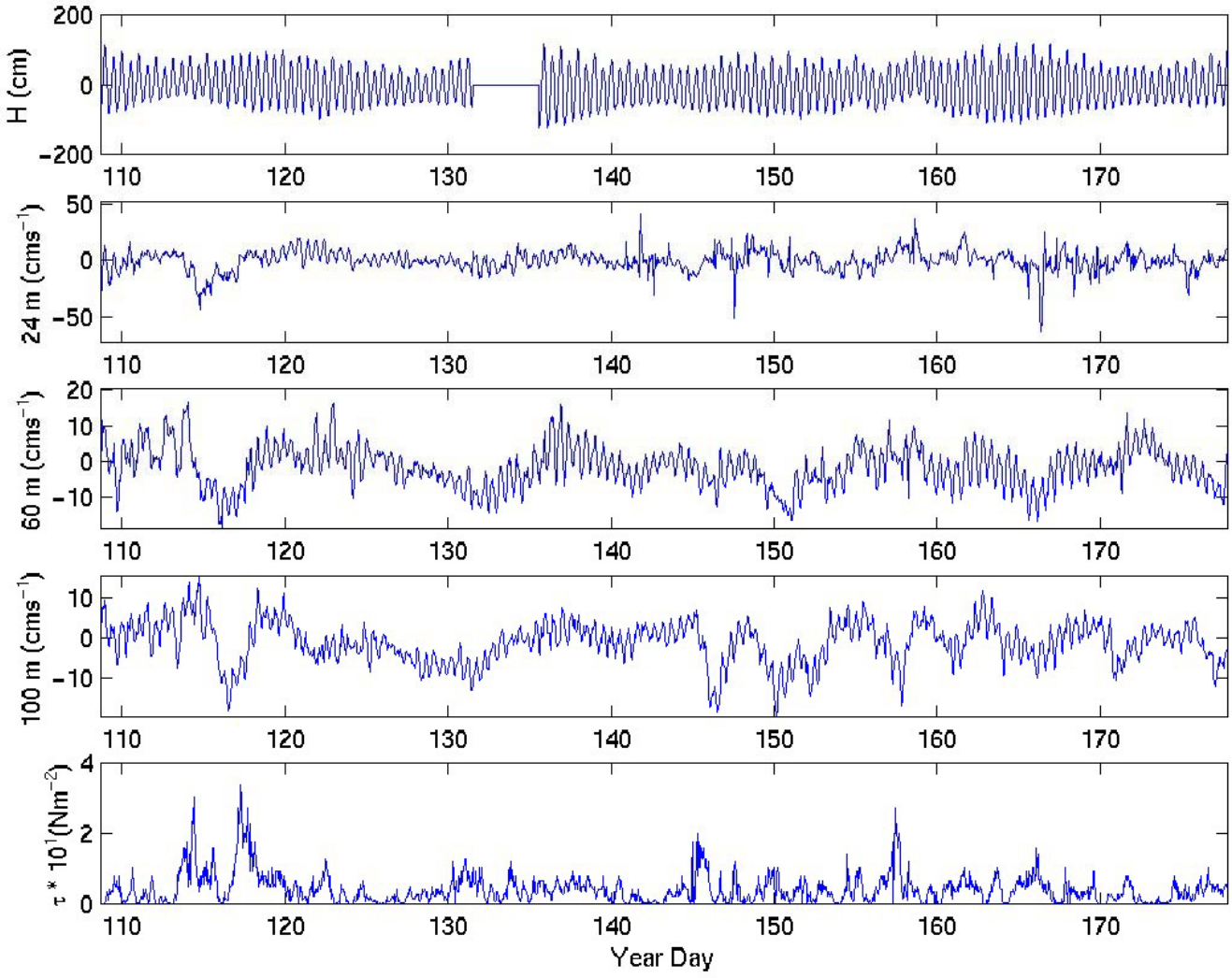

Figure 27: The surface elevation measured at Argentia, current velocities of the along bay component for 24, 60 and 100 m at mooring M6, and the magnitude of the wind stress at Argentia.

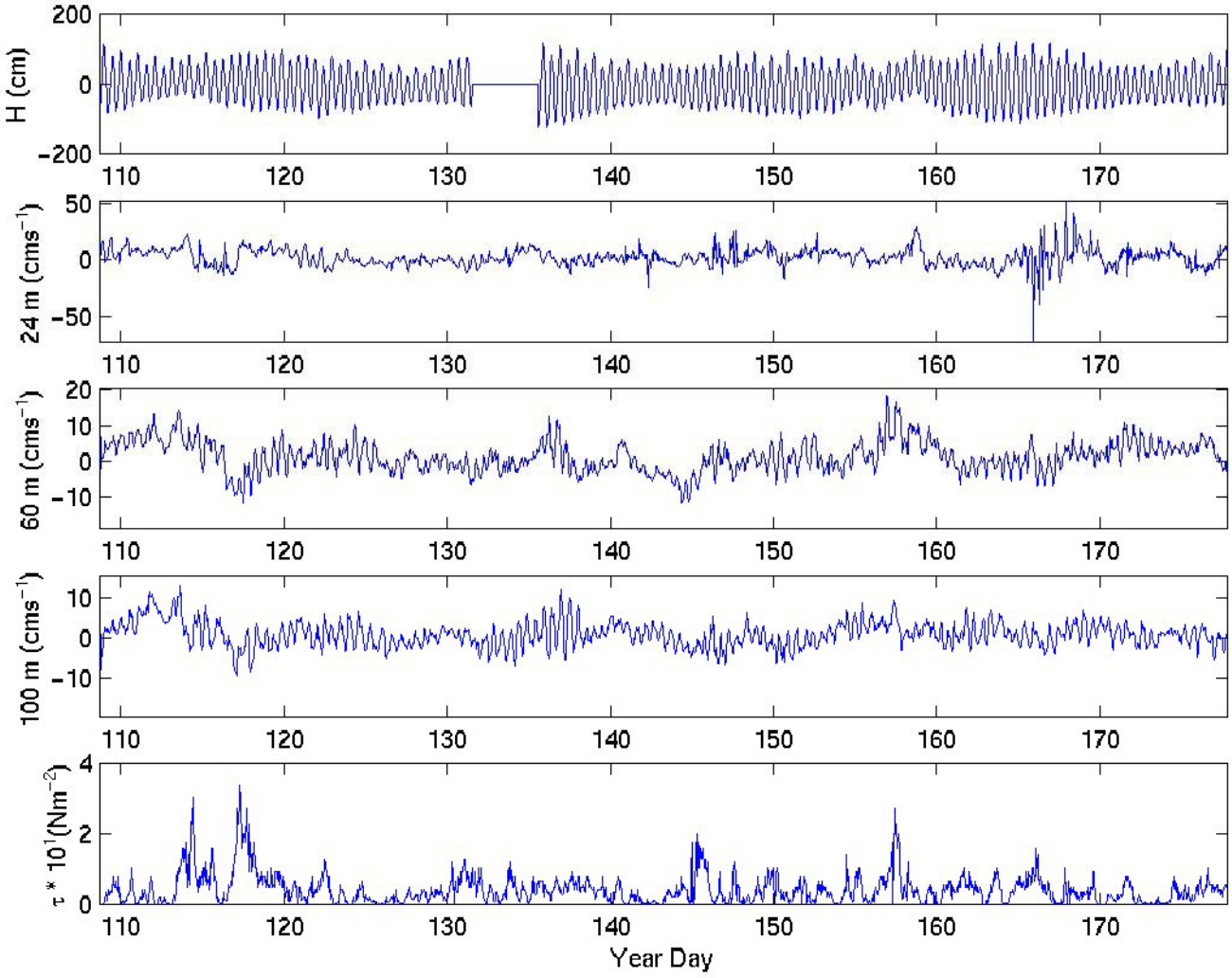

Figure 28: The surface elevation measured at Argentia, current velocities of the cross bay component for 26, 60 and 100 m measured at mooring M6, and the magnitude of the wind stress measured at Argentia.

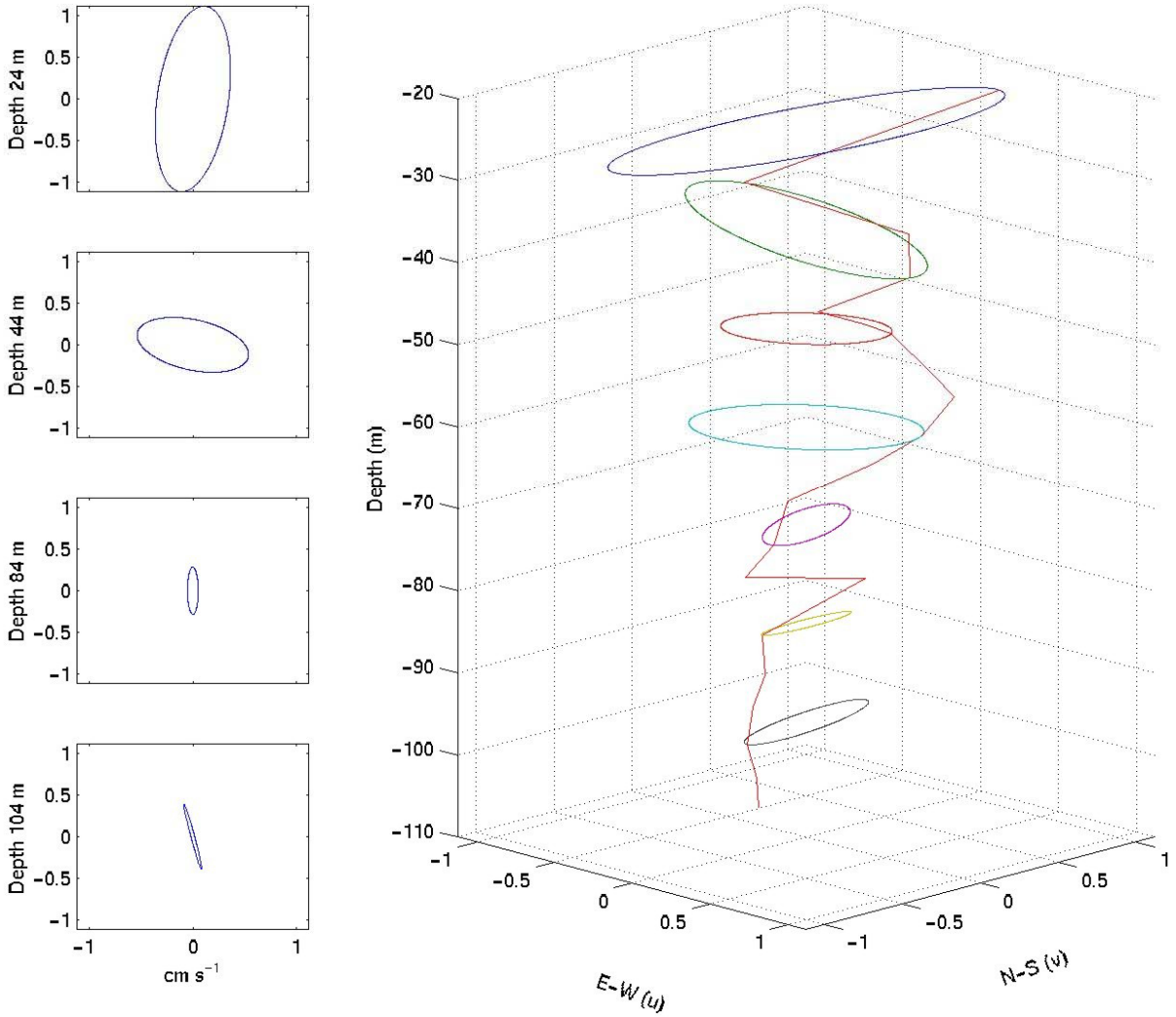

Figure 29: The K_1 tidal ellipses measured at mooring M6. The N-S axis is the cross bay axis, while the E-W axis is the along bay axis. The red line connects the inclination of each ellipse for all depths.

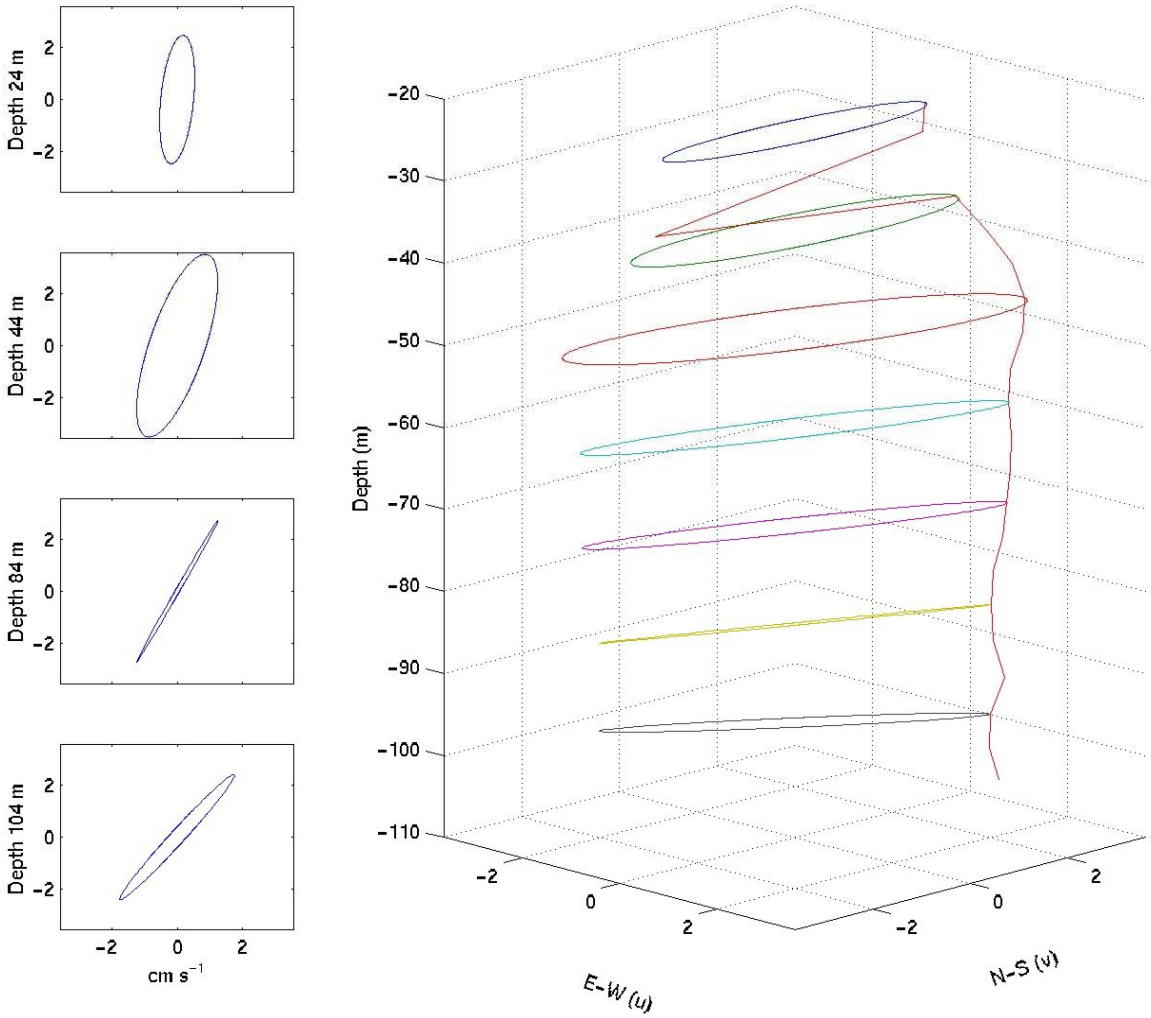

Figure 30: The M_2 tidal ellipses measured at mooring M6. The N-S axis is the cross bay axis, while the E-W axis is the along bay axis. The red line connects the inclination of each ellipse for all depths.

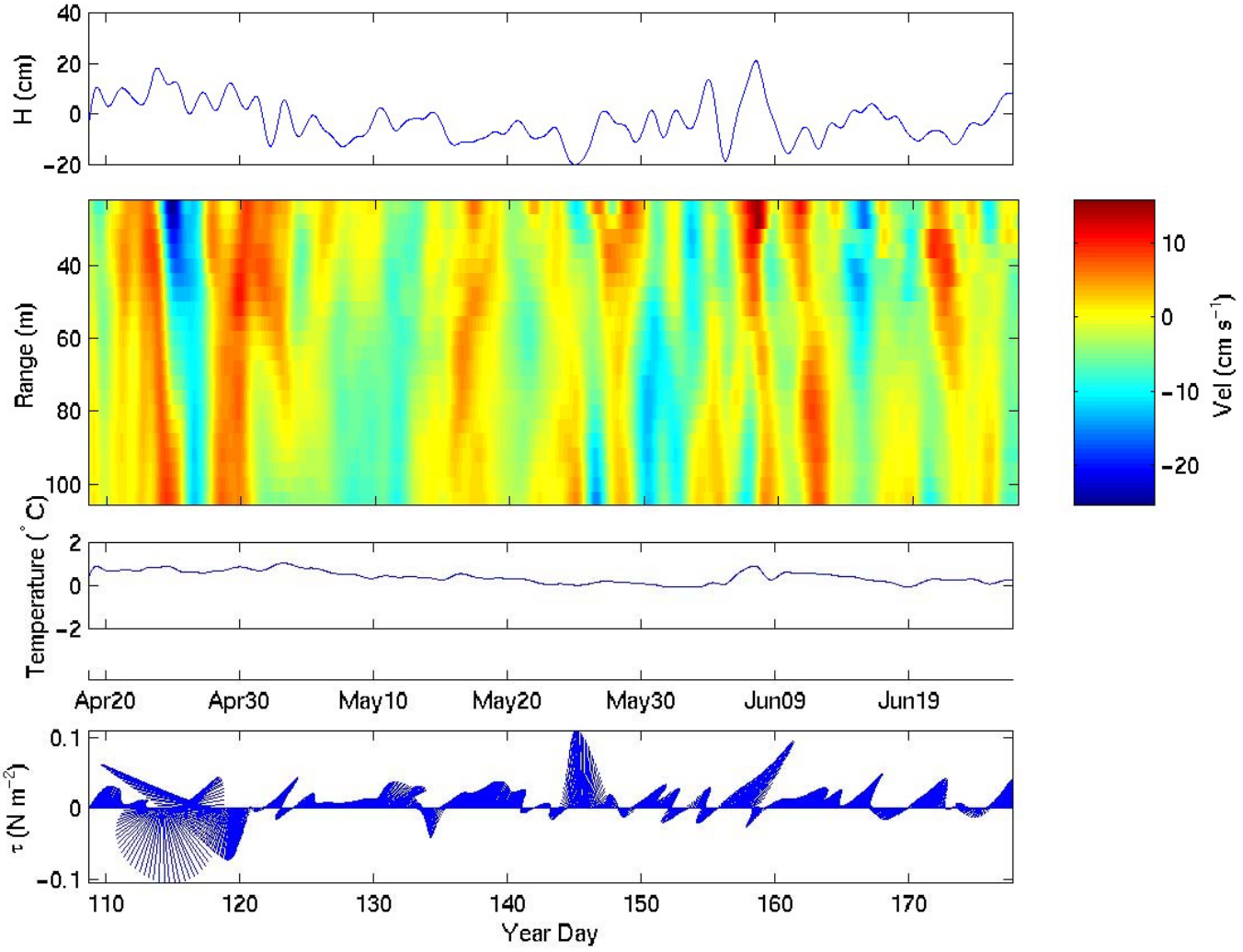

Figure 31: The subtidal along bay velocity and temperature measured by the ADCP at mooring M6 along with the surface elevation and wind stress measured at Argentia. For the stick plot, wind is presented in the direction towards which the wind is blowing, with North at the top.

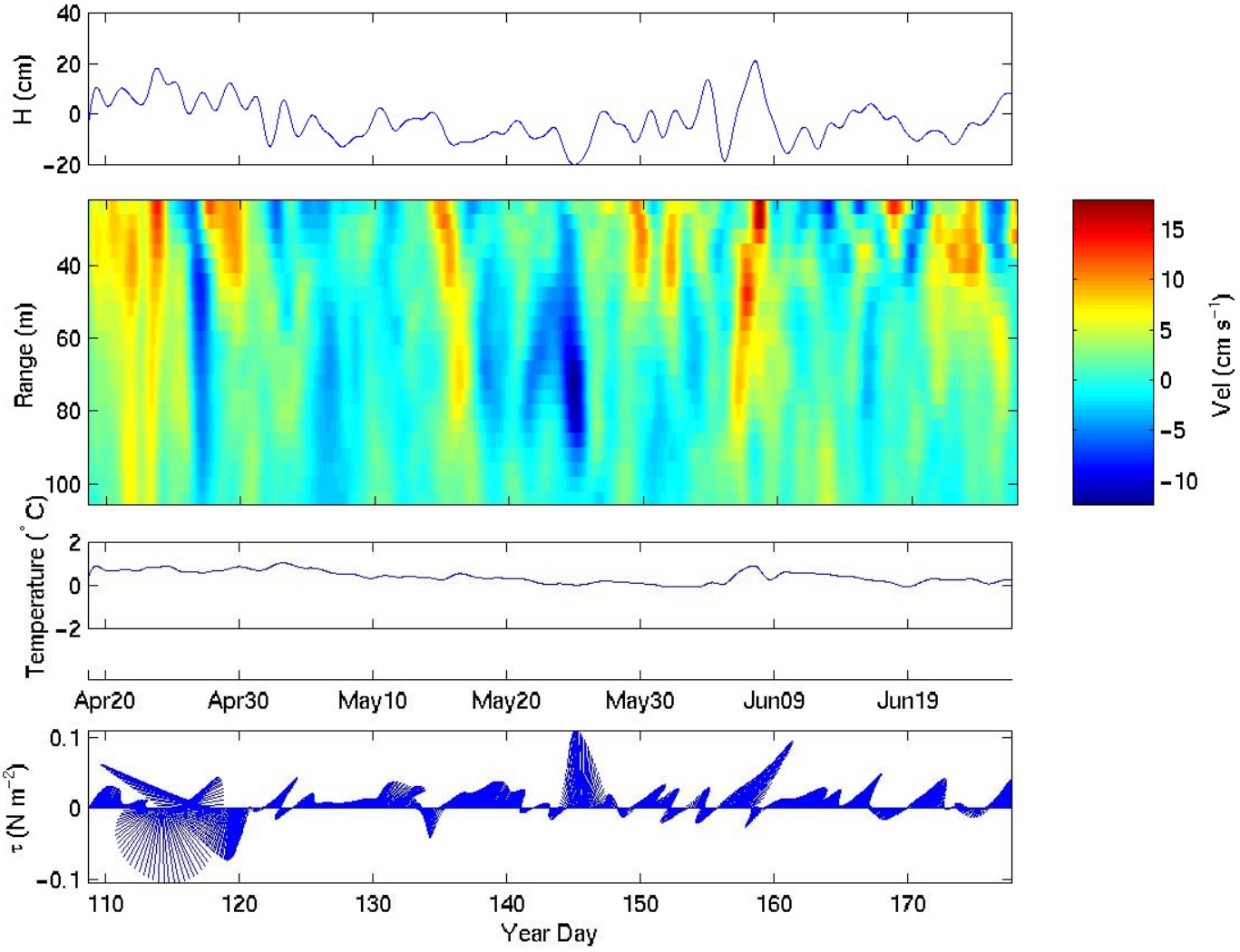

Figure 32: The subtidal cross bay velocity and temperature measured by the ADCP at mooring M6 along with the surface elevation and wind stress measured at Argentia. For the stick plot, wind is presented in the direction towards which the wind is blowing, with North at the top.

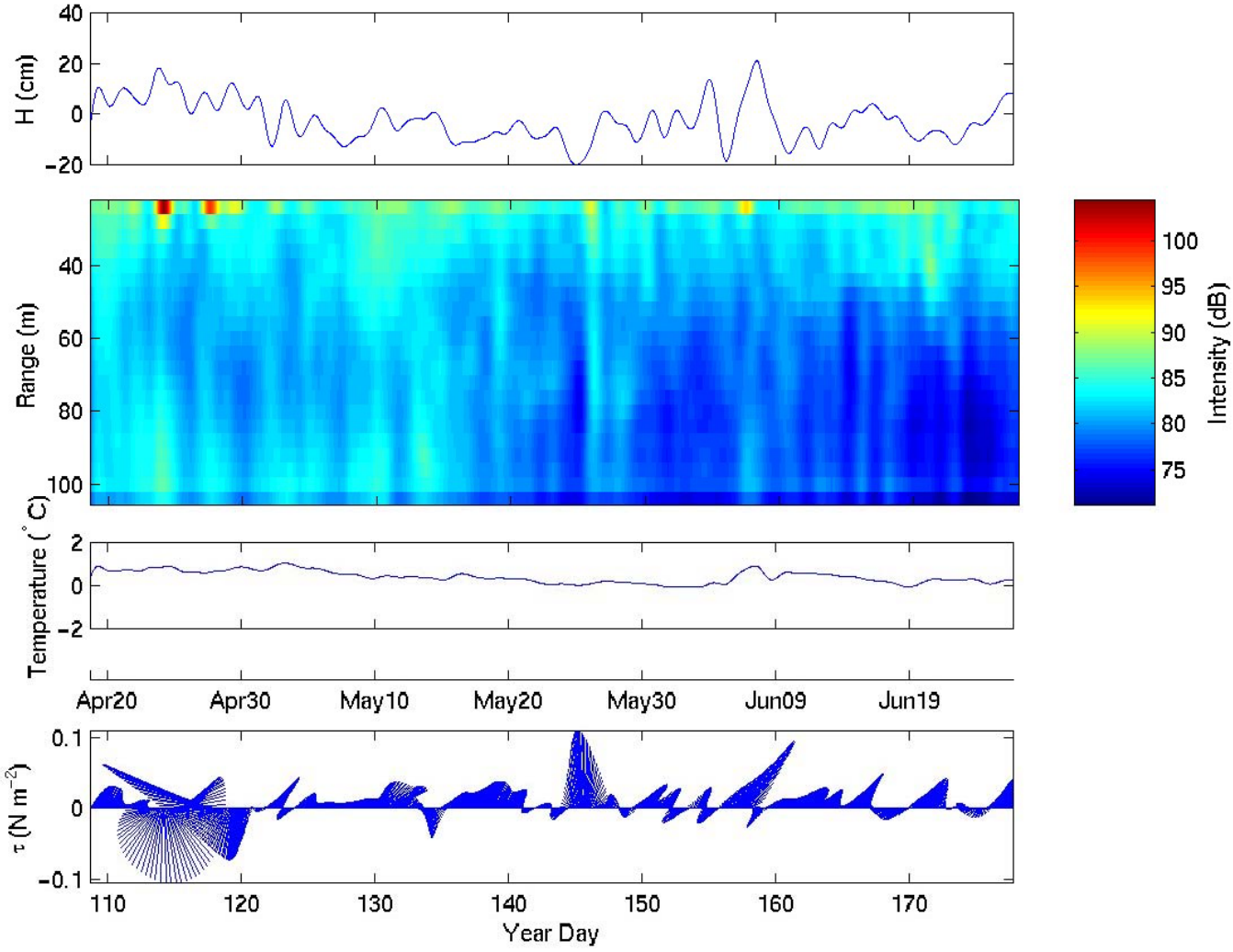

Figure 33: The subtidal backscatter intensity and temperature measured by the ADCP at mooring M6 along with the surface elevation and wind stress measured at Argentia. For the stick plot, wind is presented in the direction towards which the wind is blowing, with North at the top.

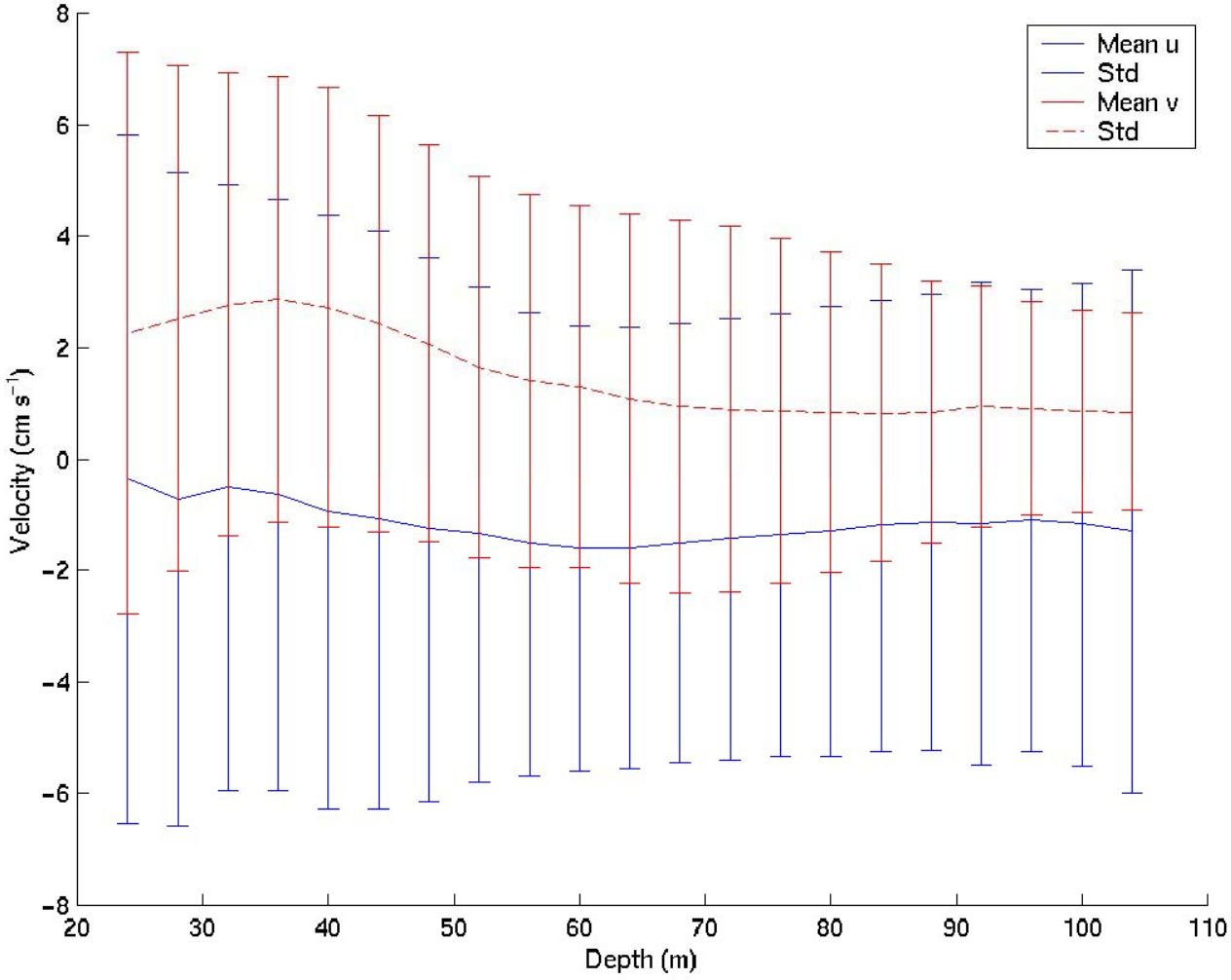

Figure 34: The subtidal along (blue solid line) and cross bay (red dashed line) velocity profiles measured at mooring M6. The standard deviations are indicated by the error bars.

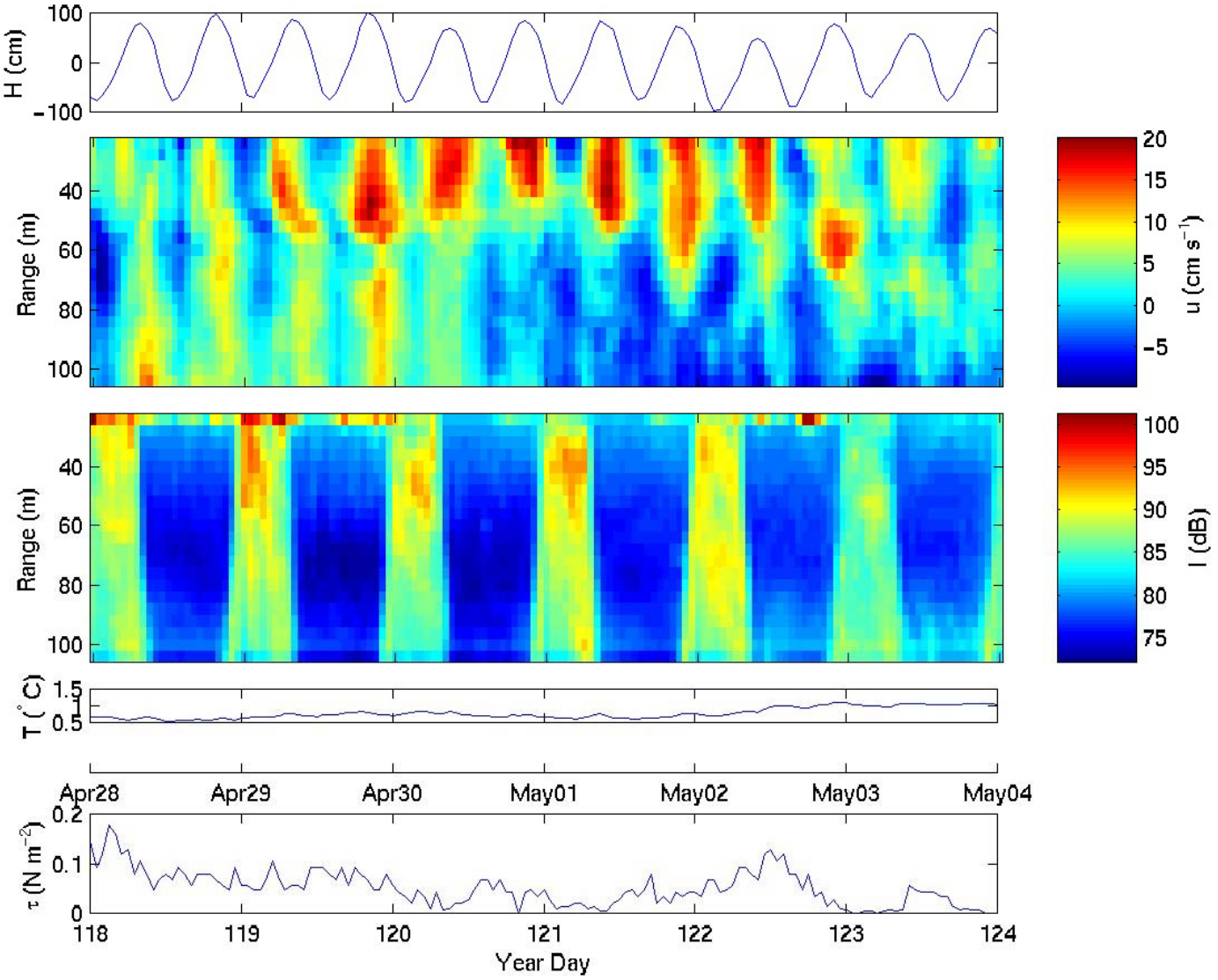

Figure 35: The surface elevation, along bay velocity, backscatter intensity, temperature and the wind stress for the hourly sampled data at mooring M6 for Year Day 118 to 124.

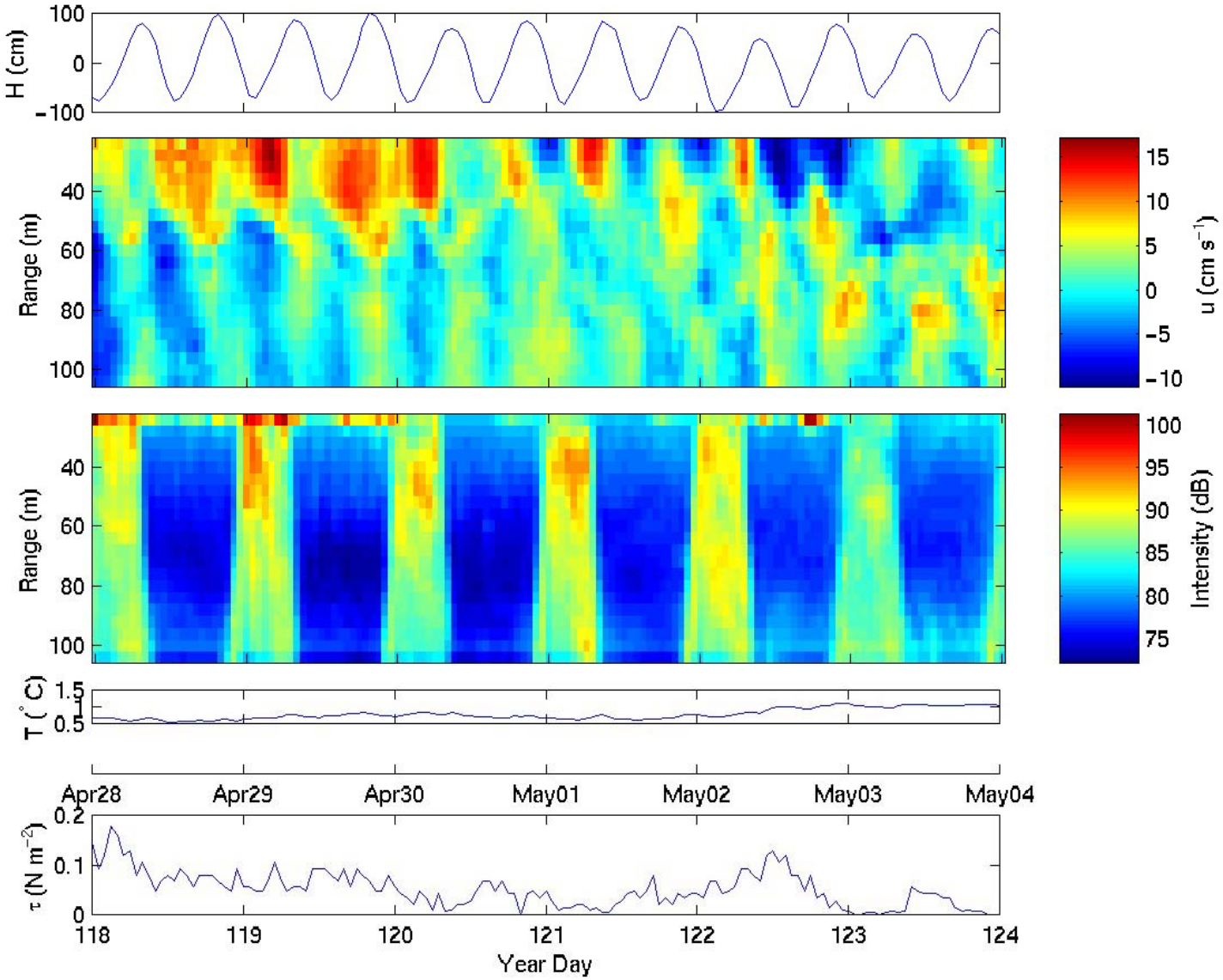

Figure 36: The surface elevation, cross bay velocity, backscatter intensity, temperature and the wind stress for the hourly sampled data at mooring M6 for Year Day 118 to 124.

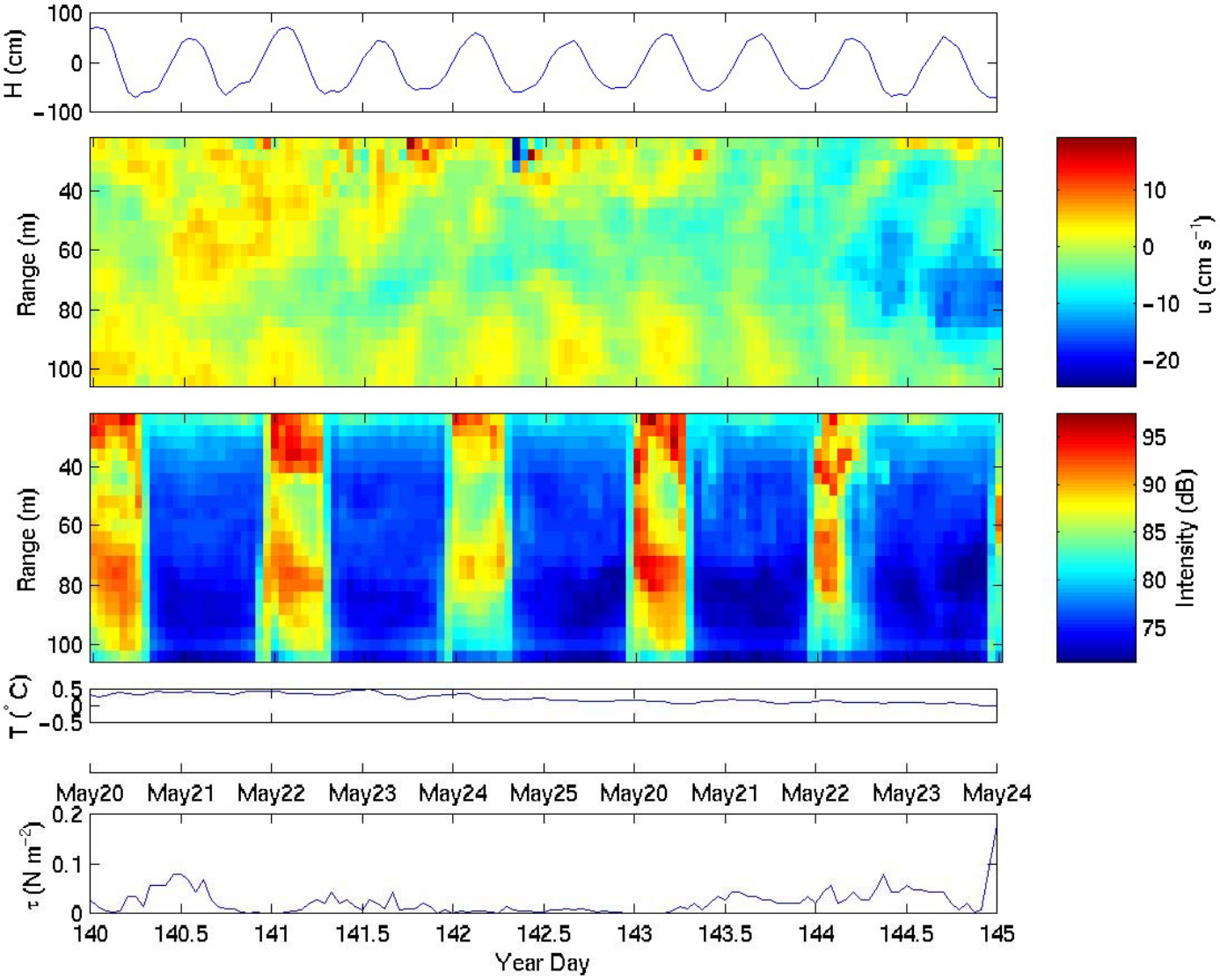

Figure 37: The surface elevation, along bay velocity, backscatter intensity, temperature and the wind stress for the hourly sampled data at mooring M6 for Year Day 140 to 145.

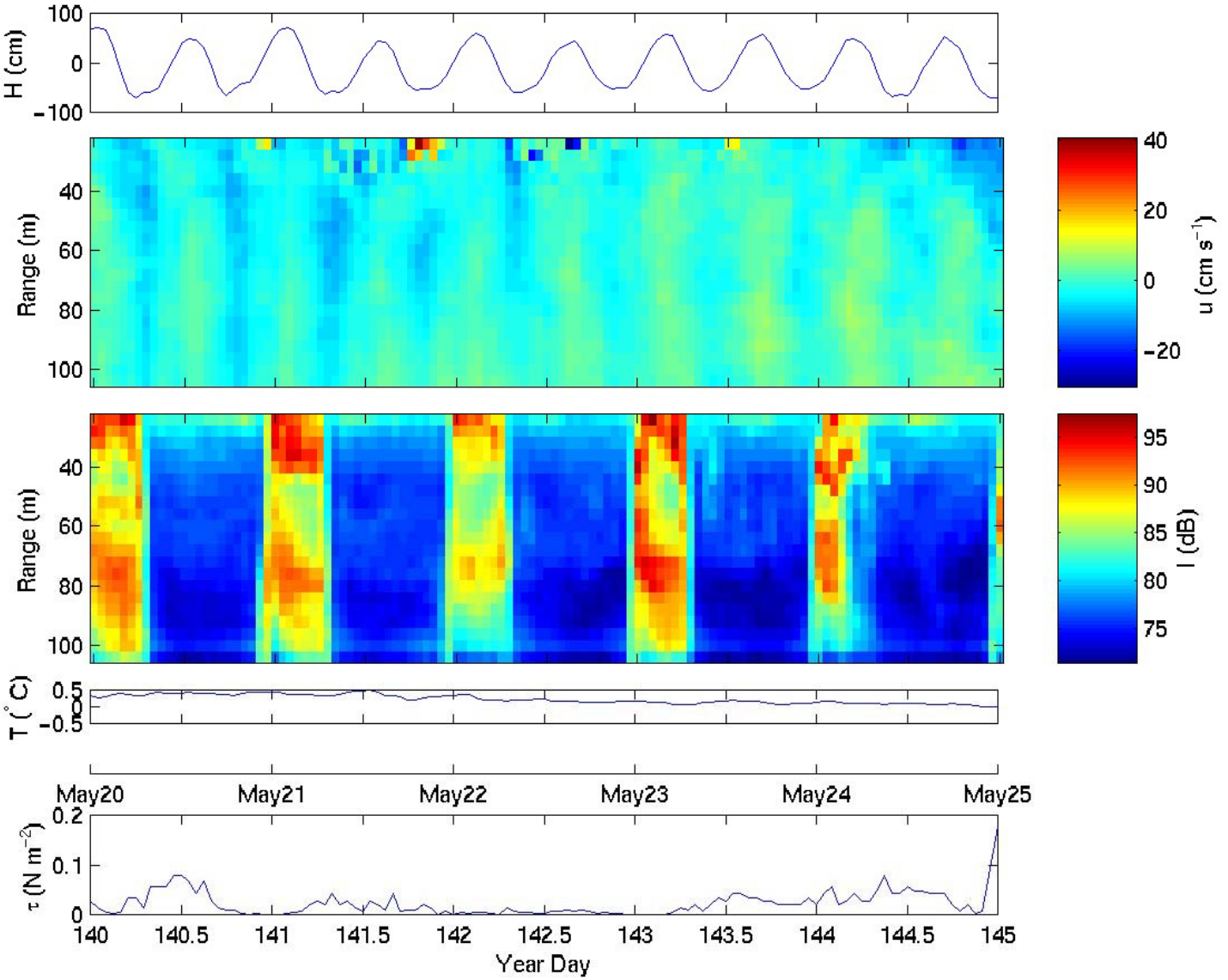

Figure 38: The surface elevation, along bay velocity, backscatter intensity, temperature and the wind stress for the hourly sampled data at mooring M6 for Year Day 140 to 145.

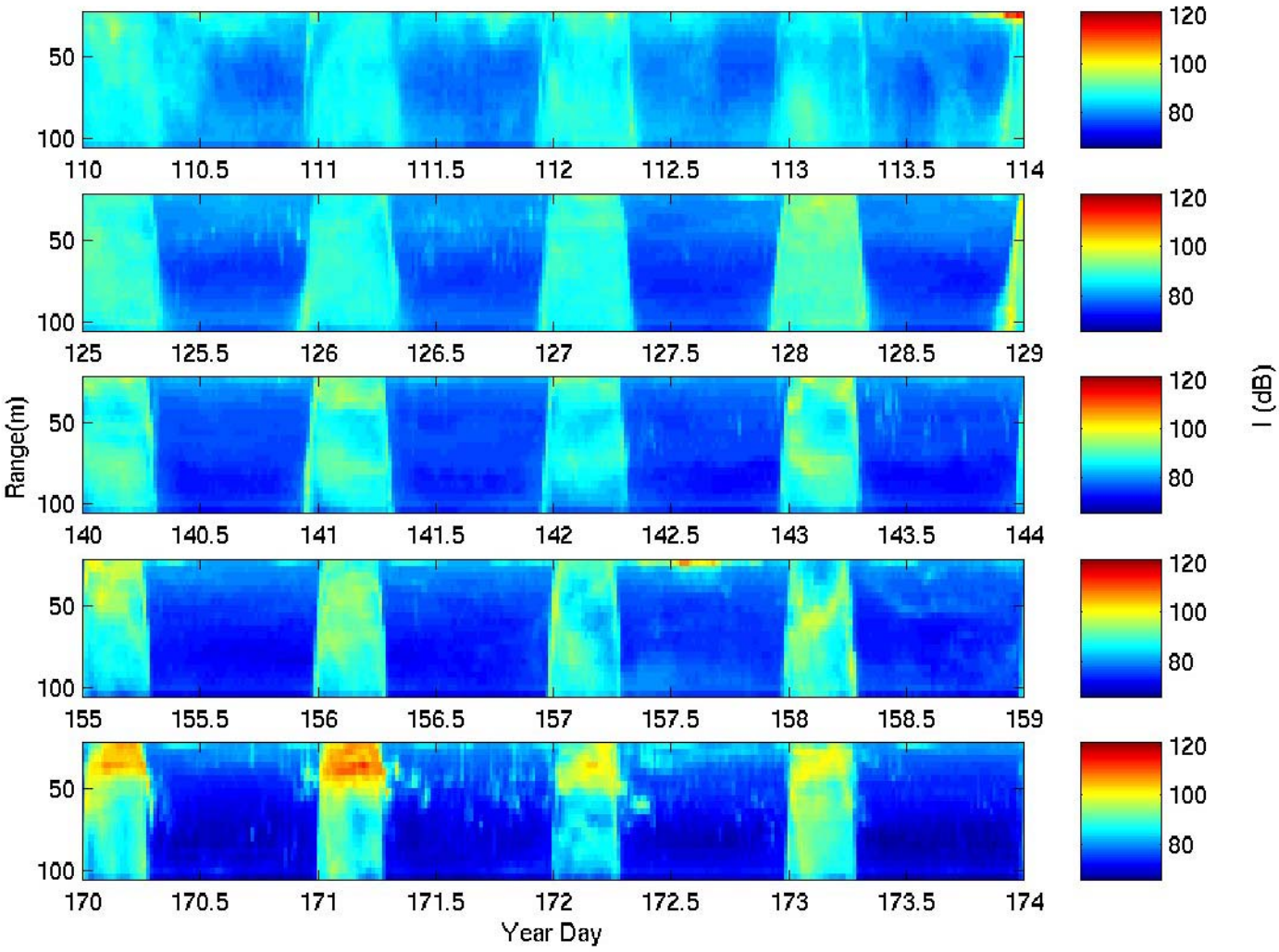

Figure 39: The backscatter intensity at M6 at 20 minute intervals for four-day periods from days 110 to 170. The backscatter intensity is in arbitrary dB, while the y-axis is the depth in metres and the x-axis is the time line in Year Day.

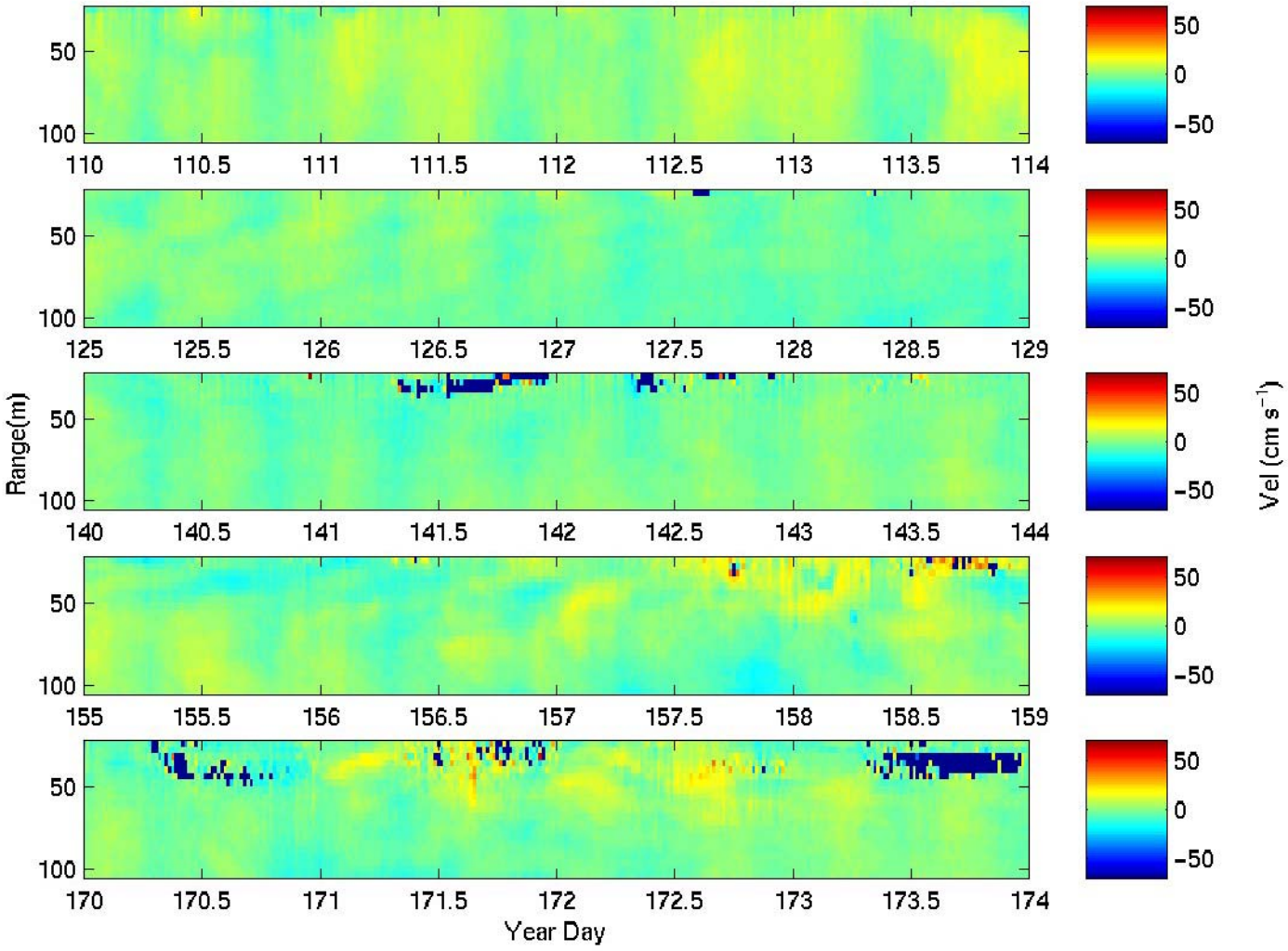

Figure 40: The along bay component of current velocity (in cm s^{-1}) measured at M6 at 20 minute intervals for selected ranges of Year Day. The y-axis is the depth in metres and the x-axis is the time line in Year Day. Bad data are indicated by the black points in the plots.

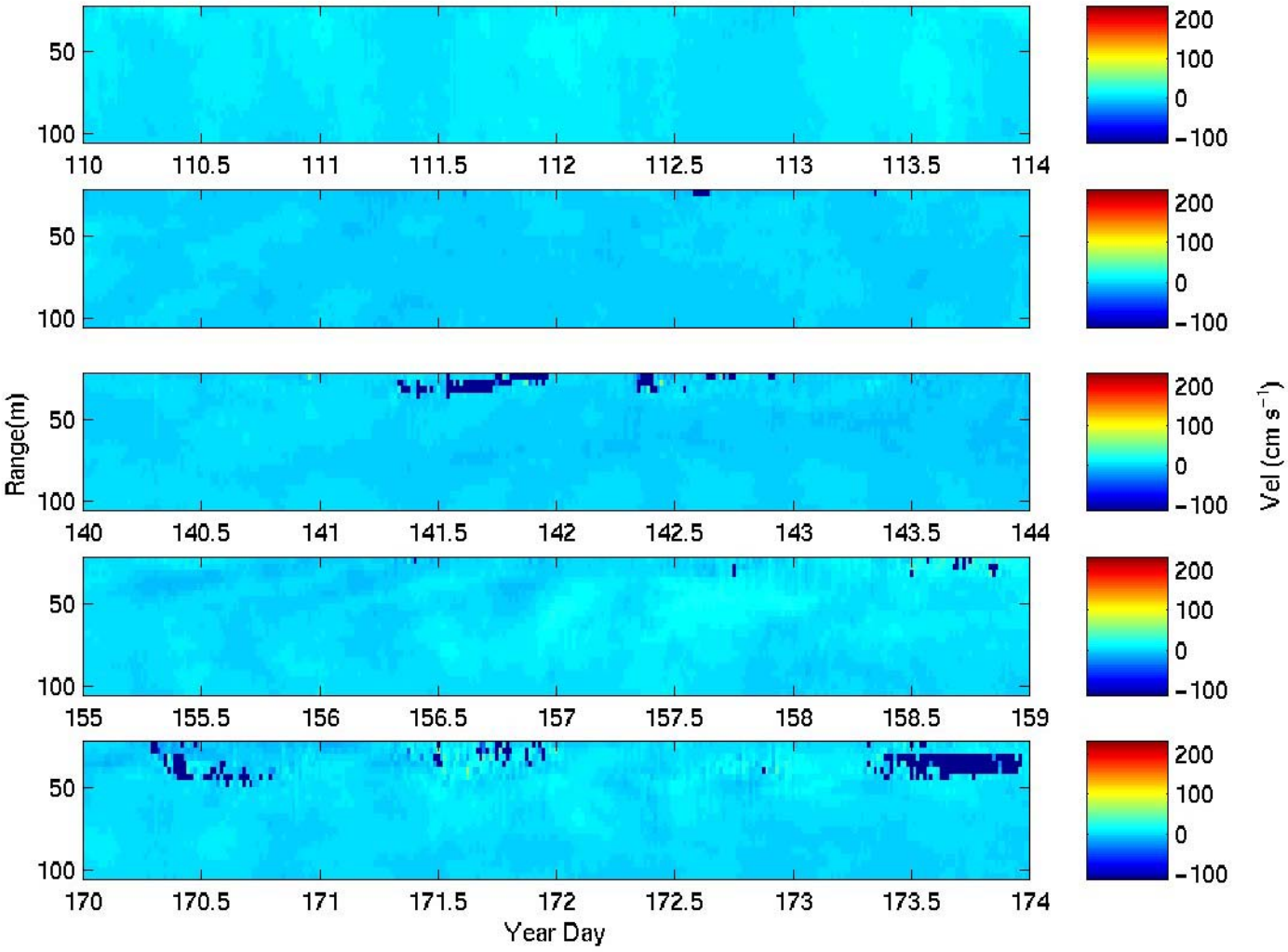

Figure 41: The cross bay component of current velocity (in cm s^{-1}) measured at M6 at 20 minute intervals for selected ranges of Year Day. The y-axis is the depth in metres and the x-axis is the time line in Year Day. Bad data are indicated by the black points in the plots.

Results from Mooring M7, in bay co-ordinates

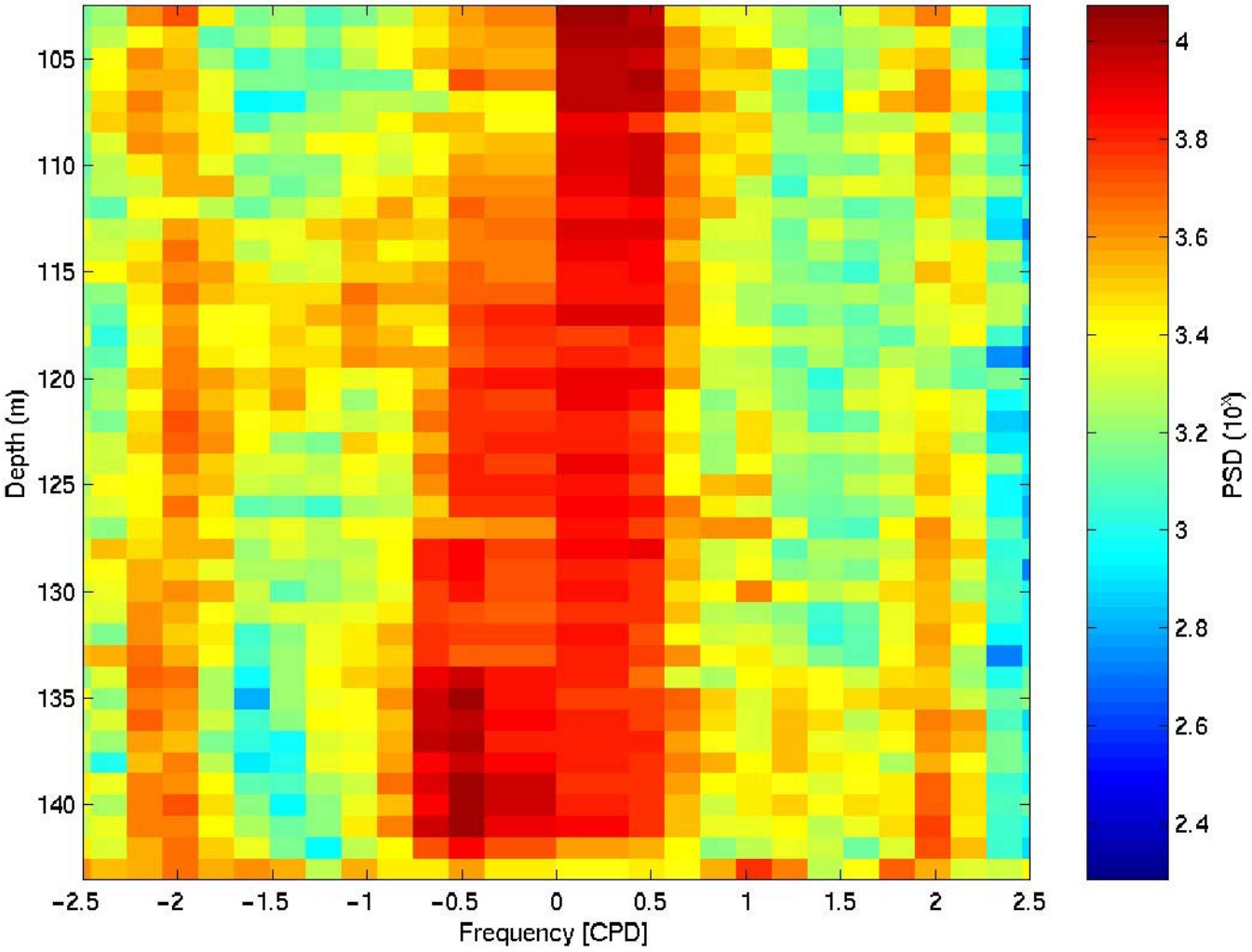

Figure 42: Rotary spectrum for the velocities recorded at Mooring M7 for each depth bin. There were 13 degrees of freedom in the rotary spectra calculation.

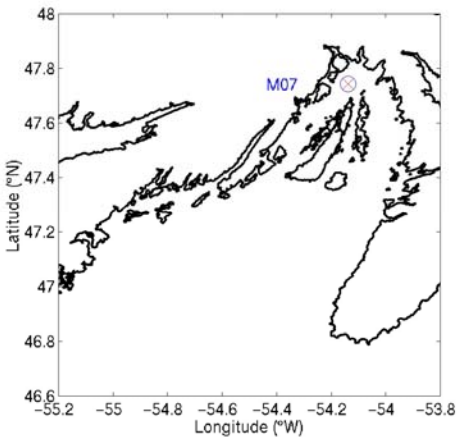

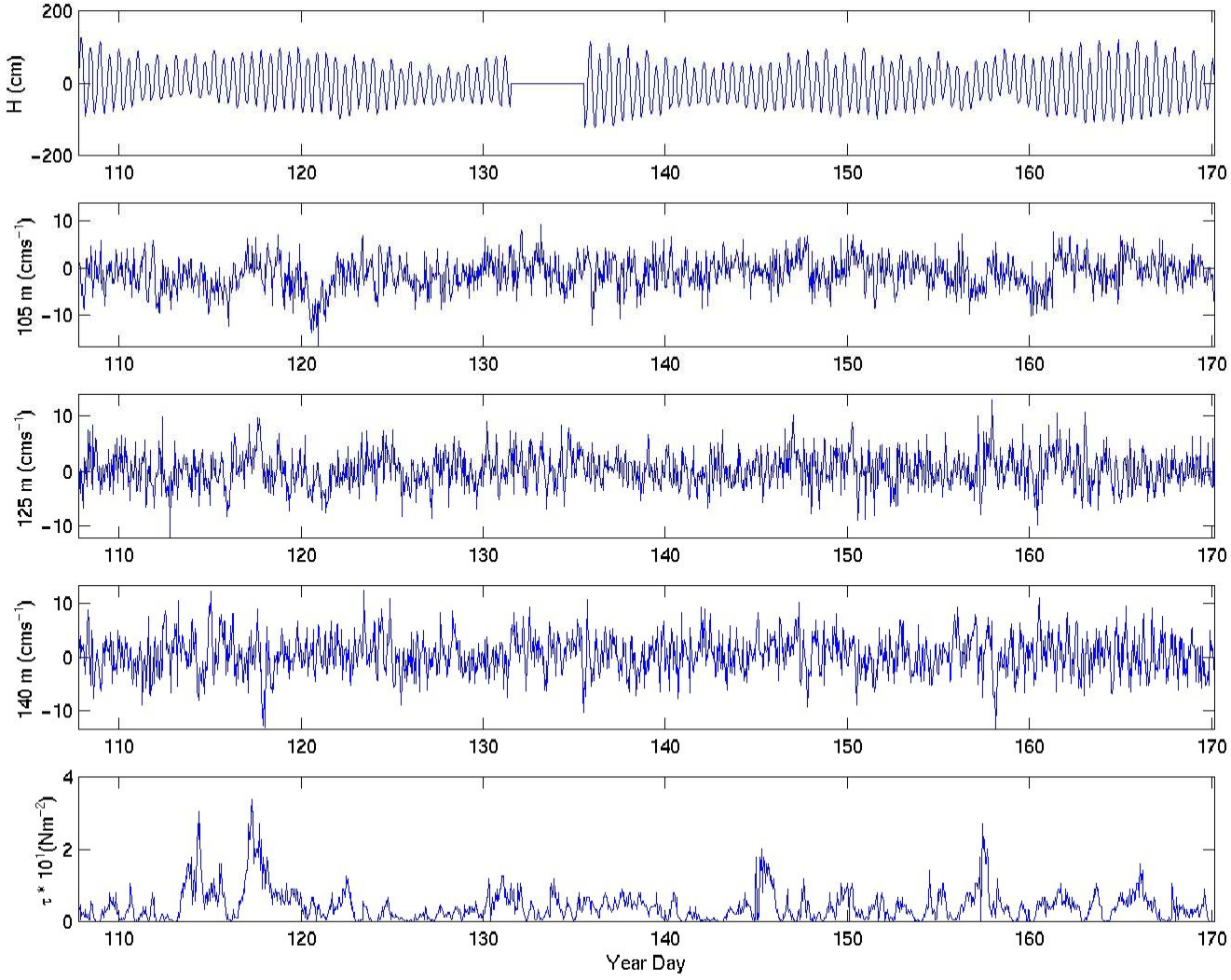

Figure 43: The surface elevation measured at Argentia, current velocities of the along bay component for 105, 125, and 140 m measured at M7, and the magnitude of the wind stress measured at Argentia.

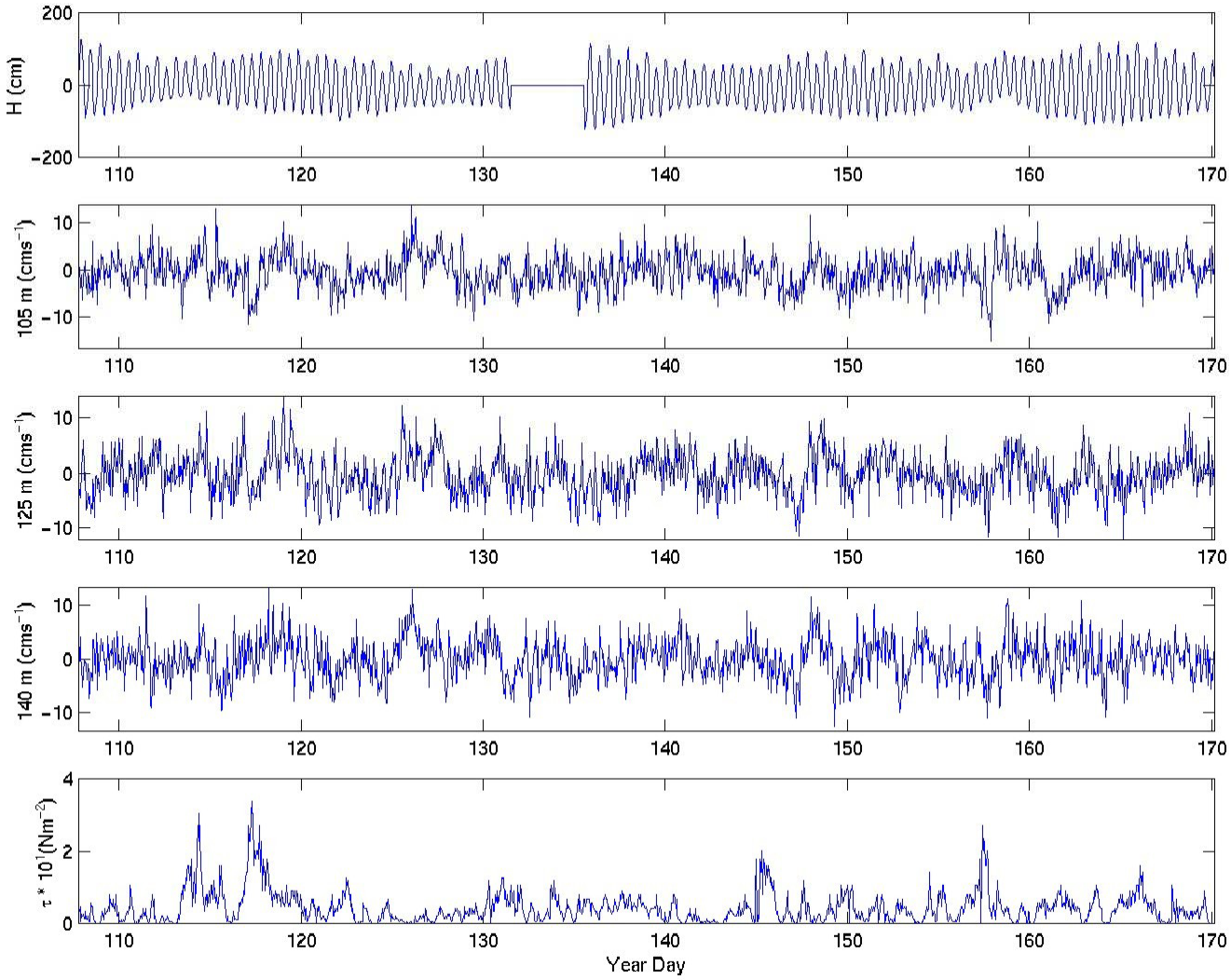

Figure 44: The surface elevation measured at Argentia, current velocities of the cross bay component for 105, 125 and 140 m measured at M7, and the magnitude of the wind stress measured at Argentia.

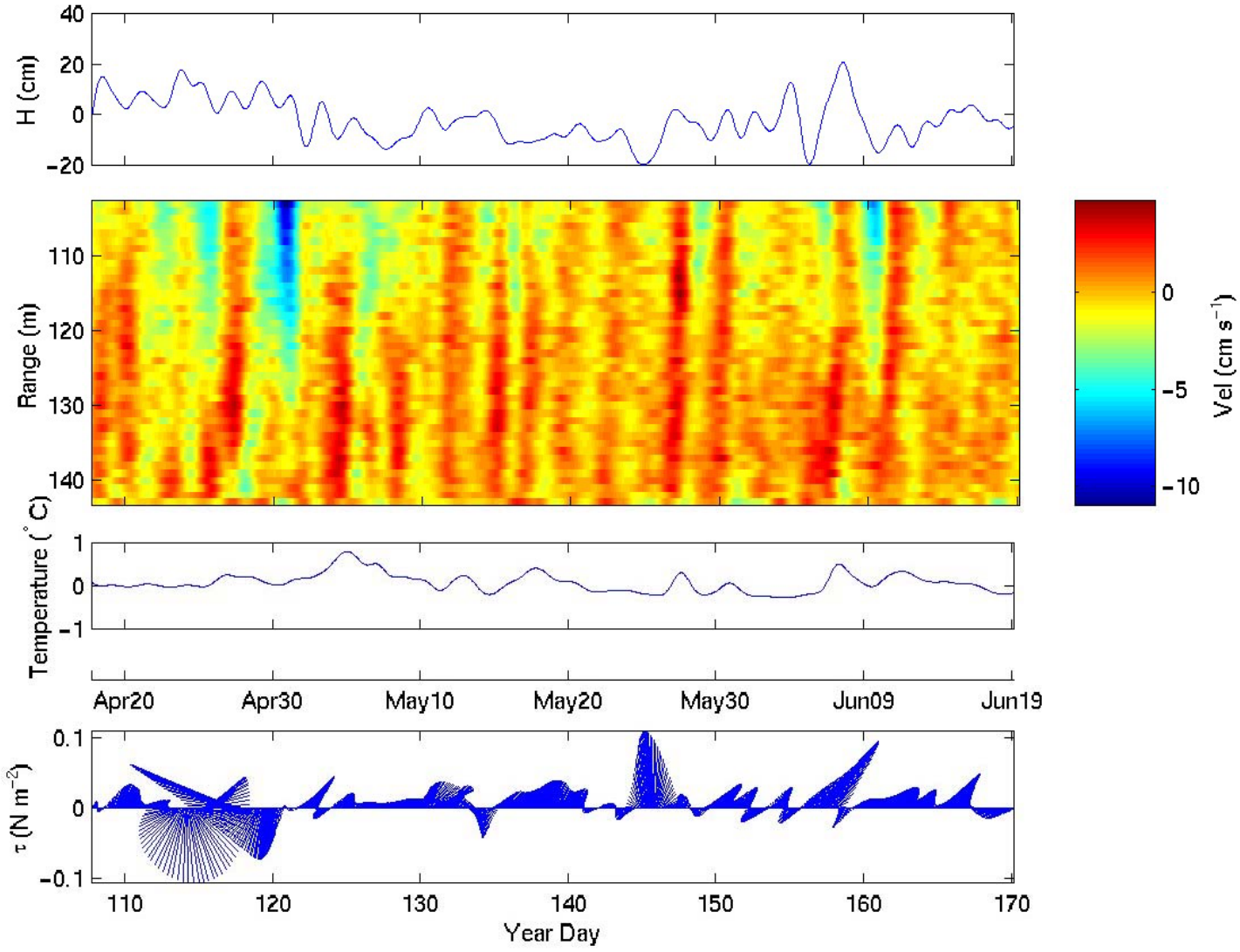

Figure 45: The subtidal along bay velocity intensity and the temperature measured by the ADCP at M7 along with the surface elevation and the wind stress measured at Argentia. For the stick plot, wind is presented in the direction towards which the wind is blowing, with North at the top.

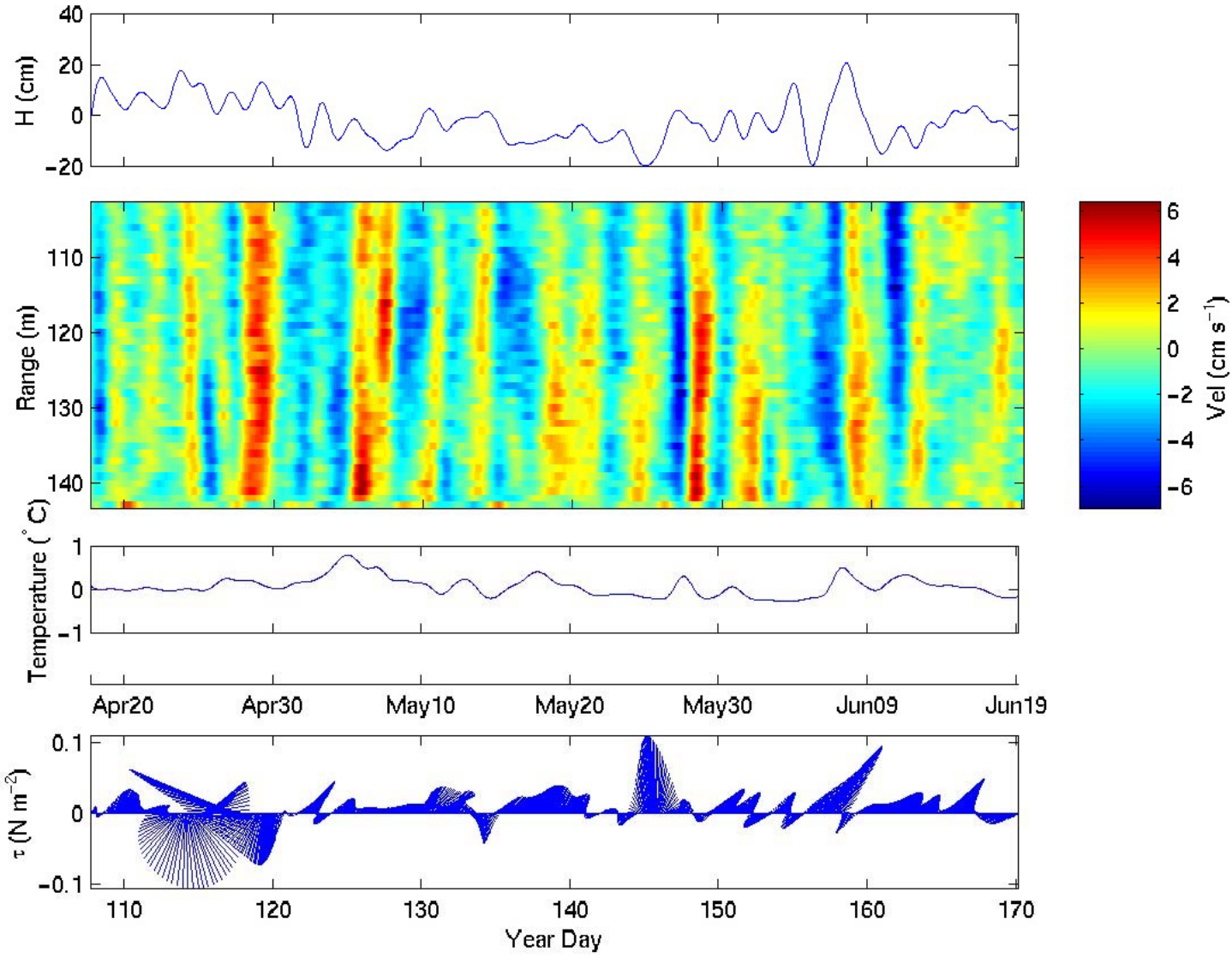

Figure 46: The subtidal cross bay velocity intensity and the temperature measured by the ADCP at M7 along with the surface elevation and the wind stress measured at Argentia. For the stick plot, wind is presented in the direction towards which the wind is blowing, with North at the top.

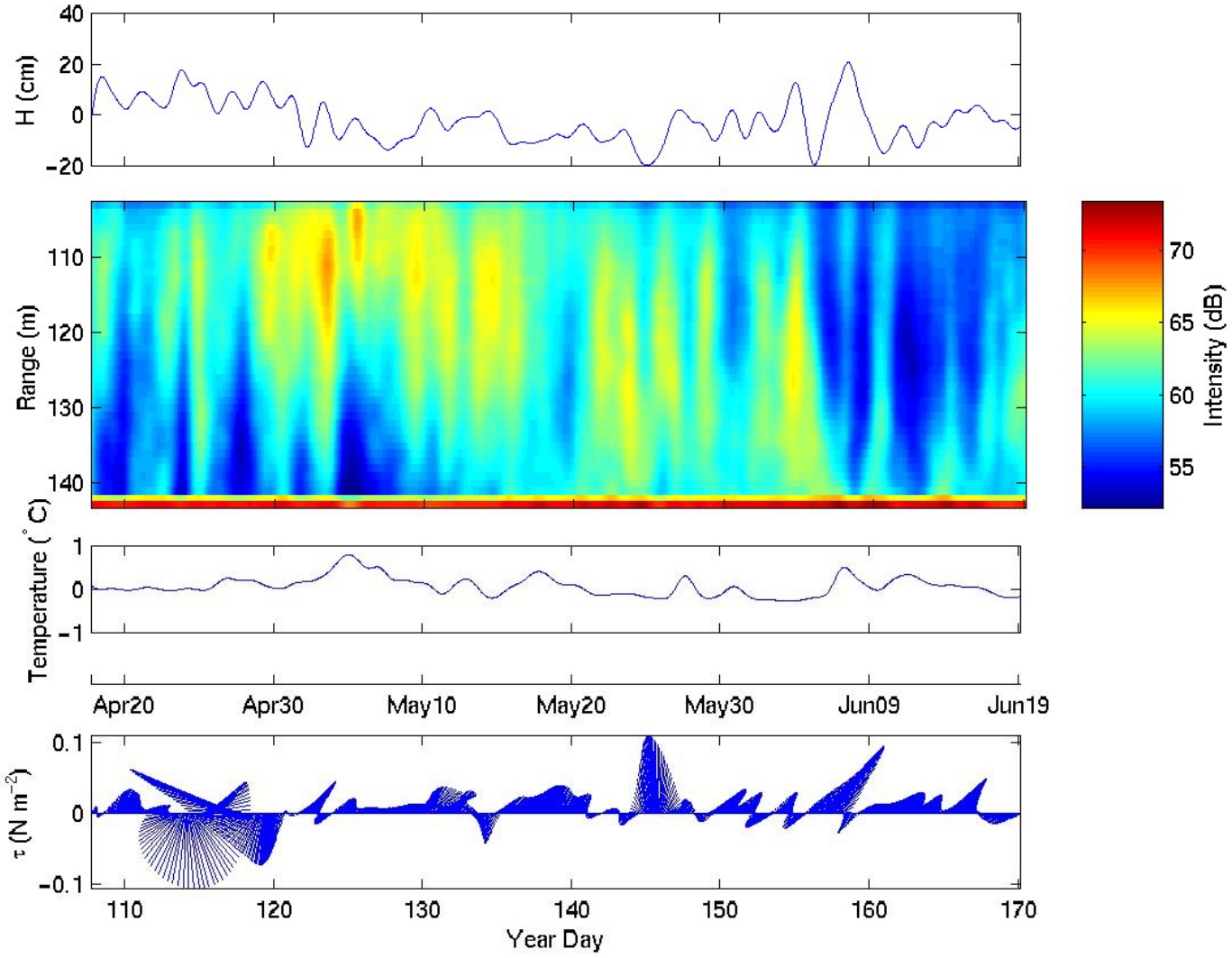

Figure 47: The subtidal backscatter intensity and the temperature measured by the ADCP at M7 along with the surface elevation and the wind stress measured at Argentia. For the stick plot, wind is presented in the direction towards which the wind is blowing, with North at the top.

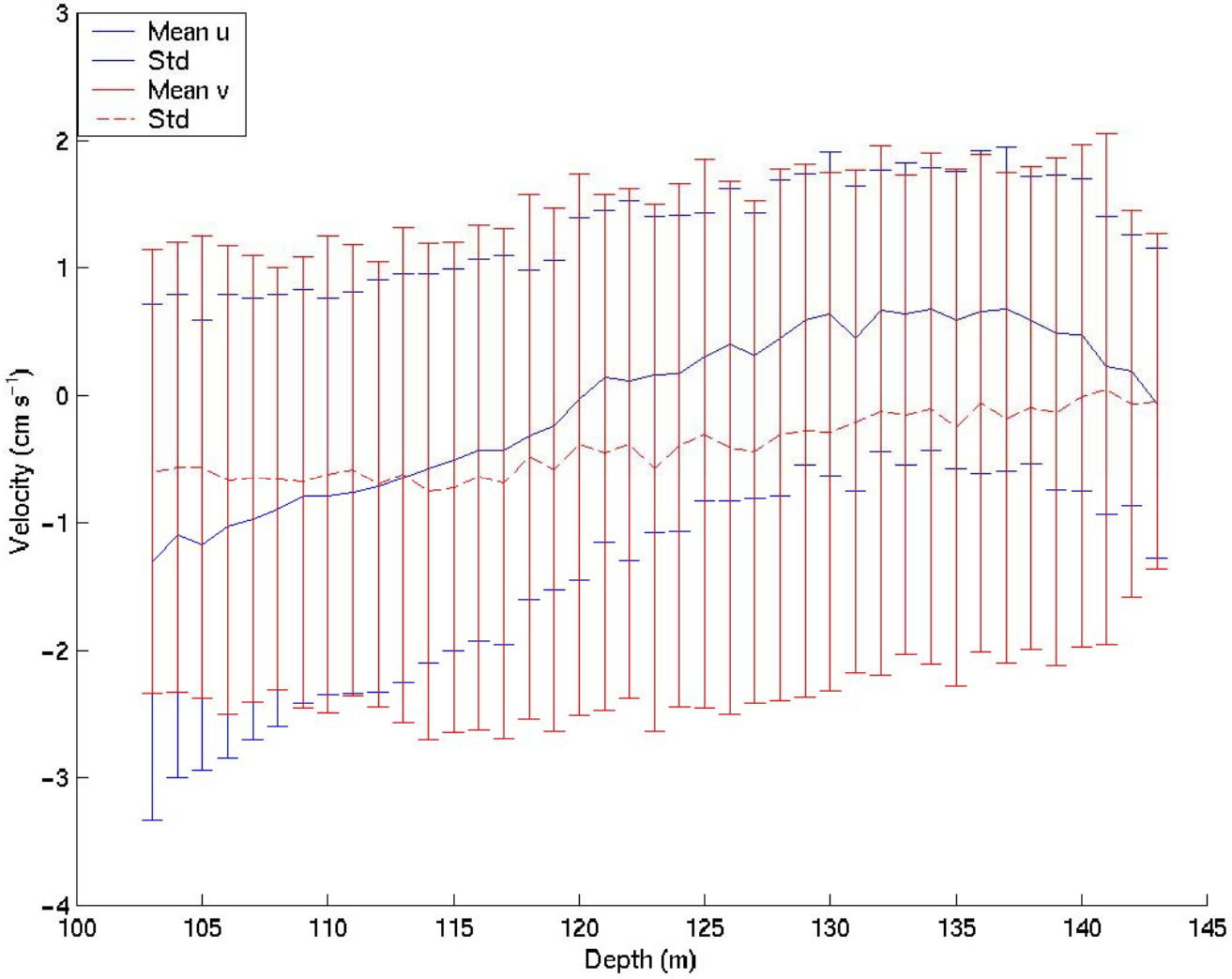

Figure 48: The subtidal along and cross bay velocity profiles measured at M7. The standard deviations are indicated by the error bars.

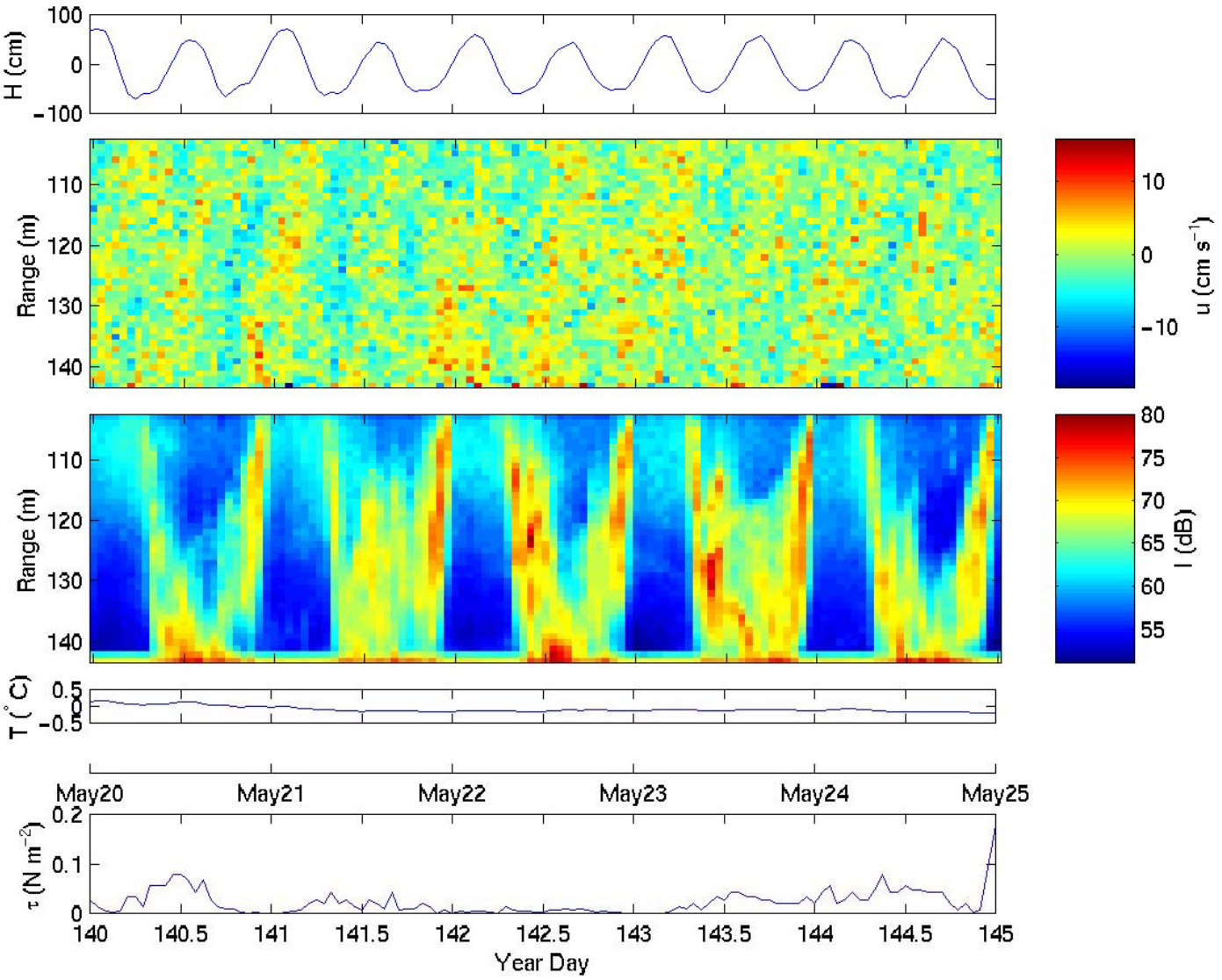

Figure 49: The surface elevation, along bay velocity, backscatter intensity, temperature and the wind stress for year day 140 to 145.

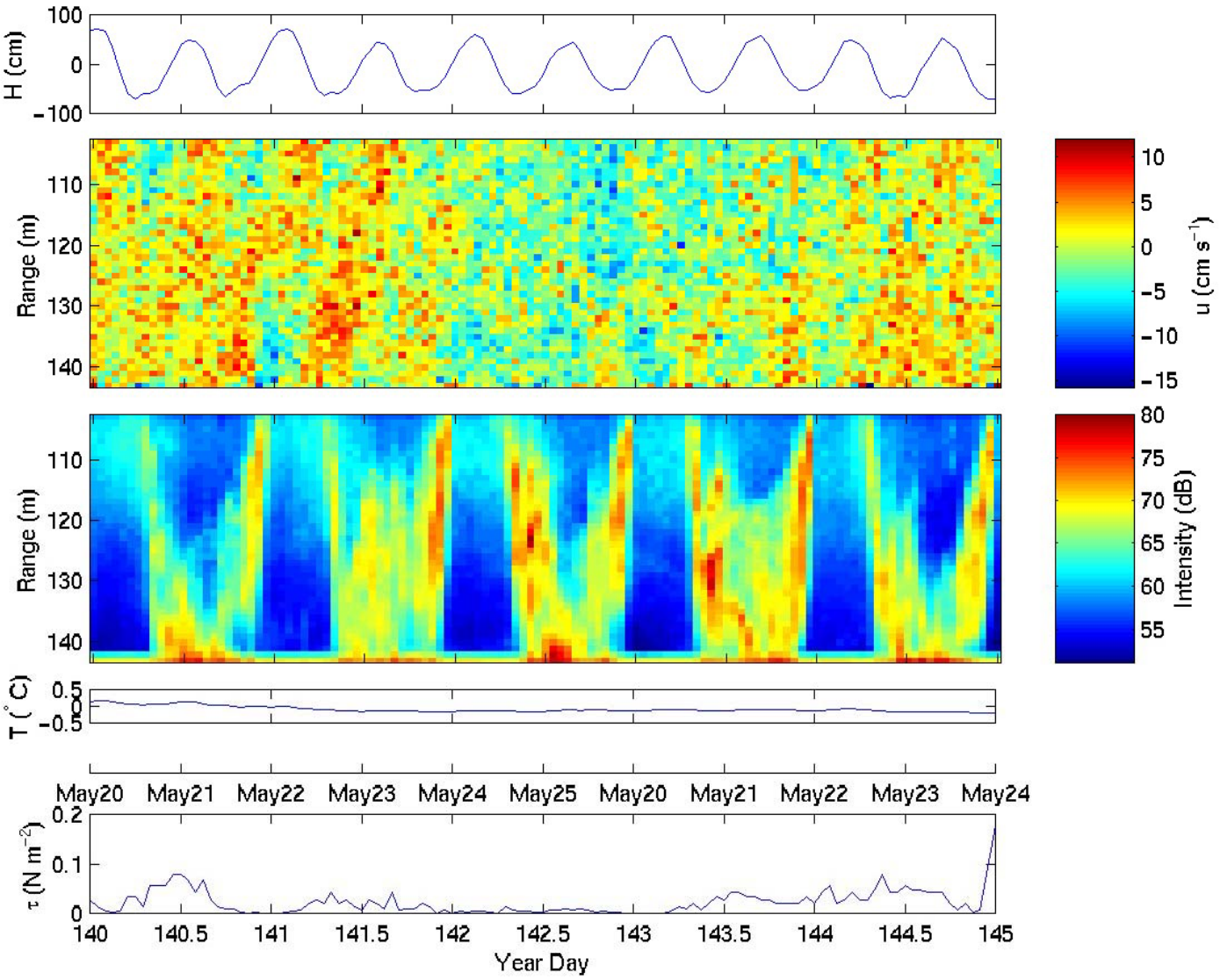

Figure 50: The surface elevation, along bay velocity, backscatter intensity, temperature and the wind stress for year day 140 to 145

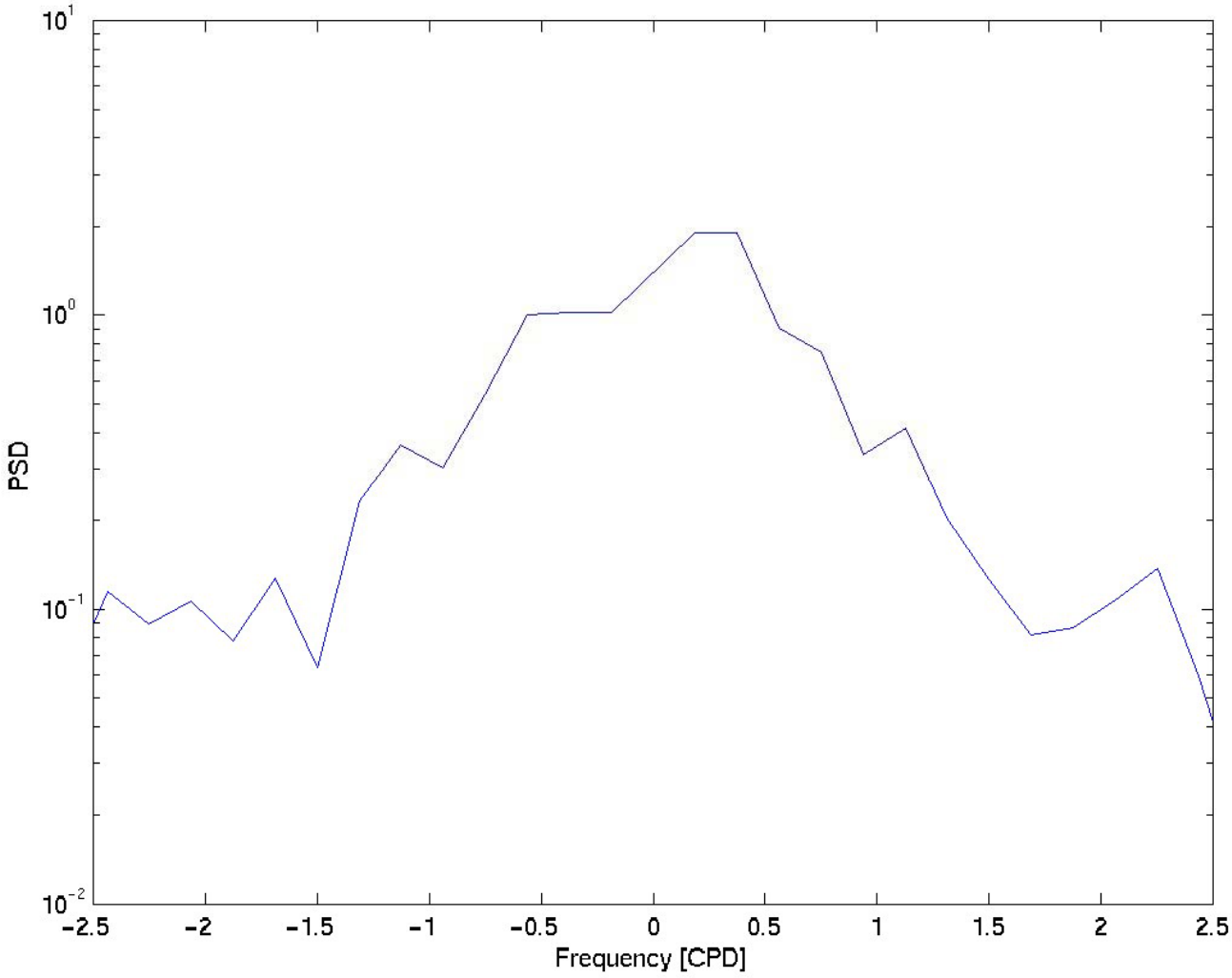

Figure 51: The rotary spectrum of the wind as measured at Argentia. There were 13 degrees of freedom in the rotary spectral calculation.